With the support of the Erasmus+ Programme of the European Union

UAlg
UNIVERSIDADE DO ALGARVE

Department of Chemistry and Pharmacy

Faculty of Science and Technology

Searching for Bioactive Compounds in the Microalgae *Nanofrustulum shiloi*

ERASMUS MUNDUS MASTER IN QUALITY IN ANALYTICAL LABORATORIES (EMQAL)

Ugonna Darlington Nwankpa

Faro, July 2023

Searching for Bioactive Compounds in the Microalgae *Nanofrustulum shiloi*

Erasmus Mundus Master in Quality in Analytical Laboratories (EMQAL)

Department of Chemistry and Pharmacy
Faculty of Science and Technology
Universidade do Algarve

Author: Ugonna Darlington Nwankpa

Supervisor: Prof. Luísa Afonso Barreira

July 2023

Searching for Bioactive Compounds in the Microalgae *Nanofrustulum shiloi*

Disclaimer

Searching for Bioactive Compounds in the Microalgae *Nanofrustulum shiloi*

Declaration of authorship of work

I declare I am the author of this work, which is original and unpublished. The sources consulted have been duly cited in the text and included in the list of references.

Ugonna Darlington Nwankpa

Acknowledgements

I am grateful to the European Union for funding my MSc. studies and this project, and to the EMQAL organizing committee for giving me the opportunity to participate in this life-changing adventure.

I acknowledge the unequalled support of my supervisor, Prof. Luísa Afonso Barreira, throughout the course of this work. I wish every student would have a taste of working with a supportive supervisor like her. I also acknowledge the guidance and contributions of Mélanie Vanessa Silva, who made my work ten times easier than normal, and translated the abstract of this work to portuguese. I appreciate the support of the entire Marbiotech group, working with You is a memory that will linger for a long time.

To my family, who never stopped praying and believing in my academic success, friends and well-wishers, this story will not be complete without the part you played. Imela nke ukwuu, muchas gracias, muito obrigado, thank you so much.

Finally, I am grateful to God for guidance and direction in this journey.

Sumário

A hipertensão arterial é um dos principais fatores de risco para o desenvolvimento de doenças cardiovasculares (DCs), tendo também sido associados à etiologia deste tipo de patologias a enzima conversora da angiotensina (ECA), o *stress* oxidativo e a inflamação cardíaca. A medicação anti-hipertensiva disponível de momento no mercado apresenta inúmeros efeitos adversos, tais como hipercalemia, tosse seca e angioedemas, existindo a necessidade para o desenvolvimento de terapias medicinais alternativas, de preferencialmente de origem natural. *Nanofrustulum shiloi* é uma microalga pouco estudada, mas apresenta-se como uma fonte sustentável com um repositório de compostos químicos potencialmente interessantes, como pigmentos, ácidos gordos polinsaturados, entre outros, tendo reportadamente inibido a atividade da ECA num estudo anterior. O presente trabalho pretende aprofundar conhecimento potencialmente identificado no estudo anterior, visando avaliar as atividades anti-hipertensiva, antioxidante e anti-inflamatória de *N. shiloi*, tal como identificar os metabolitos responsáveis por estas atividades. A biomassa foi extraída separadamente por etanol e acetato de etilo, fracionada por cromatografia líquida de alto desempenho e a sua bioatividade avaliada por ensaios *in vitro* espectrofotométricos de Difenilo-1-picrilhidrazilo (DPPH) e Poder redutor do ião férrico (FRAP), inibição fluorométrica da ECA e ensaios anti-inflamatórios do gene repórter. As frações ativas do extrato de etanol menos coradas foram analisadas posteriormente com espectrometria de massa por cromatografia em fase líquida (LC-MS). Algumas frações apresentaram bioatividades promissoras; FRAP (até 59,4% [etanol] e 94,4% [acetato de etilo] da atividade do ácido gálico) e inibição da ECA (até 94,4% [etanol] e 95,0% [acetato de etilo] da atividade do captopril). As frações de etanol também inibiram a expressão de genes humanos que codificam marcadores pró-inflamatórios TNFα, IL-6 e NF-kβ. A análise por LC-MS identificou alguns metabólitos sem usos ou atividades reportadas. Recomendamos confirmar as bioatividades dos metabólitos identificados purificados, e posteriormente criar estratégias para estimular a sua produção ao cultivar *N. shiloi* em diferentes condições (a)bióticas. Esta(s) estratégias(s) poderão auxiliar na criação de novas perspetivas sobre a utilização de alimentos funcionais e nutraceuticos como tratamentos naturais para o tratamento de hipertensão e doenças cardiovasculares.

Palavras-chave

Inflamação cardiovascular, hipertensão, *Nanofrustulum shiloi*, ensaio de gene repórter e Metabolómica não direcionada.

Abstract

Hypertension remains the greatest risk factor of cardiovascular diseases (CVDs) and the roles of angiotensin converting enzyme (ACE), oxidative stress and cardiovascular inflammation in its etiology are well established. Current hypertension medications present some side effects such as increased risk of hyperkalemia, dry cough, and angioedema, and thus the search for alternative therapies is needed, especially with the increasing emphasis on natural alternatives. *Nanofrustulum shiloi* is an understudied microalga, but a sustainable and economic repository of nutritive chemicals such as pigments, poly-unsaturated fatty acids (PUFAs), etc., and has been found to inhibit ACE, in a previous study. The present study intends to deepen the previous one and aims at evaluating *N. shiloi's* antihypertensive, antioxidant, and anti-inflammatory activities and identifying the metabolites responsible for such activities. The biomass was separately extracted with ethanol and ethyl acetate, fractionated with preparative high-performance liquid chromatography, and analyzed with spectrophotometric Diphenyl-1-picrylhydrazyl (DPPH) free radical scavenging and ferric reducing antioxidant power (FRAP), *in vitro* fluorometric ACE inhibition, and high throughput screening reporter gene anti-inflammatory assays. Active non-color-intensive ethanol fractions were further analyzed with liquid chromatography mass spectrometry (LC-MS). Some fractions displayed interesting bioactivities; FRAP (up to 59.4% [ethanol] and 94.4% [ethyl acetate] of the activity of gallic acid), and ACE inhibition (up to 94.4% [ethanol] and 95.0% [ethyl acetate] of the activity of captopril). Ethanol fractions also inhibited the expression of human genes coding for the proinflammatory cytokines TNFα, IL-6, and NF-kβ. LC-MS analysis was able to identify some metabolites with no recorded uses or activities. We recommend confirming the bioactivities of the pure metabolites, upon which they can be overproduced by culturing *N. shiloi* under different biotic/abiotic conditions. This might provide fresh perspectives on the production of functional foods and nutraceuticals as all-natural treatments for hypertension and CVDs.

Keywords

Cardiovascular inflammation, hypertension, *Nanofrustulum shiloi,* reporter gene assay, & untargeted metabolomics.

List of Tables

List of Figures

Abbreviations

Abz-Gly: o-aminobenzoylglycine,

Abz-Gly-Phe(NO2)-Pro: o-aminobenzoylglycyl-p-nitro-L-phenylalanyl-L-proline,

ACE: angiotensin-converting enzyme,

ACE2: angiotensin-converting enzyme 2,

ACEIs: angiotensin-converting enzyme inhibitors,

ACN: acetonitrile,

ALA: alpha-linolenic acid,

Ang I: angiotensin I,

Ang II: angiotensin II,

Ang-(1–7): angiotensin-(1–7),

Ang-(1–9): angiotensin-(1–9),

AT1R: angiotensin II type 1 receptor,

AT2R: angiotensin II type 2 receptor,

ARA: arachidonic acid,

ARBs: angiotensin receptor blockers,

ARNIs: angiotensin receptor neprilysin inhibitors,

b-Gal: beta-Galactosidase,

CAT: catalase,

CAT: chloramphenicol acetyltransferase,

CAWG: Chemical Analysis Working Group,

CO_3^{2+}: carbonate,

COX-2: cyclooxygenase-2,

CVD: cardiovascular disease,

DAD: diode array detector,

DMSO: dimethyl sulfoxide,

DPPH: 2,2-Diphenyl-1-picrylhydrazyl,

dSPE: dispersive solid phase extraction,

DW: dry weight,

EC: enzyme Commission number

EC_{50}: half maximal effect concentration,

ELISA: enzyme-linked immunosorbent assay,

EPA: eicosapentaenoic acid,

ESI: electrospray ionization,

ERK: extracellular signal-regulated kinase,

FRAP: ferric reducing antioxidant power,

gACE: germinal form ACE,

GC-MS: gas chromatography-mass spectrometry,

GFP: green fluorescent protein,

GPX: glutathione peroxidases,

H_2O_2: hydrogen peroxide,

HAT: hydrogen atom transfer reaction,

HEPEs: hydroxyeicosapentaenoic acids,

HepETEs: hydroxy-epoxy-eicosatetraenoic acids,

HHMEs: hydroxyhexadecenoic acids,

HPLC: high performance liquid chromatography,

HTS: high-throughput screening,

IL-1β: interleukin 1β,

IL-6: interleukin 6,

IUPAC: the International Union of Pure and Applied Chemistry,

KHMEs: ketohexadecenoic acids,

KKS: Kallikrein-kinin System,

LC-MS: liquid chromatography-mass spectrometry,

LOX: lipoxygenase,

LPS: lipopolysaccharide,

Luc: Luciferase,

m/z: mass to charge ratio,

MAPK: mitogen-activated protein kinase,

MAS: mitochondrial assembly protein,

MHC: major histocompatibility complex,

MS: mass spectrometry,

MSI: Metabolomics Standards Initiative,

NF-κB: nuclear factor kappa-light-chain-enhancer of activated B cells,

NMR: nuclear magnetic resonance,

NO•: nitric oxide,

NO_2•: nitrogen dioxide,

NOXs: NADPH oxidases,

O_2•$^-$: superoxide anion,

O_2NOO−: peroxynitrate,

ONOO−: peroxynitrite,

PAMPs: pathogen-associated molecular patterns,

PFE: pressurized fluid extraction,

PI3K/AKT: phosphatidylinositol-3-kinase/protein kinase B,

PPAR: peroxisome proliferator-activated receptors,

PRRs: pattern recognition receptors,

Prx: peroxiredoxin,

PUFAs: polyunsaturated fatty acids,

QuEChERS: Quick-Easy-Cheap-Effective-Rugged-Safe extraction,

RAAS: renin-angiotensin-aldosterone system,

RAS: renin-angiotensin system,

RAW 264: murine macrophage cell line,

RCS: reactive carbonyl species,

RNS: reactive nitrogen species,

ROS: reactive oxygen species,

RSeS: reactive selenium species,

RSS: reactive sulfur species,

sACE: somatic form ACE,

SARS-Cov-2: severe acute respiratory syndrome-corona virus-2,

SET: single electron transfer reaction,

SOD: superoxide dismutase,

TCA: trichloroacetic acid,

TE: Trolox equivalent,

THP-1: human monocytic cell line,

TNF-α: tumor necrosis factor alpha, and

UFAs: unsaturated fatty acids.

Contents

1 INTRODUCTION

1.1 Cardiovascular Diseases

Cardiovascular diseases (CVD) are a group of diseases related to the heart and blood vessels, including rheumatic heart disease, cerebrovascular disease, coronary heart disease, etc. They are the leading cause of death worldwide, claiming an estimated 17.9 million lives annually, or about 32% of all deaths (Cardiovascular Diseases – World Health Organization, 2022). Risk factors of CVDs include hypertension, and cardiovascular inflammation, among others. Additionally, oxidative stress has been implicated in the etiology of CVDs and their risk factors. Moreover, different CVDs risk factors can potentiate each other (Kjeldsen, 2018). Therefore, ascertaining the global cardiovascular risk is important in clinical decision-making.

1.1.1 Hypertension

Hypertension is a condition where circulating blood exerts much force on the arterial walls. It is generally diagnosed by a systolic blood pressure up to 140 mmHg with a diastolic blood pressure up to 90 mmHg on two consecutive days (Hypertension – World Health Organization, 2022; Magalhães et al., 2017). Hypertension is a major cause of premature death, affecting an estimated 1.3 billion people globally and about 30–45% of the general European population (Hypertension – World Health Organization, 2022; Kjeldsen, 2018). Hypertension increases the risk of kidney, brain, and heart diseases, which is why reducing its prevalence by 33% between 2010 and 2030 is one of the global targets of the World Health Organization for non-communicable diseases (Hypertension – World Health Organization, 2022). Several factors increase the risk of developing hypertension. These include unhealthy diet, physical inactivity, alcohol or tobacco intake, obesity, family history, age, and other diseases. However, the pathogenesis of hypertension is based on the action of the angiotensin converting enzyme (ACE); as such, ACE inhibitors and angiotensin receptor blockers (ARB) are used as first-line treatment for hypertension (Shrimpton et al., 2020).

1.1.1.1 Angiotensin-converting Enzyme

Angiotensin-converting enzyme (EC 3.4.15.1) is a crucial component of the renin-angiotensin system (RAS), also known as renin-angiotensin-aldosterone system (RAAS), which regulates blood pressure and fluid and electrolyte balance (Khurana and Goswami, 2022; Gaddam et al., 2014; Zhao and Xu, 2008). It is a type 1 monomeric glycoprotein, a peptidyl dipeptidase that hydrolyzes

the carboxy-terminal dipeptide of its substrates (Gaddam et al., 2014; Riordan, 2003). ACE exists mainly as a tissue-bound, transmembrane protein, and although soluble plasma forms exist, reports suggest that they have very low activities compared to the plasma-bound forms (Georgiadis et al, 2003). ACE's activity depends on the presence of chloride ions and zinc, while it is inhibited by chelating agents such as heavy metals, sulfhydryl compounds, and specific peptides (Studdy et al., 1983). There are two isoforms of ACE, the ubiquitous somatic form (sACE) is expressed in different tissues, including the brush-border membranes of the kidney, the endothelial surface of the lungs, vascular endothelium, brain, renal proximal tubule epithelium, intestinal epithelium, macrophages, placenta, etc. In contrast, the sperm-specific germinal form (gACE), also called testicular ACE (tACE), is only expressed in adult testes (Masuyer et al., 2014; Riordan, 2003). sACE has two catalytic domains, the C- and the N-domains, while gACE has only the C-domain (Riordan, 2003). ACE plays significant roles in two biological pathways, the RAS and the Kallikrein-kinin System (KKS) but is mainly known for its role in the RAS (Khurana and Goswami, 2022; Zhao and Xu, 2008).

In the RAS (Figure 1.1), the enzyme renin, which is made in the juxtaglomerular complex of the nephrons, hydrolyzes the liver-made glycoprotein angiotensinogen into the decapeptide angiotensin I (Ang I). ACE cleaves off a dipeptide from the C-terminal of Ang I, forming the octapeptide Angiotensin II (Ang II; Khurana and Goswami, 2022). Ang II has two receptors: the Angiotensin II types 1 and 2 receptors (AT1R and AT2R; Gaddam et al., 2014). When Ang II binds to AT1R, it acts as a vasoconstrictor by stimulating androsterone secretion from the adrenal cortex, which causes sodium and water retention, an increase in blood volume, vascular smooth muscle contraction, and ultimately an increase in blood pressure (Zhao and Xu, 2008). These activities lead to cell growth and proliferation. Conversely, Ang II binding to AT2R causes vasodilation, apoptosis, and inhibition of cell growth and proliferation (Gaddam et al., 2014). It is noteworthy that AT2R expression is much reduced after birth than during fetal development; therefore, Ang II acts mostly as a vasoconstrictor than a vasodilator (Masuyer et al., 2014).

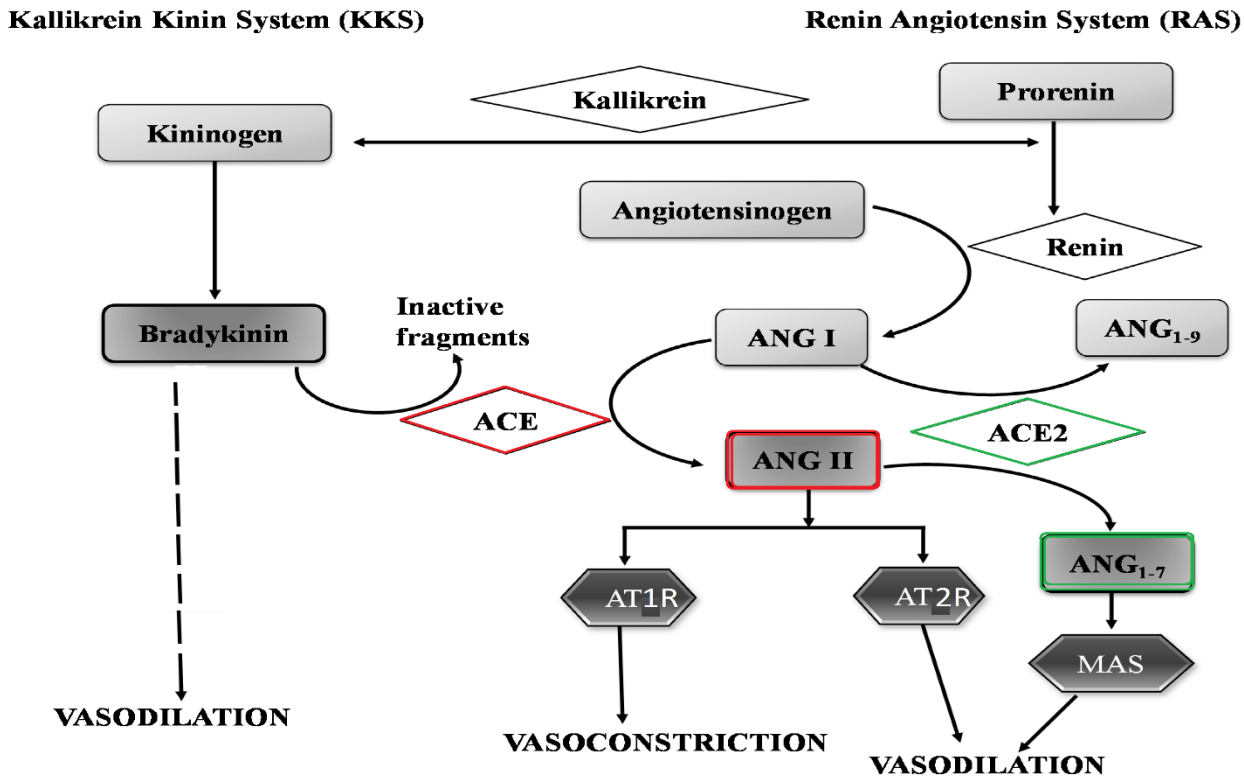

Figure 1.1: The roles of ACE and ACE2 in the RAS and KKS (adapted from Majumder & Wu, 2014).
ACE: Angiotensin-converting enzyme; ACE2: Angiotensin-converting enzyme 2; Ang-(1–7): Angiotensin-(1–7), Ang-(1–9): Angiotensin-(1–9), Ang I: Angiotensin I; Ang II: Angiotensin II; AT1R: Angiotensin type 1 receptor; AT2R: Angiotensin type 2 receptor; MAS: Mitochondrial assembly protein.

In the KKS, ACE acts as a kininase in hydrolyzing the vasodilator bradykinin (Khurana and Goswami, 2022). However, the increase in blood pressure is mainly elicited by an increase in Ang II level as the reduction in bradykinin level has little effect (Bernstein et al., 2013). ACE also hydrolyzes other vasoactive peptides such as neurotensin, enkephalin, and substance P (Zhao et al., 2008). It has been demonstrated *in vivo* that selectively inhibiting ACE's C-domain significantly reduced Ang I hydrolysis, whereas a complete inhibition of both domains was required to achieve a similar effect for bradykinin (Figure 1.2). Hence, sACE's C-domain has much more efficiency in hydrolyzing Ang I than the N-domain. The C-domain alone appears sufficient for regulating blood pressure *in vivo* while the N-domain plays other physiological roles such as hematopoietic stem cell differentiation and proliferation (Harrison and Acharya, 2015; Zhao and Xu, 2008; Georgiadis et al, 2003; Riordan, 2003).

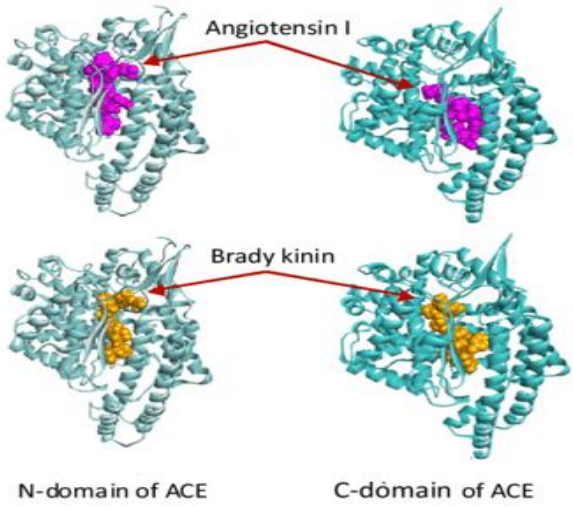

Figure 1.2: ACE domains and their interaction with Ang I and bradykinin (adapted from Widodo et al., 2017).

1.1.1.2 Angiotensin Converting Enzyme-2 (ACE2).

Angiotensin-converting enzyme-2 (ACE2; EC 3.4.17.23) is similar to ACE in being a zinc metallopeptidase and a transmembrane glycoprotein (Gaddam et al., 2014). However, it has several differences from ACE. Unlike ACE, it is a mono-carboxypeptidase with high specificity (Huentelman et al., 2005). Although it has two domains, the extracellular amino- and intracellular carboxy-terminal domains, only the amino domain is catalytic (Douglas et al., 2004). Its primary biological function is the degradation of Ang II to Angiotensin-(1–7; Ang-(1–7)), but it also hydrolyzes Ang I to Angiotensin-(1–9; Ang-(1–9)), a substrate which ACE hydrolyzes to Ang-(1–7; Gaddam et al., 2014). Either way, it counteracts ACE activity by reducing the concentration of Ang II and increasing the production of Ang-(1–7) which has opposing activities to Ang II. ACE2 is not inhibited by ACE inhibitors (Huentelman et al., 2005). It is found mainly in the lungs, heart, kidneys, intestine, and placenta (Gaddam et al., 2014).

1.1.1.3 Cardiovascular Inflammation

Inflammation is a local response caused by the immune system to limit injury-induced damages to a local site and to eliminate the cause of the injury. It induces illness responses such as fever, sleep, loss of appetite, etc., which enables the body to adjust and fight diseases, and initiate tissue repair processes (Zhang and An, 2007). Inflammation activates macrophages, monocytes, and endothelial cells which increases secretion of proinflammatory cytokines and expression of

adhesion molecule. This results in inflammation of the vascular tissues, including those of the myocardium (Li et al, 2021). Inflammation appears to be both a cause and consequence of several diseases, cardiovascular diseases inclusive (Sorriento and Iaccarino, 2019).

Inflammatory cytokines are small, secreted proteins that play a role in the body's inflammatory processes, and are produced predominantly by macrophages, monocytes, and helper T cells of the immune system (Figure 1.3). The role of nuclear factor kappa-light-chain-enhancer of activated B cells (NF-κB), and pro-inflammatory cytokines such as interleukin (IL)-1β, IL-6, and tumor necrosis factor alpha (TNF-α) in the upregulation of inflammatory reactions is well established (Zhang and An, 2007). NF-κB is a protein complex that is involved in immune system regulation, control of DNA transcription and cytokine production, among other things (Brasier, 2006). Dysregulation of NF-κB, such as undue activation by some proinflammatory cytokines, lead to immunological disorders including inflammatory diseases. IL-1β induces the expression of cyclooxygenase-2 (COX-2), an enzyme that plays important roles in inflammation (National Library of Medicine, 2023). IL-6 plays proinflammatory roles in monocytes and macrophages, but anti-inflammatory roles in muscle cells (Brandt and Pedersen, 2010). It is secreted when specific microbial molecules called pathogen-associated molecular patterns (PAMPs) bind to recognition molecules in the immune system called pattern recognition receptors (PRRs). This triggers an intracellular signaling cascade that leads to secretion of inflammatory cytokines including IL-6. TNF-α activates endothelial cell and multiple cellular signaling pathways such as NF-κB and mitogen-activated protein kinase (MAPK) pathways, which mediate inflammation (Li et al, 2021).

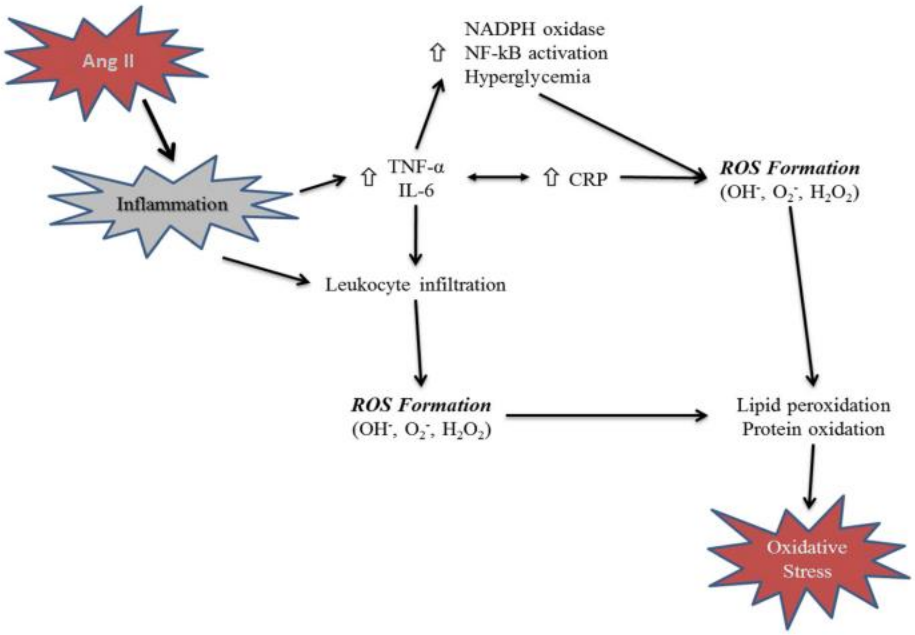

Figure 1.3: Relationship between Ang II, inflammation markers, and oxidative stress.
Ang II: Angiotensin II; CRP: C reactive protein; H_2O_2: hydrogen peroxide; IL-6: interleukin 6; NF-κB: nuclear factor kappa-light-chain-enhancer of activated B cells; $O_2\bullet^-$: superoxide anion; OH•: hydroxyl radical; ROS: reactive oxygen species; TNF-α: tumor necrosis factor alpha (adapted from Huang et al., 2015)

1.1.1.4 Opposing Roles of ACE/Ang II/AT1R and ACE2/Ang-(1–7)/MAS in Hypertension and Cardiovascular Inflammation

The ACE/Ang II/AT1R and ACE2/Ang-(1–7)/MAS have been described as two counterregulatory pathways within the RAS (Parajuli et al., 2014). As discussed earlier, ACE hydrolyzes Ang I into the vasoconstrictor Ang II. Ang II binding to its AT1R causes an increase in blood volume and constriction of blood vessels, which ultimately increases blood pressure. ACE further increases blood pressure by degrading the vasodilator bradykinin. Conversely, ACE2 reduces the quantity of Ang II by hydrolyzing Ang II and Ang I to Ang-(1–7) and Ang-(1–9), respectively. The latter is converted to Ang-(1–7) which is an AT1R antagonist (Gaddam et al., 2014). Therefore, by reducing the quantity of Ang II and increasing Ang-(1–7), ACE2 displays the opposite activity to ACE and reduces blood pressure.

Furthermore, reports suggest that ACE plays a role in regulating the expression of cytokines such as TNF-α, and IL-12, and on the production of the proinflammatory compound, nitric oxide (NO), in monocytes and macrophages (Gonzalez-Villalobos et al, 2013). Ang II binding to AT1R causes myocardial remodeling, fibrosis, and oxidative stress, which trigger inflammation (Shrimpton et

al., 2020). Ang II downregulates inflammation-regulating peroxisome proliferator-activated receptors (PPAR; Tham et al., 2002). Also, a direct link has been found between Ang II and the activation of NF-κB regulated genes (Nakamura et al., 2000). Hence, Ang II has been described as a proinflammatory molecule (Dagenais and Jamali, 2005).

Conversely, by the action of its product Ang-(1–7), ACE2 is described as an anti-inflammatory protein (Gaddam et al., 2014). As an AT1R antagonist, Ang-(1–7) counters the actions of Ang II. Ang-(1–7) activates MAS receptors, thereby playing a role in MAS receptor-mediated anti-inflammatory effects (Iyer et al., 1998). Together, Ang-(1–7) and MAS receptors regulate the Phosphatidylinositol-3-kinase/protein kinase B (PI3K/AKT) and extracellular signal-regulated kinases (ERK) signaling pathways. They also downregulate COX-2 and NO production, both of which play essential roles in inflammation (Passos-Silva et al., 2013). Table 1.1 summarizes the physiological functions of Ang II and Ang-(1–7).

Table 1.1: Physiological Roles of Ang II and Ang-(1-7; adapted from Shrimpton et al., 2020).

Molecule	*Ang II*	*Ang II and Ang-(1–7)*
Receptor	**AT1R**	**AT2R**
Cardiovascular	Vasoconstriction	Vasodilation
	↑ Cardiac remodeling	↓ Cardiac remodeling
	Myocyte hypertrophy	
Immune	↑Inflammation	↓ Inflammation
	↑ Oxidative stress	↓ Oxidative stress
	↑ Cell proliferation	↓ Cell proliferation
Renal	↑Aldosterone	
	↑Vasopressin	

1.1.1.5 Other Roles of ACE

Apart from its role in RAS and KKS, ACE plays other vital and protective roles in the cell. ACE is involved in the outside-in signaling of cells, disruption of which leads to health disorders (Fleming, 2006; Kohlstedt and Brandes, 2004). ACE also plays a role in innate and adaptive immune responses possibly by trimming major histocompatibility complex (MHC) class I and II peptides (Kenneth et al., 2018). In fact, ACE's overexpression can enhance immune response over a wide range of stimuli such as infection by antibiotic-resistant bacteria (Khan et al., 2017) at levels beyond the normal ability of white blood cells (Coe et al., 2020). Although the latter response was elicited by ACE C-domain, known C-domain peptides such as Ang I, bradykinin, and substance P

did not achieve this effect in macrophages and neutrophils. Hence, identifying compounds with this ability might be a breakthrough as such peptides are possible therapeutic agents to boost the immune response against infections, tumors, and similar stimuli (Khurana and Goswami, 2022). Of course, any such therapeutic interventions must be considered carefully, and their administration should be evaluated on a case-to-case basis, given the role of ACE in cardiovascular diseases.

ACE has also been implicated in the pathogenesis or progression of other diseases apart from hypertension and inflammation. ACE overexpression in myelomonocytes can prevent cognitive decline in Alzheimer's (Bernstein et al., 2014). Serum ACE levels increase significantly in people suffering from silicosis (Huuskonen et al., 1986), tuberculosis (Lopez-Sublet et al., 2018), and sarcoidosis (Baudin, 2005), but decrease during pneumonia and increase during recovery from it (Meijvis et al., 2011). ACE is also implicated in the COVID-19 disease, as severe acute respiratory syndrome-corona virus-2 (SARS-Cov-2) enters the cell by binding to ACE2, and afterwards, causes ACE2 downregulation, creating an imbalance between ACE and ACE2. This leads to the unopposed action of Ang II which is likely involved in the acute lung injury related to Covid-19 (Zheng and Cao, 2020). Figure 1.4 depicts ACE's involvement in different diseases.

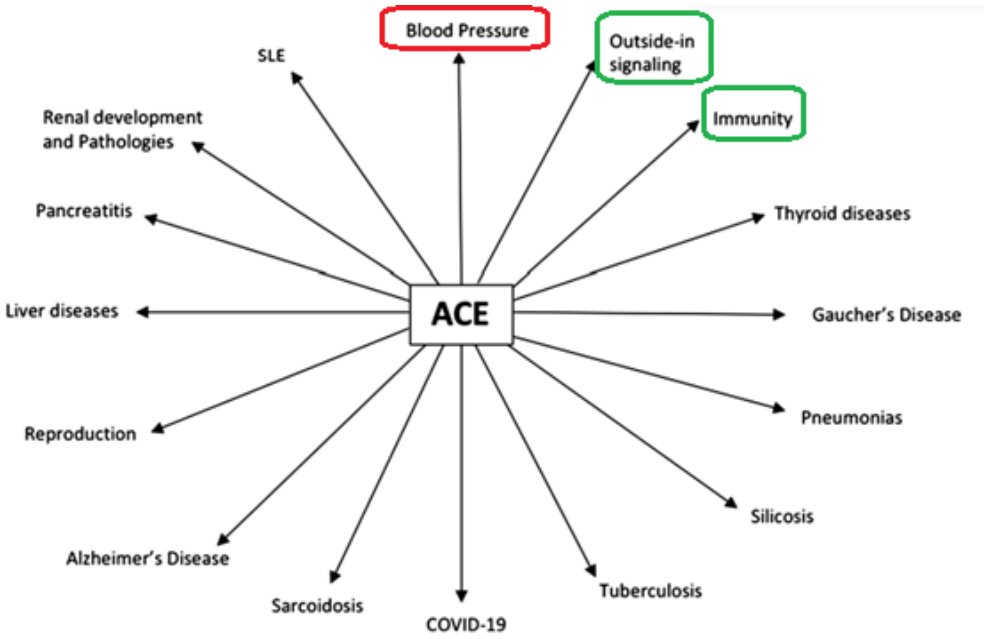

Figure 1.4: Diverse roles of ACE in the body's metabolism and in diseases (adapted from Khurana and Goswami, 2022).

1.1.2 Oxidative Stress

Oxidative stress is implicated in more than a hundred diseases including CVDs, inflammation, hypertension, cancer, diabetes, etc. and appears to be both a cause and consequence of hypertension (Reis et al., 2012; Grossman, 2008). It is an imbalance between pro- and antioxidants in favor of prooxidants, disrupting redox signaling and control and causing molecular damage (Sies and Jones, 2007). The deviation from the redox steady state is essential for redox signaling, that is the transmission of a redox signal via an important redox element from a source to a target. Redox signaling is necessary to maintain homeostasis in the living system. A minor deviation from the redox steady state is a physiological oxidative stress condition termed "metabolic eustress" (Sies et al., 2017). However, this deviation can be excessive, either because of the excess production of free radicals or the inability of the antioxidant system to counteract their effect (Sies et al., 2017). This condition is termed "metabolic distress" but is usually referred to as "oxidative stress." Henceforth, the term 'oxidative stress' will refer to metabolic distress.

Normally, biological macromolecules such as proteins, DNA, and lipids withstand oxidative alterations using the body's antioxidant defense system. Under oxidative stress conditions, free radicals initiate a cascade of redox reactions which nonspecifically modify these biomolecules, disrupting their biological roles in cell structure, transport, catalysis, etc., and interferes with physiological redox signaling (Sies et al., 2022). Oxidative stress leads either to direct effects, such as cell injury, or protracted impacts, such as apoptosis, DNA damage, inflammation, etc. (Rawat et al., 2022).

Oxidants (free radicals) generated in the living system are usually referred to as reactive oxygen species (ROS) as they primarily originate from molecular oxygen but include other reactive species such as reactive nitrogen species (RNS), reactive sulfur species (RSS), reactive carbonyl species (RCS), and reactive selenium species (RSeS), all of which undergo redox reactions (Sies et al., 2022).

1.1.2.1 Reactive Oxygen Species

ROS are generated on several cellular compartments, including the cytosol, plasma membrane, mitochondria, endoplasmic reticulum, peroxisomes, and lysosomes, and in the extracellular space by NADPH oxidases (NOXs; Di Meo et al., 2016). They are generated by different biological

processes, including the mitochondrial oxidative phosphorylation in the electron transport chain, the microsomal cytochrome P450 system, immune response, and NADPH oxidases (Panfoli et al., 2018). ROS can abstract a hydrogen atom from a methylene group of unsaturated fatty acids (UFAs), forming radicals that trigger lipid peroxidation and the formation of secondary oxidation products (Rawat et al., 2022).

Under physiologic conditions, dioxygen (O_2) undergoes tetravalent reduction to water (H_2O). However, in the prevalence of prooxidants or due to electron leakage in the biological processes mentioned above, monovalent, divalent, or trivalent reduction occurs, leading to the generation of radical species: superoxide anion ($O_2\bullet^-$), hydrogen peroxide (H_2O_2), and highly reactive hydroxyl radical (OH•), respectively (Lyle and Griendling, 2006). Superoxide is a precursor of many other ROS as its dismutation produces hydrogen peroxide which is relatively stable but cytotoxic. Hydrogen peroxide plays a role in redox signaling; it generates hydroxyl radicals in the presence of reduced transition metals such as Fe^{2+} via the Fenton reaction (Rawat et al., 2022). Other ROS include singlet oxygen ($^1O_2$), triplet oxygen ($^3O_2$), ozone (O_3), hydroxide ion (HO^-), alkoxyl radical (RO•), and peroxyl radical (ROO•; Sies et al., 2022). Figure 1.5 shows the formation and interconversion of the most prevalent ROS.

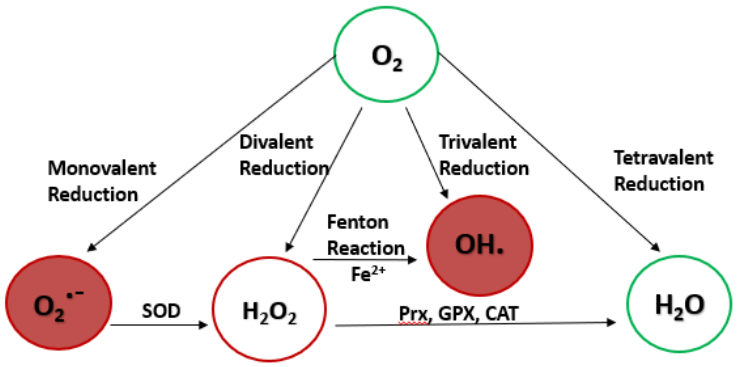

Figure 1.5: Mechanism of generation and interconversion of some reactive oxygen species.
CAT: catalases; GPX: glutathione peroxidases; H_2O: water; H_2O_2: hydrogen peroxide; O_2: oxygen gas; $O_2\bullet^-$: superoxide anion; OH•: hydroxyl radical; Prx: peroxiredoxins; and SOD: superoxide dismutase.

The biological system boasts of enzymatic and non-enzymatic antioxidant defense systems against some ROS. In extracellular fluids, cytosol, and mitochondria, superoxide dismutase (SOD) catalyzes the dismutation of superoxide into hydrogen peroxide and molecular oxygen, as noted earlier. In turn, catalases (CAT), glutathione peroxidases (GPX), and peroxiredoxins (Prx) directly

reduce hydrogen peroxide to water (Rawat et al., 2022). No enzymes are known to deactivate electronically excited states, such as singlet molecular oxygen; this must be done by non-enzymatic components of the antioxidant system (Sies et al., 2022). Non-enzymatic components include vitamins such as vitamins C (ascorbic acid) and E (tocopherol), citric acid, gallic acid, and phytochemicals such as carotenoids, flavonoids, phenols, polyphenols, etc. (Sies et al., 2022). Unfortunately, biological systems do not have a known antioxidant defense system against hydroxyl radicals (Quinlan et al., 2013).

1.1.2.2 Reactive Nitrogen Species

Nitric oxide (NO•) is the primary precursor of other RNS and is generated by NADPH-dependent NO synthase (NOS) during arginine breakdown to citrulline (Rawat et al., 2022). It reacts with hydrogen peroxide, superoxide anion, and transition metals to generate cytotoxic nitrogen species, including peroxynitrite ($ONOO^-$) and peroxynitrate (O_2NOO^-). Peroxynitrite reacts with carbon dioxide to form toxic nitrogen dioxide (NO_2•) and carbonate (CO_3^{2+}; Rawat et al., 2022). Nitrogen dioxide is also generated by the reaction of peroxynitrate and superoxide anion. This reaction has a significantly higher rate constant than the dismutation of superoxide anion. Therefore, peroxynitrate competes favorably for superoxide anion over SOD (Radi, 2018). Figure 1.6 shows the formation of some NOS. Excess ROS and RNS production leads to aberrant signaling as these free radicals attack membrane lipids, structural and enzymatic proteins, and DNA.

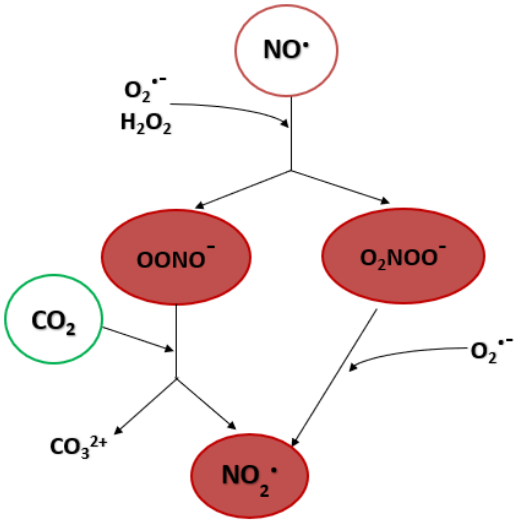

Figure 1.6: Mechanism of generation and interconversion of reactive nitrogen species.
CO_2: carbon dioxide; CO_3^{2+}: carbonate; H_2O_2: hydrogen peroxide; NO•: Nitric oxide; NO_2•: nitrogen dioxide; ONOO−: peroxynitrite; O_2NOO-: peroxynitrate; O_2•−: superoxide anion.

1.1.3 Pharmaceutical Agents for the Management of Cardiovascular Diseases and Their Drawbacks

Angiotensin-converting enzyme inhibitors and Angiotensin receptor blockers are currently used as first-line therapy in managing hypertension, post-myocardial infarction, stroke, chronic renal disease, and diabetes mellitus (Shrimpton et al., 2020). Also, Angiotensin receptor neprilysin inhibitors are reported as effective in managing chronic heart failure (Shrimpton et al., 2020). However, the beneficial actions of these pharmaceutical agents are accompanied by various side effects.

Angiotensin-converting enzyme inhibitors (ACEIs), such as captopril, enalapril, benazepril, etc., competitively inhibit ACE hydrolysis of Ang I to Ang II (Figure 1.7; Shrimpton et al., 2020). While the reduction in Ang II production decreases the stimulation of harmful AT1R, it also has the same effect on protective AT2R. ACEIs-induced inactivation of RAS reduces aldosterone secretion, causing potassium retention, which increases the risk of hyperkalemia. Also, buildup of the vasodilator bradykinin contributes to an anti-hypertensive effect but also triggers refractory dry cough and fatal angioedema, experienced by up to 20% and 0.5%, respectively, of patients taking ACEIs (Shrimpton et al., 2020; Riordan, 2003). As noted earlier, selectively inhibiting ACE's C-domain can bypass the side effects of commercially available ACEIs since bradykinin hydrolysis will not be significantly affected but Ang I hydrolysis will (Georgiadis et al., 2003).

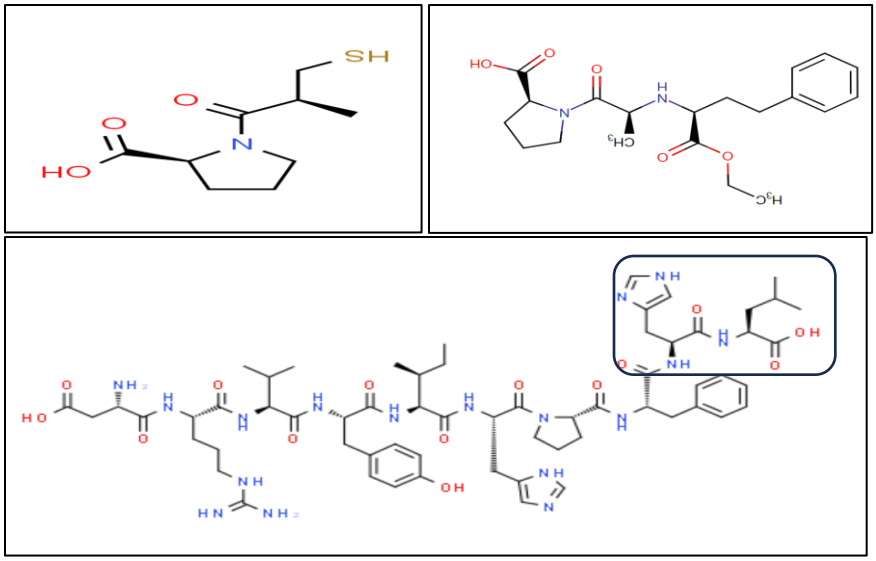

Figure 1.7: Structures of (A) captopril, (B) Enalapril, and (C) Angiotensin I (adapted from Chemspider).

Angiotensin receptor blockers (ARBs), such as valsartan, are structural analogs of Ang II and therefore block Ang II binding to the AT1R (Shrimpton et al., 2020). Since they do not interfere with Ang II production, they bypass the side effects of bradykinin buildup and are preferentially used for patients with symptoms associated with such. However, like ACEIs, their interference with AT1R reduces aldosterone secretion and increases the risk of hyperkalemia (Shrimpton et al., 2020). Figure 1.8 summarizes the mechanism of action of ACEIs and ARBs.

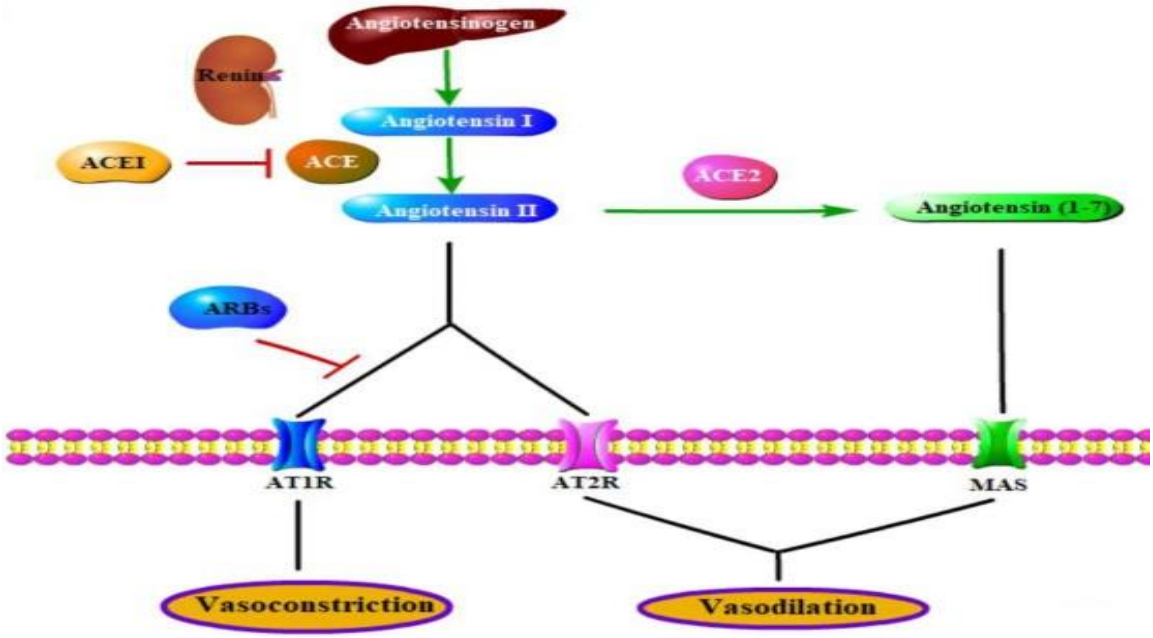

Figure 1.8: Mechanism of action of ACEIs and ARBs (adapted from Gao et al., 2021).
ACE: Angiotensin-converting enzyme; ACE2: Angiotensin-converting enzyme 2; ACEI: ACE inhibitors; ARBs: Angiotensin receptor blockers; AT1R: Angiotensin type 1 receptor; AT2R: Angiotensin type 2 receptor; MAS: Mitochondrial assembly protein.

Neprilysin degrades atrial natriuretic peptides, which counteract the harmful effect of Ang II; neprilysin inhibitors, such as sacubitril, hinder this activity (Shrimpton et al., 2020). However, as neprilysin also breaks down bradykinin, symptoms accompanying bradykinin accumulation were recorded with the administration of neprilysin inhibitors (Shrimpton et al., 2020). A combination of Angiotensin receptors blocker (valsartan) and neprilysin inhibitor (sacubitril) lead to a better-tolerated class of drugs, Angiotensin receptor neprilysin inhibitors (ARNIs) such as sacubitril/valsartan (Shrimpton et al., 2020). ARNIs seem promising in managing patients with cardiovascular diseases, but neprilysin also hydrolyses Ang I to Ang-(1–7), which activates AT2R

(Shrimpton et al., 2020). As AT2R plays cellular protective roles, ARNIs still face some drawbacks. Table 1.2 summarizes the functions of these drug classes and their drawbacks.

Table 1.2: Effects and Drawbacks of Some Cardiovascular Disease Medications.

	MODE OF ACTION	SIDE EFFECT	IMPLICATION
ACEIs	Competitively inhibits ACE	Decrease AT2R stimulation. Reduce aldosterone secretion. Hinder bradykinin breakdown.	Decrease cell protection. Increase risk of hyperkalemia. Dry cough, Angioedema.
ARBs	Blocks AT1R	Reduce aldosterone secretion.	Increase risk of hyperkalemia.
ARNIs	Blocks AT1R and inhibits neprilysin	Decrease AT2R stimulation.	Decrease cell protection.

The various side effects of pharmaceutical agents for managing hypertension and heart diseases, as with many other orthodox medications, highlight the need for all-natural alternatives such as functional foods and nutraceuticals which can be derived from plants and algae.

1.2 Bioprospecting Microalgae for Disease Management

There is rising interest in formulating functional foods, nutraceuticals, and pharmaceuticals from natural substances such as plants and algae. Nutraceuticals are substances considered as food or part of food that provide medical or health benefits such as prevention and treatment of diseases, while functional foods are foods that promote health apart from providing basic nutrition. Although similar, the most distinguishable difference between them is the mode of intake; while nutraceuticals are mainly taken as pills and drugs, functional foods are eaten as foods (Chandra et al., 2022; Zeisel, 1999). While several studies have been targeted isolating bioactive compounds in plants, little effort has been channeled to aquatic organisms. The marine environment hosts countless species that produce interesting bioactive compounds such as polyphenolic compounds, polyunsaturated fatty acids (PUFAs), polysaccharides, essential minerals, vitamins, pigments, enzymes, and peptides (Nieri et al., 2023), and therefore marine's potentials in therapeutics is large and remains largely underexplored.

1.2.1 Diatoms

Algae are a diverse group of eukaryotic organisms (except blue-green algae), ranging in complexity and color (Nieri et al., 2023). They serve as food for almost all aquatic organisms, and their products have been used in the food and pharmaceutical industries. A subgroup of algae, the microalgae, are unicellular organisms which contribute to about 50% of global carbon fixation

and oxygen production (Chapman, 2013). The potential of microalgae for the pharmaceutical and other industries lies in their ability to overproduce desirable metabolites and compounds when grown under manipulated conditions, their relatively cheap media requirements, and ability to grow in different environments, including freshwater and marine, and in environments that are less favorable for the growth of many plants (Sahin et al., 2019; Begum et al., 2016). Although microalgae have gained application in the industries where their high-value compounds have been marketed, they are still underexplored and industrial production is dominated by a few species such as *Arthrospira* spp. (*Spirulina*), *Chlorella* spp., *Dunaliella* spp., for the food market and *Tetraselmis* spp., *Nannochloropsis* spp. and *Phaeodactylum tricornutum* for the feed. A few other species such as *Haematococcus pluvialis* (a dinoflagellate) and *Nitzschia laevis* (a diatom) have also gotten some industrial application in recent years (Nieri et al., 2023).

Diatoms, a subclass of microalgae, are gaining interest in research. Diatoms produce about 20% of global oxygen and are noted for their capacity to mitigate carbon dioxide, thereby contributing to environmental sustainability (Sahin et al., 2019; Ruocco et al., 2018). They also play important roles in the biogeochemical cycles of carbon, nitrogen, phosphorus, and silica (Nieri et al., 2023). They have been documented to accumulate lipids and carotenoids such as fucoxanthin, lutein, astaxanthin, and β-carotene when cultivated under high-light intensity, high salt concentration, and nutrient stress (Minhas et al., 2016). They are a good source of metabolites such as proteins, peptides, polysaccharides, fatty acids, sterols, carotenoids, and polyphenols (Nieri et al., 2023; Figure 1.9).

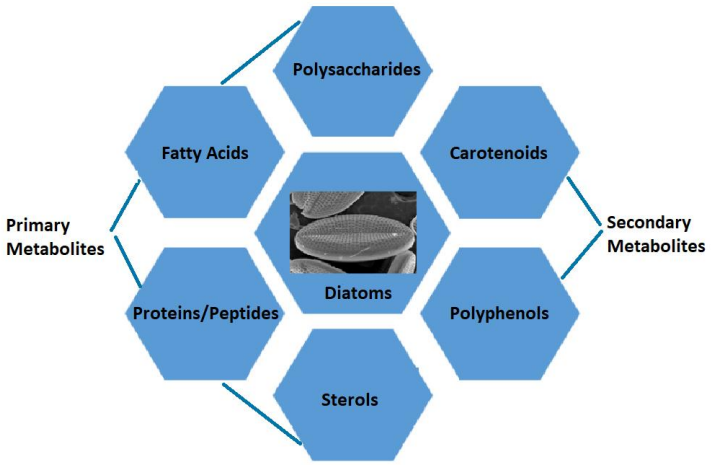

Figure 1.9: Class of metabolites derived from diatoms (adapted from Nieri et al., 2023).

Diatoms are found in different habitats, hence their classification as freshwater or marine species. They can be planktonic (living in the water column) or benthic (attached to a single substratum; Ruocco et al., 2018). The benthic diatoms have been grossly understudied, possibly due to their tiny size (Ruocco et al., 2018). An interesting member of this group, *Nanofrustulum shiloi*, has been reported with exciting bioactivities that makes it promising in the search for natural remedies for cardiovascular diseases.

1.2.2 Nanofrustulum shiloi

Nanofrustulum shiloi (taxonomy ID NCBI: txid210602), originally named *Fragilaria shiloi* by Lee, Reimer & McEnery in 1980, was renamed as such by Round, Hallsteinsen & PaascheIt in 1999. It is a tiny benthic marine diatom (diameter: 2-6 um) of short-chained cells, linked by interlocking marginal spine and having rectangular frustules (Ruocco et al., 2018; Round et al., 1999). Figure 1.10 shows the light microscopy and scanning electron micrograms of *N. shiloi*. It has the taxonomical classification: kingdom Chromista, subkingdom Harosa, infrakingdom Heterokonta, phylum Ochrophyta, subphylum Khakista, class Bacillariophyceae, subclass Bacillariophyceae *incertae sedis*, genus *Nanofrustulum*, and specie *Nanofrustulum shiloi* (Kociolek et al., 2023). The complete *N. shiloi* chloroplast genome has been sequenced by Li et al. (2019), placing it in the araphid 2 clade.

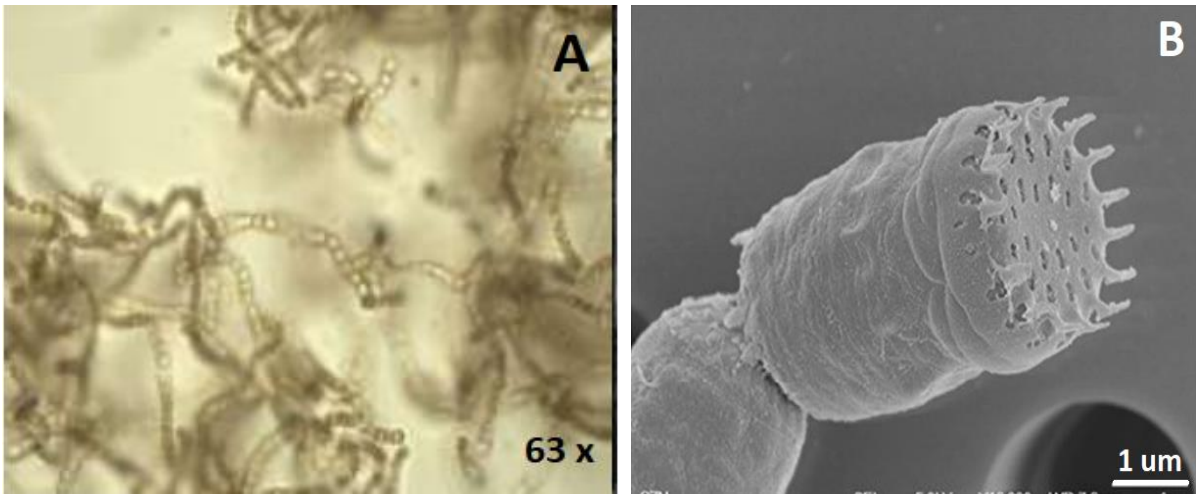

Figure 1.10: Appearance of *N. shiloi;* (A) Light microscopy observation: 63 x magnification and (B) scanning electron micrographs (adapted from Demirel et al., 2020, and Ruocco et al., 2018, respectively).

1.2.2.1 Chemical Composition of *N. shiloi*

Recently, Grubišić et al. (2022) extensively studied the macro and micromolecular composition of *N. shiloi* and other microalgae and their antioxidant and antimicrobial activities. The study reports the macromolecular contents as protein, lipid, and carbohydrate at 56.2, 32.7, and 17.1% DW, respectively. The most abundant carbohydrate is glucose (73.1%), but xylose, glucuronic acid, and fucose were also found in significant levels. As with other diatoms, the primary fatty acids were palmitic (C16:0) and palmitoleic (C16:1) acids, making up 70% of fatty acids. In addition, polyunsaturated fatty acids (PUFAs), including arachidonic acid (ARA, C20:4; 9.29%), eicosapentaenoic acid (EPA, C20:5; 6.79%), and alpha-linolenic acid (ALA, C18:2; 1.88%) were found. The lipid class is reported as mainly neutral lipids such as free fatty acids, mono-, di-, and tri-acyl glycerols, sterols and steryl esters, and less of polar lipids such as phosphatidylcholine, phosphatidyl ethanolamine, etc.

High protein content gives *N. shiloi* some potential for food and feed production, and its lipid content makes it a valuable feedstock for biodiesel production. *N. shiloi* has been employed in the bioproduction of EPA with high yield (Bárcenas-Pérez et al., 2022). Omega fatty acids (such as EPA) are considered essential fatty acids as they cannot be made by the human body but are necessary for health maintenance, infant development, and reduction in the risk of chronic and heart diseases (Fleith and Clandinin, 2005).

1.2.2.2 Bioactive Compounds in *N. shiloi*

N. shiloi also contains some interesting pigments and antioxidants that make it promising in the pharmaceutical, nutraceutical, and cosmetic industry. Fucoxanthin, beta-carotene, and chlorophyll-*a* were found by Grubišić et al. (2022) at 39.5, 0.36, and 131 mg/100 g, respectively, in *N. shiloi.* Fucoxanthin, the brown-colored xanthophyll that gives brown macroalgae their characteristic color, has been reported to possess antioxidant and anti-inflammatory activities, apart from anti-carcinogenic, anti-obesity, anti-diabetic, neuroprotective, and anti-angiogenic activities (Sahin et al., 2019). Antioxidants such as flavonoids (0.38 mg quercetin/g DW), phenols (11.7 mg DAE/g DW), and carotenoids (39.9 mg/100 g DW) were also found in *N. shiloi*, with DPPH free radical scavenging activity of 36.6 umol TE/g (Grubišić et al., 2022).

Further, Ruocco et al. (2018; 2020) found some toxigenic oxylipins in *N. shiloi*. Oxylipins are oxygenated fatty acid derivatives, including polyunsaturated aldehydes (PUA), which are cytotoxic to microalgal grazers (Lauritano et al., 2016) and have been found to specifically activate apoptosis in human cancer cell lines without affecting normal cells (Sansone et al., 2014). The PUA content of *N. shiloi* was found to be mostly composed of lipoxygenase (LOX) products of C16 polyunsaturated fatty acids, palmitoleic acid, and EPA, and include hydroxyeicosapentaenoic acids (HEPEs), hydroxy-epoxy-eicosatetraenoic acids (HepETEs), hydroxyhexadecenoic acids (HHMEs), and ketohexadecenoic acids (KHMEs; Ruocco et al., 2018; 2020). Some peaks not correlated with known oxylipins found in diatoms were also observed, indicating that there may be interesting unidentified *N. shiloi* cytotoxic compounds.

1.2.2.3 Cultivation of *N. shiloi*

As with other microalgae and benthic marine diatoms, several physical and chemical parameters affect the growth of *N. shiloi*. These parameters include light intensity, pH, temperature, mixing, CO_2, dissolved oxygen, nutrient supply, etc. (Demirel et al., 2020). Cultivation can be done in a closed or open system, each with its advantages and drawbacks. Varying the culture conditions, such as cultivation system, physical and chemical cultivation parameters, etc., influences the growth and accumulation of specific desired metabolites, and the optimal conditions appear to be specie dependent. For example, Demirel et al. (2020) reported an increased growth rate and lipid composition of *N. shiloi* when cultivated in photobioreactors with a combination of aeration and stirring than those grown with one or none of the parameters. Also, Sahin et al. (2019) found that *N. shiloi* accumulated fucoxanthin, EPA, and total lipids when cultured under nitrogen- and iron-enriched conditions, which is interesting since the same work reported differing results for another diatom specie, *Nitzschia* sp., cultivated under the same conditions. A combination of the studied and other parameters might lead to an even greater accumulation of the studied metabolites and others.

1.3 Methods for bioactivity assessment

Antioxidant Assays

The determination of antioxidant activity of plant and food constituents involves the use of different instruments. Straight chemical assays can be classified into two groups: assays

associated with lipid peroxidation and assays associated with hydrogen or electron transfer or radical scavenging (Moon and Shibamoto, 2009). Assays associated with electron or hydrogen transfer, or radical scavenging have been used in many studies involving food and plant samples possibly because they are simple and highly sensitive (Moon and Shibamoto, 2009). By definition, reduction involves the transfer of either a hydrogen atom or an electron. To capture all compounds that display antioxidant activities by any of these two mechanisms, this study employed two antioxidant assays, the 2,2-Diphenyl-1-picrylhydrazyl (DPPH) free radical scavenging assay which involves hydrogen atom transfer, and the ferric reducing antioxidant power (FRAP) assay which involves a single electron transfer mechanism.

ACE Inhibition Assay

Several methods are used to measure ACE-inhibitory activity, many of which are modifications of the method initially described by Cushman and Cheung (1971). However, the fluorimetry assay (used in this study) described by Sentandreu and Toldrá (2006) is simple, can be used for large number of samples in a relatively small time, and eliminates some extraction steps which could add to measurement uncertainty. This method is based on the principle of hydrolysis of the tripeptide o-aminobenzoylglycyl-p-nitro-L-phenylalanyl-L-proline (Abz-Gly-Phe(NO2)-Pro) by ACE to give the fluorescent product o-aminobenzoylglycine (Abz-Gly) whose excitation and emission wavelengths are 355 and 405 nm, respectively (Sentandreu and Toldrá, 2006). Substances that inhibit ACE lead to less generation of the reaction product. Being fluorometric, this method has the advantage of not suffering the interference of the strong color of microalgal extracts, a common problem of colorimetric assays.

Reporter Gene Assay for the assessment of anti-inflammatory activity

High-throughput screening (HTS) reporter gene assays were used to measure the expression of pro-inflammatory cytokines (TNFα and IL-6) and the activity of NF-κB in this study. The reporter gene technology is based on changes in gene expression by transient signals such as cytokines interacting with receptors in or outside the cell. Such interaction can lead to activation of transcription factors, such as phosphorylation, and stimulate their interaction with response factors in the gene (Naylor, 1999). Response factors are cis-regulatory genetic sequences responsible for alteration of gene expression and regulation in host cells. By attaching specific

response elements to reporter genes (genes that code for a protein with easily measurable phenotype such as fluorescense, luminescence, etc.), the effects of the signals can be measured by the alterations of the expression of the reporter gene. The promoter-reporter gene vector is transfected into a cell where the expression of the reporter can be monitored (Naylor, 1999).

Several reporter genes from different sources have been developed, each with their advantages and drawbacks. These include the Chloramphenicol acetyltransferase (CAT; bacterial), beta-Galactosidase (b-Gal; bacterial), Luciferase (Luc; firefly and bacterial), Alkaline phosphatase (human placental), and the Green fluorescent protein (GFP; jellyfish). The Luc firefly has the advantage of having a broad dynamic range and high specificity as it has no endogenous activity while the Luc bacterial is suited for measuring prokaryotic gene transcription (Naylor, 1999). A combination of these two methods plus HTS increases the specificity of results of this study.

1.4 Non-targeted Metabolomics

Metabolomics constitutes the techniques and methods employed to study the metabolome, which consist of low-molecular-weight metabolites, typically less than 1500 Da, present in materials such as biological tissues. These include the precursors, intermediates, and products of biological pathways, and therefore provides a fingerprint that could be used to elucidate such pathways (Viant et al., 2017). The two main techniques used to generate metabolomic data are nuclear magnetic resonance (NMR) and mass spectrometry (MS; Fuhrer and Zamboni, 2015). Metabolomic studies can be 'targeted' hypothesis-driven experiments that measure predefined sets of metabolites with high precision and accuracy or 'non-targeted' analysis of the entire metabolomic profile of a sample without prior specific hypothesis (Alonso et al, 2015). Also, there are different levels of metabolomic studies. Level 1, metabolite identification, involves elucidating the structure of metabolites using such tools as fractionation, high resolution accurate mass MS, and 1D and 2D NMR and requires exhaustive analytical validation. On the other hand, putative annotation of compounds and characterization of compound classes (levels 2 and 3) require less rigorous validation (Sumner et al., 2007). In the present work, liquid chromatography-mass spectrometry (LC-MS)-detected peaks were screened against online libraries of identified and annotated compounds.

Due to their complexity, biological materials' metabolomic analyses involve sample preparation and fractionation, before NMR or MS analysis. General sample preparation steps include drying, milling, extraction, filtration, and purification. Lyophilization is a method of choice for drying biological materials as it avoids exposure to extreme temperatures which may denature biological compounds, and bypasses prolonged exposure to oxygen which can lead to oxidation. Several techniques have been employed in extraction of solid biological materials, including, headspace microextraction, Soxhlet, pressurized fluid extraction (PFE), dispersive solid phase extraction (dSPE), supercritical fluid extraction, Quick-Easy-Cheap-Effective-Rugged-Safe (QuEChERS), etc., each with its advantages and disadvantages. The energized dispersive guided extraction (EDGE) by CEM (CEM Corporation, 2017), used in this study, is an automated system that combines dSPE and PFE, and is claimed to be 'faster than Soxhlet, more automated than QuEChERS, and simpler than other solvent extraction systems' (CEM Corporation, 2017). In this method, pressure generated by heat forces the extracting solvent to expand and disperse into the sample which causes the analytes to partition into the solvent. This method combines extraction, filtration, and cooling in one step, thereby reducing sample losses and chances of contamination by multiple sample preparation steps. It is applied to a wide range of samples including environmental, food, pharmaceutical, and polymer samples (CEM Corporation, 2017), and has been reported to be 4.5 times faster than PFE in extracting pesticides from leaves (Kinross et al., 2020).

High performance liquid chromatography (HPLC) is an efficient method used to analyze the components of food, drug, and plant samples. This technique involves the partitioning of the sample between two phases, the mobile and stationary phases. Analytes elute at different times based on their affinities with the mobile phase; the higher the affinity, the faster the elution. HPLC could be analytical or preparative. The purpose of analytical HPLC is to qualitatively or quantitatively measure the analytes in a sample, while the eluent goes to waste. On the other hand, preparative HPLC fractionates the components of the sample, collecting the fractionated eluent in different vials. Also, analytical columns are of smaller dimensions than preparative columns. Fractions can be tested for bioactivity with bioactive fractions further subjected to MS analysis for metabolite identification, annotation, or screening.

Mass spectrometry is a high throughput technique used to determine the molecular fingerprint of metabolites by analyzing their mass to charge ratio (m/z). It allows the identification/annotation and structure elucidation of unknown metabolites, or the screening of the peaks in spectra by comparison to a vast mass spectra library. Unlike gas chromatography (GC)-MS, LC-MS is not limited to analysis of volatile and heat-stable compounds, and therefore identifies a broader spectrum of metabolites in biological samples (Viant et al., 2017). Analysis of such samples using LC-MS required suitable ionization sources such as electrospray ionization (ESI) and mass analyzers such as orbitrap which were employed in this study.

1.5 Justification of study

Despite advances in medication, the agents used for first-line treatment of some cardiovascular diseases and hypertension present interesting drawbacks and side effects. In a study to valorize three diatom species using three different extracting solvents (carried out in our research group), Kautzmann (2022; unpublished) reported exciting antioxidant, ACE inhibitory, and COX-2 inhibitory bioactivity of *N.shiloi*, an understudied but promising benthic marine diatom. Specifically, 58.93 and 56.97% ACE inhibitory activity were reported for its ethanol and ethyl acetate extracts, respectively. The study also tentatively identified some known antioxidant compounds in *N. shiloi*. However, the latter part of this study was conducted using GC-MS, which is limited to only volatile and heat-stable compounds. From our review of literature, no study has attempted to identify the full range of bioactive compounds in *N. shiloi* using LC-MS. Hence, it is necessary to validate the bioactivities reported by Kautzmann and attempt identification of a broader spectrum of compounds responsible for them. Dissecting this promising algae's components could provide fresh insights into developing all-natural products for the treatment of hypertension, cardiovascular inflammation, and some cardiovascular diseases for which ACE is implicated in their pathogenesis. These proposed natural alternatives might help reduce the side effects of the synthetic drugs used in treating these diseases, besides reducing the pharmaceutical footprints of unmetabolized medicines in the environment, thereby promoting environmental sustainability in line with the United Nations' sustainable development goals.

1.6 Aim and Objectives

This study aims to identify bioactive compound(s) that might be responsible for ACE inhibition and decrease of pro-inflammatory cytokines in ethanol and ethyl acetate extracts of *N. shiloi* and determine their structure(s). To achieve this, the following specific objectives were set:

- To confirm the inhibitory activity of ethanol and ethyl acetate extracts of *N. shiloi*, and
- To identify bioactive metabolites possibly responsible for the bioactivities determined.

2 MATERIALS AND METHODS

2.1 Materials

2.1.1 Chemicals

Laboratory reagent grade ethanol (>= 99%; Fisher Chemicals, Portugal) and analytical reagent grade ethyl acetate (>=99.8%) were used for microalgal biomass extraction. Analytical reagent grade dimethyl sulfoxide (DMSO; >= 99.8%) was used in the reconstitution and dilution of the extracts and fractions to use in the biological assays. For HPLC analysis, HPLC gradient grade acetonitrile (ACN; >=99,9%; Fisher Chemicals, Portugal) and milli-Q water obtained through Milli-Q® Advantage A10 Ultrapure Water Purification System (Merck, Germany) were used. ACN was also used for HPLC sample reconstitution. For DPPH assay, 2,2-diphenyl-1-picrylhydrazyl (DPPH) and pure methanol (Valente & Ribeiro, Portugal) were used. For ferricyanide reducing power assay, iron (III) chloride hexahydrate (Valente & Ribeiro, Portugal), 98% pure potassium ferricyanide (Arcos Organics, Spain), trichloroacetic acid (TCA), and distilled water by Elix/Gradient Water Purification System (Merck, Germany) were used. Gallic acid (Acros Organics, USA) was used as positive control for both assays. For angiotensin converting enzyme (ACE) inhibitory assay, angiotensin converting enzyme from rabbit-lung (cat. No. A-6778) and the positive control captopril (≥98%) were obtained from Sigma–Aldrich (Munich, Germany). O-aminobenzoylglycyl-p-nitro-L-phenylalanyl-L-proline (Abz-Gly-Phe(NO2)-Pro-OH; Bachem, cat. No. M-1100) was used as substrate. Other reagents used for this assay included zinc chloride (Labkem, Spain), sodium chloride (Acros Organics, USA), and Tris (Amresco, USA).

2.2 Methods

2.2.1 Biomass Preparation

N. shiloi biomass was obtained as deep-frozen paste from Necton S.A., Olhão, Algarve, Portugal, where it was produced during the summer in outdoor tubular photobioreactors, with Nutribloom® Plus (NB+; 2 mM) and silica (0.11 mM) as nutrients. The biomass was lyophilized with Christ Alpha 1-2 LDplus (Germany) freeze dryer. It was ground to fine powder in a planetary ball mill PM 100 (Retsch GmbH, Germany) with 5 stainless steel mill balls of 20 mm diameter each. This allowed breaking of the cell walls to enable the release of cell components. The grinding was done at room temperature and 450 rpm speed for 5 min. A 30 sec cooling interval

was allowed after each minute to dissipate heat and avoid temperature upshifts which could degrade heat labile compounds.

2.2.2 Biomass Extraction

The disrupted biomass was extracted using an energized dispersive guided extractor (EDGE) by CEM (CEM Corporation, 2017). Absolute ethanol (99.9%) and ethyl acetate (99.8%) were used separately as solvents. These two solvents of different polarities were chosen to enable extraction of a wide range of compounds and because they are food grade solvents with less toxicity than most organic solvents. The extraction conditions were set at 10 min per cycle and 30 °C, which is the least temperature possible allowed by EDGE, to avoid degradation of heat labile compounds. For each extraction, 1 g of biomass was mixed with 1 g of inert sand and extracted with 20 ml of solvent, with three extraction cycles, making a total of 60 ml extract. The three extracts were combined and evaporated under a gentle nitrogen stream using Techne sample Concentrator (USA). Enough biomass was extracted to obtain a sufficient amount of extract to perform all the experiments. Ethanol and ethyl acetate extracts were reconstituted in absolute ethanol and acetonitrile, respectively, and filtered with a 0.45-µm nylon filter before each use.

2.2.3 High Performance Liquid Chromatography

To reduce extract and solvent wastage, the elution program was optimized in an analytical column until a good peak separation of most of the peaks in the chromatogram was obtained. Both photo diode array detector (DAD) and the evaporative light scattering detector (ELSD) were used to allow the observation of a wide range of compounds in the sample, since ELSD can detect compounds that do not absorb light and hence do not give a signal in the DAD. Increasing the gain of the ELSD amplifies the peaks, making them more observable. The result of this analysis was used to optimize the parameters for the preparative HPLC column. The adapted elution program, flow rate and injection volume for the preparative HPLC were determined by the Shimadzu system software LabSolution version LCGC ensuring that the retention time of the eluted compounds is the same in the preparative column as in the analytical column. The chromatogram of this analysis was used to set the fraction collection program. Table 2.1 shows a list of the final chromatographic conditions employed with the analytical and preparative columns for the two extracting solvents.

Preparative HPLC fractionation yielded 37 fractions each for ethanol and ethyl acetate extracts. The fractionation program was prepared to collect pure or close to pure compounds in different fractions, or on a time/volume-based way when peak resolution was not optimal, or no peaks were observed in the chromatogram. Whenever fractions had very little volume and negligible weight upon drying, they were pooled. For the ethanol extract, the 37 fractions were pooled into 21 fractions for reporter gene assays and 14 fractions for bioactivities and LC-MS. For the ethyl acetate extract, the 37 fractions were pooled into 13 fractions for all assays.

For all analyses, the pressure was allowed to stabilize before sample injection as this will affect the retention times. Also, the injector was purged, and the column cleaned between injections to remove all residual materials. The mobile phases were filtered and degassed while filtering under vacuum to remove particles and gases which could damage the column. Besides this, the HPLC system is equipped with a solvent degassing system. The chromatograms were analyzed using OpenChrome 1.5.0. from Lablicate GmbH.

The fractions were dried under gentle nitrogen flow using the Techne Sample Concentrator. To facilitate drying, the fractions were placed in a block digester set at 20 °C. The dried fractions were stored in amber vials at -20 °C until use for bioactivity assays. These steps were taken to prevent exposure to oxygen, light, and heat which could lead to oxidation, and photo or heat degradation of some components.

Table 2.1: HPLC Conditions for Analytical and Preparative Columns

Parameters	*Analytical Column: Ethanol*	*Analytical Column: Ethyl Acetate*	*Preparative Column: Ethanol*	*Preparative Column: Ethyl Acetate*
HPLC model	LC-20AP (Shimadzu)	LC-20AP (Shimadzu)	LC-20AP (Shimadzu)	LC-20AP (Shimadzu)
Column type	Luna 5u C18(2)	Luna 5u C18(2)	Luna 5u C18(2)	Luna 5u C18(2)
Column dimensions	250 x 4.60 mm	250 x 4.60 mm	250 x 10 mm	250 x 10 mm
Phase type	Reverse phase	Reverse phase	Reverse phase	Reverse phase
Mobile phase	(A) Milli-Q water (B) Acetonitrile	(A) Milli-Q water (B) Acetonitrile	(A) Milli-Q water (B) Acetonitrile	(A) Milli-Q water (B) Acetonitrile
Gradient elution program	Initial 65% B; 30 min, 100% B; 55 min, 100% B; 60 min, 65% B	Initial 60% B; 35 min, 100% B; 55 min, 100% B; 60 min, 60% B	Initial 65% B; 30 min, 100% B; 55 min, 100% B; 60 min, 65% B	Initial 60% B; 35 min, 100% B; 55 min, 100% B; 60 min, 60% B
Sample Concentration	50 mg/ml	50 mg/ml	200 mg/ml	160 mg/ml
Injection volume	50 µl	50 µl	200 µl	300 µl
Flow rate	1 ml/min	1 ml/min	4.73 ml/min	4.73 ml/min
Recorded back pressure	10.1 MPa	10.1 MPa	15.8 MPa	17.4 MPa
Oven temperature	25 °C	25 °C	25 °C	25 °C
Detector	SPD-M40 DAD LTII low temperature ELSD (gain=4)	SPD-M40 DAD LTII low temperature ELSD (gain=4)	SPD-M40 DAD	SPD-M40 DAD LTII low temperature ELSD (gain=8)

2.2.4 Liquid Chromatography Mass Spectrometry

Liquid chromatography mass spectrometry (LC-MS) analysis was performed on the fractions obtained with the preparative HPLC, that were deemed active, to identify possible bioactive compounds.

Chromatographic separation was performed on a Thermo Scientific ultimate 3000 UHPLC. The ionization source and mass analyzer were Electrospray Ionization and Orbitrap mass spectrometer, respectively. Fragmentation spectra were obtained by running the system in data dependent mode using dynamic exclusion, in negative and positive polarities. LC-MS profiles were analyzed using XCalibur 4.1.50 from Thermo Scientific Inc. Details of the LC-MS parameter values are provided in Table 2.2.

Table 2.2: Conditions for UHPLC

Parameters	***Value***
UHPLC model	Thermo Scientific ultimate 3000 UHPLC
Column type	Thermo Scientific Accucore RP-18
Column dimensions	2.1 × 100 mm, 2.6 µm
Mobile phase	(A) Water (with 0.1% of formic acid) (B) Acetonitrile (with 0.1% of formic acid)
Gradient Elution program	Initial 0% B; 2 min, 0% B; 13 min, 30% B; 16 min, 100% B, 20 min, 100% B; 21 min, 0% B; 25 min, 0% B
Injection volume	10 µl
Flow rate	0.3 ml/min
Ionization source	Electrospray Ionization (HESI-II)
Spray voltages	3.7 kV (positive polarity) and 4.0 kV (negative polarity)
Sheath gas	40 arbitrary units
Auxiliary gas	10 arbitrary units
Heater temperature	300 °C
Capillary temperature	350 °C
S-Lenses RF level	64.9 %
Scan range	100-1000 m/z
Mass analyzer	Orbitrap Elite (Thermo Scientific)

2.2.5 Bioactivity Assays

Three assays in this work, DPPH free radical scavenging, ferric reducing antioxidant power, and ACE inhibition, were performed on the crude *N. shiloi* extracts (ethanol and ethyl acetate) and their fractions, henceforth collectively referred to as samples, all in 96 well plates. A stock of 20 mg/ml in DMSO of the samples were prepared, and a dilution of 1 mg/ml was prepared each day as working sample. These were analyzed in three replicates for each sample, plus a

color control for DPPH free radical scavenging and ferric reducing antioxidant power. For each assay, three tests were performed on three consecutive days to determine intermediate precision. Due to low extract availability, less daily replicates were performed for some fractions of the ethanol extract.

2.2.5.1 DPPH Free Radical Scavenging Assay

The DPPH free radical scavenging assay has been used in studies involving algae (Kuda et al., 2006) as in other food and plant samples. It is based on the principle of reduction by hydrogen atom transfer (HAT). In theory, a molecule can reduce a radical by donating a hydrogen atom, thereby acting as antioxidant. When the purple-colored 2,2-Diphenyl-1-picrylhydrazyl radical (DPPH•) gains a hydrogen atom, it is reduced to the stable, yellow-colored DPPH. The disappearance of DPPH• is proportional to the amount of hydrogen atoms gained, that is the scavenging activity of the sample. This is conveniently monitored by UV-vis spectrometry at 517 nm, although electron spin resonance spectroscopy and nuclear magnetic resonance monitoring have also been used (Calliste et al., 2001). The result is standardized using the Trolox equivalent (TE) unit. Trolox is the commercial water-soluble vitamin E. Gallic acid can equally be used. The antioxidant activity is expressed in terms of micromoles of equivalents of Trolox per 100 g of sample (TE/100 g). The result can also be reported as half maximal effect concentration (EC_{50}) which is the amount of the antioxidant sample required to reduce the initial DPPH• concentration by half (Brand-Williams et al., 1995). Figure 2.1 depicts the DPPH• scavenging reaction mechanism.

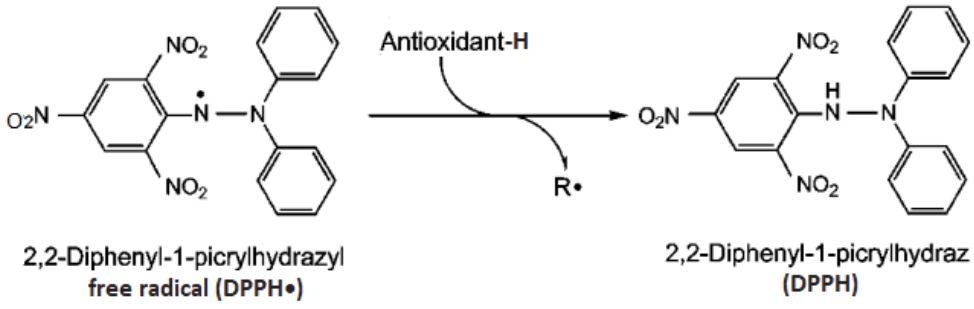

Figure 2.1: DPPH free radical scavenging reaction mechanism (adapted from Moon and Shibamoto, 2009).

In the present work, 120 µM DPPH radical in methanol was used as the hydrogen acceptor. The samples and positive control (Gallic acid) were tested at 1 mg/ml in DMSO, while 100%

DMSO was used as negative control. For each sample, positive control, and negative control, 22 µl were added in triplicates plus a color control to a 96-well plate. To the color controls, 200 µl methanol was added, while 200 µl of the prepared DPPH radical solution was added to the replicates. The plate was incubated in the dark for 30 min at room temperature, and the absorbance read in a spectrophotometer plate reader Synergy 4 from Biotek (Agilent, USA) at 517 nm. The results were calculated as % DPPH radical scavenging compared to the negative control using the following equation:

$$\% \text{ DPPH scavenging} = \frac{\text{Abs Neg. Control} - \text{Abs Sample}}{\text{Abs Neg. Control}} \times 100$$

2.2.5.2 Ferric Reducing Power (FRAP) Assay

The reducing power was assayed using a slightly modified version of the method described by Megías et al. (2006) which is a modification of the original method by Oyaizu (1986). This method is based on a chain of single electron transfer (SET) reactions in which ferricyanide is reduced to ferrocyanide, which in turn reduces ferric chloride to form Perl's Prussian blue, a ferric-ferrous complex which absorbs at 700 nm. The reagents used include 1% ferricyanide, 0.1% ferric chloride, and 10% trichloroacetic acid (TCA), all in distilled water. In this modification of Megías's method, 0.2M phosphate buffer (pH 6.6) was replaced with distilled water. The method was verified using gallic acid, the positive control used in this work, over a range of concentrations (2 – 2.38×10^{-07} mg/ml) to calculate the EC_{50}.

In the present work, samples, and positive control (gallic acid) were tested at 1 mg/ml in DMSO. Briefly, 50 µl of the samples, negative control (100% DMSO), and a color control were placed in their respective wells in triplicate. Distilled water (160 µl) was added to the color control, while 50 µl distilled water and 50 µl ferricyanide solution were added to the replicates. The plate was shaken gently to mix, then incubated for 20 min at 50 °C. After incubation, 50 µl of TCA and 10 µl of the ferric chloride solutions were added. The plate was incubated for 10 min at 50 °C and read in a spectrophotometer plate reader Synergy 4 from Biotek (Agilent, USA) at 700 nm. The results were calculated as a percentage of the reducing power obtained for the positive control, using the following equation:

$$\% \text{ FRAP} = \frac{\text{Abs Pos. Control} - \text{Abs Sample}}{\text{Abs Pos. Control}} \times 100$$

2.2.5.3 ACE-inhibitory Activity Assay

The fluorometric method used in this study is based on the theory that ACE inhibitors will decrease the activity of ACE in hydrolyzing the tripeptide o-aminobenzoylglycyl-p-nitro-L-phenylalanyl-L-proline (Abz-Gly-Phe(NO_2)-Pro) to the dipeptide o-aminobenzoylglycine (Abz-Gly). This fluorescent product has excitation and emission wavelengths of 355 and 405 nm, respectively (Sentandreu and Toldrá, 2006).

The assay materials include three buffers stored at 4 °C until use: buffer A (300 mM Tris-base with 2 µM $ZnCl_2$), pH 8.3; buffer B (150 mM Tris-base), pH 8.3; and buffer C (150 mM Tris-base pH 8,3 with 1.125 M NaCl). Adjustment of the pH of the buffers was done by dropwise addition of 1M HCl in a calibrated pH meter. The assay was performed in a dark 96-well plate to avoid interference from light. The enzyme solution used was 18 mU/ml ACE from rabbit-lung prepared with buffer A; the substrate solution was 0.45 mM Abz-Gly-Phe(NO_2)-Pro-OH prepared in buffer C, the positive control was 1 uM captopril prepared with buffer B, while buffer B was used as negative control. The working solutions were prepared daily.

In the present work, aliquots of 50 µl each of the samples, positive control (1 mg/ml in buffer B), and negative control (buffer B) were placed in their respective wells in triplicate. Aliquots of 50 µl ACE solution were added to each well with gentle shake to avoid cross contamination. The plate and substrate solution were incubated for 10 min at 37 °C. Aliquots of 200 µl of substrate solution were added to each well rapidly. The emission was read at 405 nm after excitation at 355 nm, in a plate reader Synergy 4 from Biotek (Agilent, USA). The readings were done every 5 min for 40 min starting at time 0 min, and the results were calculated as the slope of absorbance of the samples with time compared to that of the negative control, using the following equation:

$$\% \text{ ACE Inhibition} = 100 - \left(\frac{\text{Slope of Abs Sample} \times 100}{\text{Slope of Abs Neg. Control}}\right)$$

2.2.6 Cell-based anti-inflammatory activity

These assays were performed by a partner of the Algae4IBD project, in the CZ-Openscreen platform in Check Republic (https://www.openscreen.cz/).

The cell-based inflammatory activity was performed using cellular reporter assays monitoring the expression of human and mouse pro-inflammatory cytokines TNF-α and IL-6 and the activity of NFκB. The assays are based on the reporter vectors carrying isolated promoter

sequences corresponding to roughly 1kb region upstream of the coding sequence of the human and mouse TNF-α and IL6 and a response element for the binding of NFκB transcription factor. These reporters use two unrelated luciferase enzymes: nanoLuc and firefly luciferase, which increase the specificity of results. The reporter assays measure the activity of the cytokine promoters after stimulation with lipopolysaccharides (LPS). Reporter vectors were stably integrated in the genome of human monocytic cell line THP-1 and murine macrophage cell line RAW264.7 and clonal lines providing highest sensitivity and reproducibility were isolated. The assays were adapted to the robotic high throughput screening (HTS) in microtiter plates. Cell viability assays were also performed after 72h incubation with the extracts by determining the level of intracellular ATP using the CellTiter-Glo 2.0 luminescence assay (Promega).

These assays were applied to the ethanol and ethyl acetate extracts as well as the fractions prepared from these extracts. Each sample was tested at concentrations of 100 µg/mL, 10 µg/mL, and 1 µg/mL, with 4 replicates at each concentration. The cells were incubated with the extracts/fractions for 3 hours. Next, LPS pre-diluted in growth media was added to the cells to a final concentration of 10 ng/ml and 100 ng/ml for RAW264.7 and THP-1-reporter assays, respectively. After an additional 5 hours of incubation, luciferase activity was assessed using either the Nano-Glo® Dual-Luciferase® Reporter Assay System or the Nano-Glo® Luciferase Assay System (Promega), following the manufacturer's protocol. The data were normalized to percent activity, where 100% corresponds to the mean signal from the LPS-induced samples, and 0% corresponds to the mean signal from samples with no LPS treatment (background): %activity = 100*((LPS activity - background)/background). The median from four replicate measurements were reported. Dexamethasone is then used as a reference compound (regular sample). The significance is calculated using one-way ANOVA and Dunnett's multiple comparisons test against controls without LPS.

2.2.7 Statistical Analyses

The bioassay results were analyzed using Microsoft excel. One way ANOVA was performed using statistical package for social sciences (SPSS) version 29.0.0 from IBM and results were considered significantly different at $p < 0.05$, 0.01, and 0.001.

3 RESULTS AND DISCUSSION

This study investigated the potential of *N. shiloi* for hypertension and cardiovascular inflammation management using different assays. *N. shiloi* biomass was separately extracted with ethanol and ethyl acetate and fractionated in a preparative HPLC. All samples (extracts and fractions) were tested for bioactivity using three assays: DPPH free radical scavenging, ferric reducing antioxidant power, and ACE inhibition. The inhibitory potential of the samples on pro-inflammatory cytokines production and their cytotoxicity were assayed using HTS reporter gene assay. Promising (active) fractions were subjected to LC-MS analysis and metabolites were identified through online library search. The results of these analyses, their significance, and plausible implications are discussed below.

3.1 Extraction Yield

The yields recorded for ethanol and ethyl acetate extracts were 13.3 and 11.4% DW, respectively. This result is almost double of that obtained by Kautzmann (2021; unpublished), although the ratio of ethanol to ethyl acetate extracts are almost identical. The higher yield with ethanol, which is more polar, may be due to extraction of polar components such as carbohydrates and proteins. Ethyl acetate must have extracted more non-polar compounds which displayed more bioactivity, as discussed later. Kautzmann (2021) reported these extracts as active and so, this work, began by producing fractions to identify the compounds possibly responsible for the observed activities.

3.2 HPLC Results

3.2.1 HPLC with Analytical Column

HPLC with analytical column using the DAD and ELSD detectors was used to set the conditions for the preparative HPLC. The DAD captures compounds by their characteristic wavelengths of absorption, and therefore can only capture compounds that absorb. Knowing the wavelength at which a compound absorbs maximally can help in identifying (or at least predicting) the compound, and this can be achieved with a 3D chromatogram (in which the length of the chromatogram is the retention time, the height is the wavelength, and colors indicate intensity).

On the other hand, the ELSD captures a wider range of compounds, even those that do not absorb. It works in a similar way to electrospray ionization (used as MS ionization source in this work). It nebulizes the eluent into aerosols, evaporates the solvent using a carrier gas, and

passes light across the tube holding the analytes causing them to scatter the light irrespective of whether they absorb or not. The degree of light scattering is detected but no information about the type of analyte present is given (Waters Corporation, 2006).

Figures 3.1 and 3.2 show the chromatograms from analytical column HPLC for ethanol and ethyl acetate extracts, respectively. Since the mobile phase became less polar with time (from 65 to 100% acetonitrile [ethanol], and 60 to 100% acetonitrile [ethyl acetate]), peaks at the start of the elution correspond to more polar compounds while those toward the end of the chromatogram are less polar ones. The peaks appeared slightly earlier in the DAD detector than the ELSD since, in the HPLC setup, the eluent passed through the DAD before getting to the ELSD.

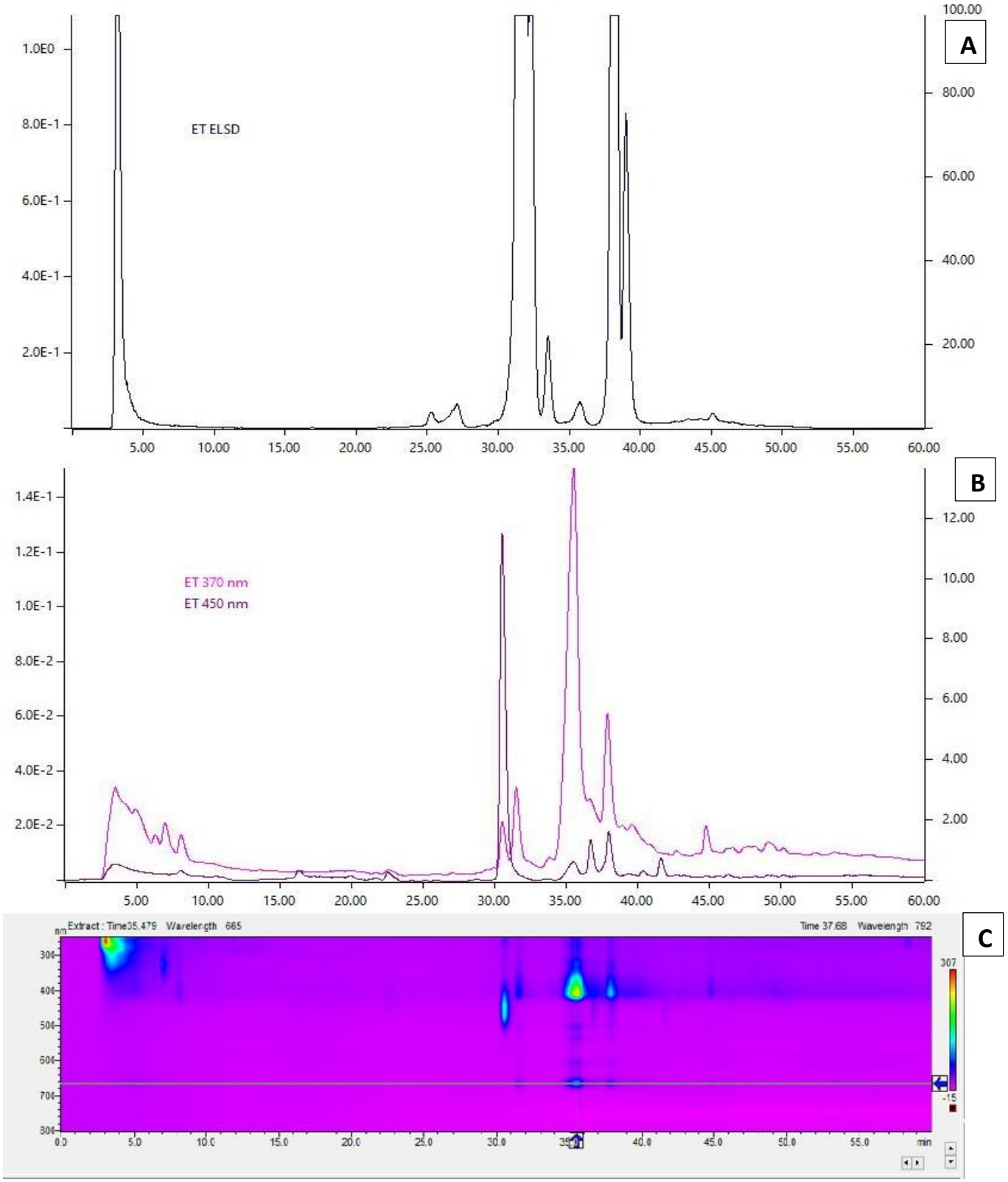

Figure 3.1**:** Chromatograms of ethanol extract ran on analytical HPLC column: (A) signal of the ELSD; gain=4, (B) Molecular spectrophotometric absorption at 370 and 450 nm, and (C) 3D signal given by the DAD.

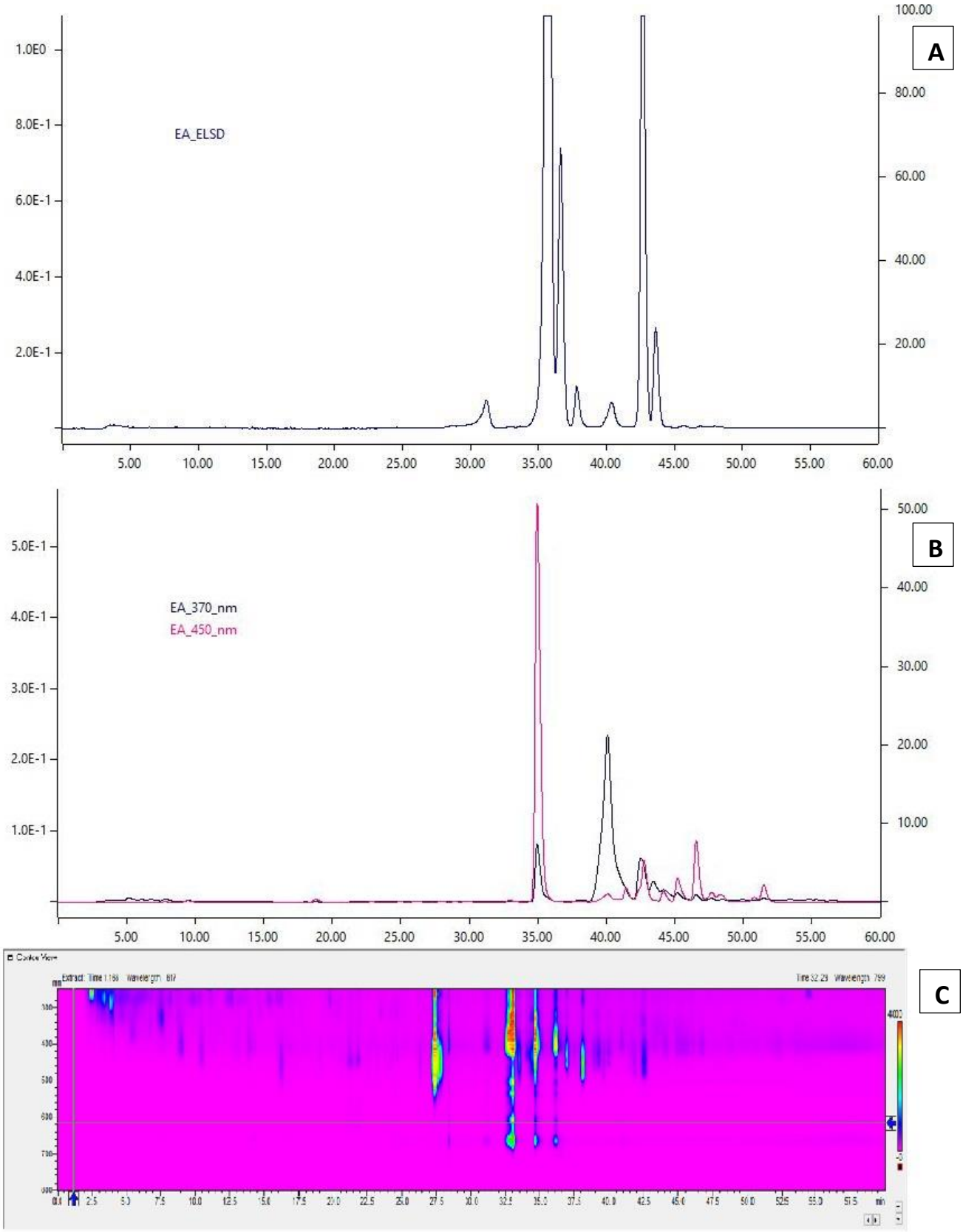

Figure 3.2**:** Chromatograms of ethyl acetate extract ran on analytical HPLC column: (A) signal of the ELSD; gain=4, (B) Molecular spectrophotometric absorption at 370 and 450 nm, and (C) 3D signal given by the DAD.

3.2.2 Preparative HPLC Fractions and Yields

To collect pure compounds in different fractions, collection programs were made although some fractions were later pooled to obtain sufficient amount of compounds to run the bioassays (Figures 3.3). The distinct colors of the pooled fractions (Figure 3.4), show that some components were separated as intended. The percentage yield of the dried fractions in relative to dry mass of injected extracts is summarized in Table 3.1. For ethanol, it can be observed that some fractions, or pooled fraction, have relatively high yields despite not having any peaks in their section of the chromatogram. This is because the chromatogram presented is DAD which cannot detect compounds that do not absorb. The ELSD chromatogram presented for ethyl acetate detected all the compounds especially since the gain was increased. Therefore, bioassays were done on all fractions irrespective of the presence or absence of peaks in their sections of preparative HPLC chromatogram.

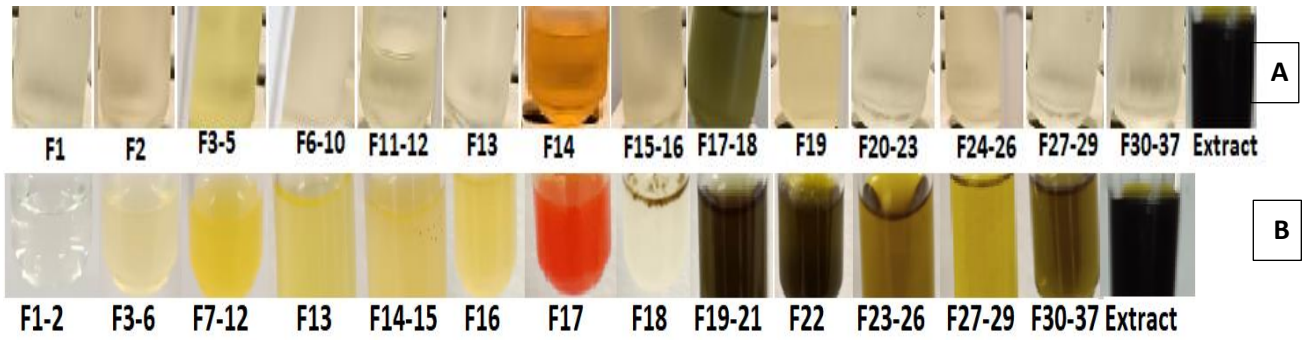

Figure 3.4: Appearance of (A) dilute pooled ethanol and (B) concentrated pooled ethyl acetate samples.

Table 3.1: Percentage yield of the dried fractions relative to dry mass of injected extracts.

Ethanol Fractions	1	2	3-5	6-10	11-12	13	14	15-16	17-18	19	20-23	24-26	27-30	31-37
Yield (%)	6.00	3.25	1.75	1.88	0.875	1.88	9.88	5.00	1.88	8.13	2.00	1.38	1.88	3.88
Ethyl Acetate Fractions	1-2	3-6	7-12	13	14-15	16	17	18	19-21	22	23-26	27-29	30-37	
Yield (%)	2.08	1.63	1.01	1.84	1.60	1.81	1.74	10.1	3.12	2.74	2.12	1.15	1.74	

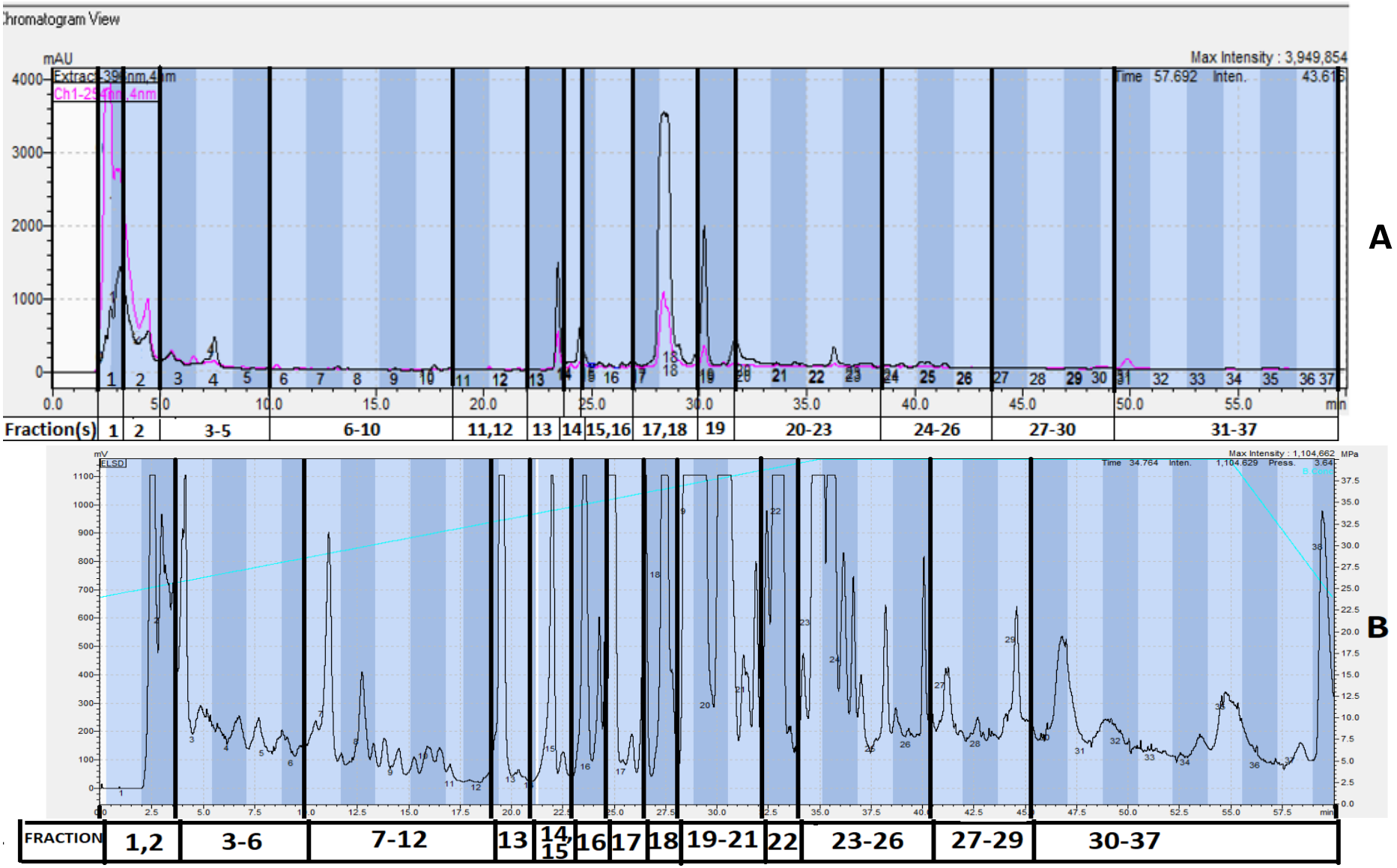

Figure 3.3: Fraction collection and pooling programmes for preparative HPLC. (A) ethanol (DAD view) and (B) ethyl acetate (ELSD view; gain = 8).

3.3 Bioactivity Results

In view of the roles of ACE and oxidative stress in the etiology of hypertension, identifying metabolites with antioxidant and ACE inhibitory activities becomes crucial in the quest for all-natural alternatives to hypertension management. In three bioactivity assays performed in this study, DPPH free radical scavenging, FRAP, and ACE inhibitory assays, comparisons were made between the activity of each fraction and its corresponding extract, and only fractions displaying significantly higher activity than the extract were considered active. This approach assumes that fractions contain pure, or close to pure, concentrated compounds, and if such compounds are bioactive, these fractions should display higher activity than the extract when assayed at the same concentration, as the extract contains very dilute concentrations of such compounds. However, it is worthy of note that this assumption would not hold true where there are synergistic interactions between active fractions, as such interactions might cause multiplicative (or at least additive) effects of bioactivity in the crude extract, in which case the fractions might be bioactive but still not show significantly higher activity than the extract. Also, not to be overruled is the possibility of antagonistic interaction of fractions, as one component (compound or fraction) could mask the activity of another component, in which case the initial assumption would hold true. These possibilities are taken into consideration in the interpretations presented below.

3.3.1 Ethanol Extract and Fractions

DPPH Free Radical Scavenging

Antioxidants counteract oxidative stress by donating a hydrogen atom to a free radical species, or by transferring a single electron to it, either of which stabilizes the radical. The DPPH free radical scavenging assay tests the ability of the sample components to scavenge free radicals by donation of hydrogen atoms.

Figure 3.5 summarizes the bioactivity results of ethanol samples. Fractions F6-10 and F17-18 displayed significantly greater DPPH scavenging activity than the extract ($p<0.05$ and $p<0.001$, respectively). F6-10 eluted from the HPLC with a mixture of water and acetonitrile as the mobile phase suggesting that it contains polar or semi-polar compound(s). Barkia et al. (2018) reported DPPH scavenging and ACE inhibitory activities for bioactive peptides in marine diatoms. Peptides and peptide derivatives with similar structures of the known ACE inhibitors captopril and enalapril (Figure 1.7) fit our suspicion of polar compounds, and although we did

not attempt to hydrolyze any present protein, some level of protein hydrolysis might have occurred during the extraction process with ethanol. But, in contrast to the observations of Barkia et al., no corresponding ACE inhibitory activity was recorded for this fraction. Since the DPPH activity of this fraction was moderate (significant at $p<0.05$) and no other activity was recorded for it in all other assays, it was not selected for further analysis with LC-MS.

Fraction F17-18 is suspected to contain pigments such as chlorophyll or chlorophyl derivatives which we believe is responsible for the radical scavenging activity observed. This is because of the deep green color of the fraction (Figure 3.4) and its maximum absorbance around 400-500 and 650-680 nm (Figure 3.3), both of which are characteristic of chlorophyll-like compounds (Grondelle and Boeker, 2017). Chlorophyll and its products have been reported to possess DPPH scavenging activities (Hsu et al., 2013), which further validates our suspicion. Generally, the scavenging activities of ethanol samples were low compared to those of pure gallic acid, that was used as a positive control.

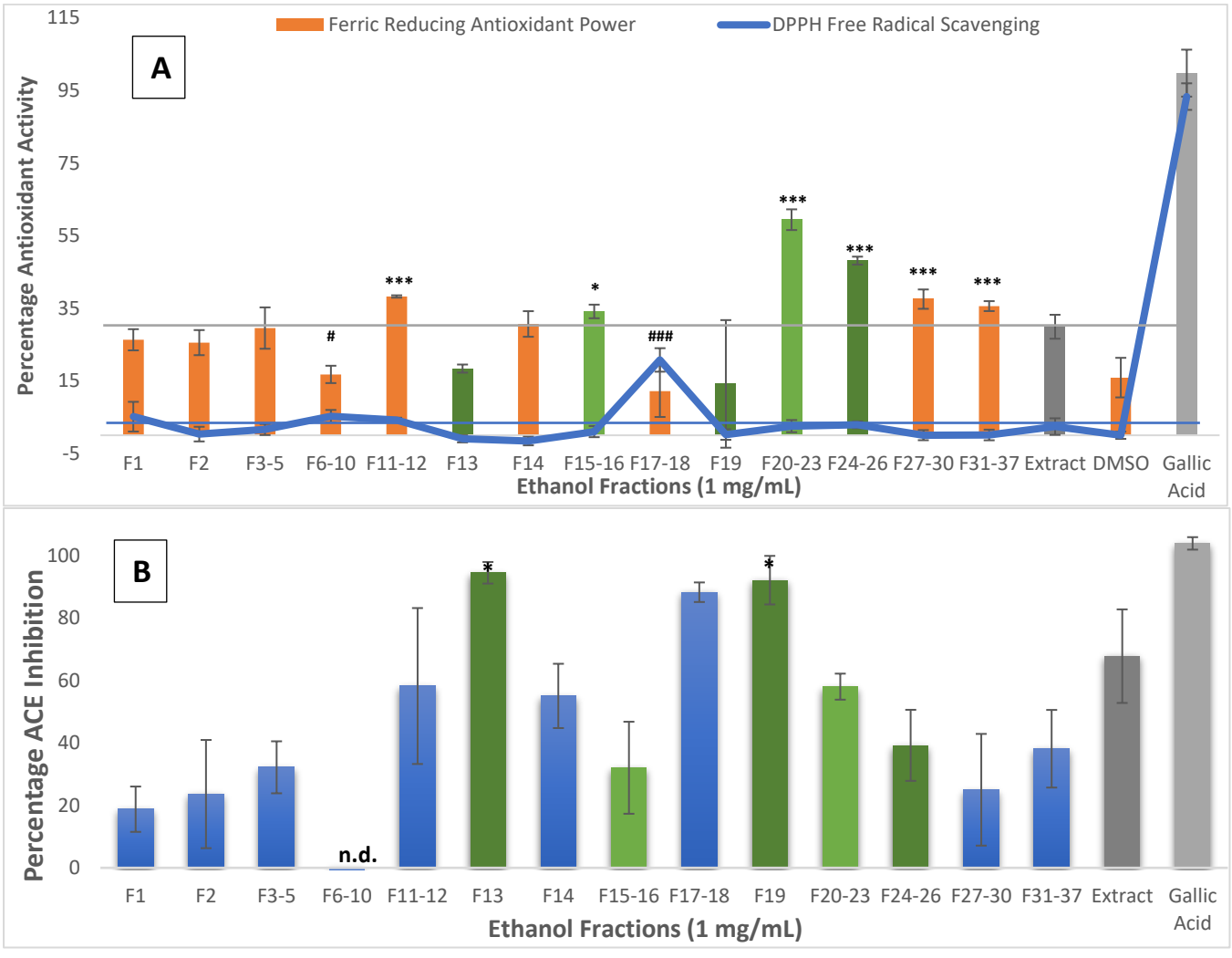

Figure 3.5: Bioactivity of ethanol extract and fractions. (A) antioxidant and (B) ACE inhibitory. Bars represent the mean ± SD of replicate samples; n = 3. Green bars indicate fractions that were analyzed with LC-MS, while grey bars denote the extract and positive control. Horizontal lines mark the level of the extract. N.d. = not detected. * and *** denote significantly higher than extract at $p<0.05$ and $p<0.001$, respectively for ferric reducing antioxidant power and ACE inhibitory assays; # and ### denote the same for DPPH free radical scavenging. For ACE inhibition, the negative control is normalized to 0%.

Ferric reducing antioxidant power

The ferric reducing antioxidant power assay evaluates the ability of sample components to transfer a single electron to ferric iron reducing it to ferrous iron. As electron transfer is also a way of counteracting free radical species, this is a simple method of determining the antioxidant power of extracts. Several ethanol fractions showed significantly higher ferric reducing properties than the extract: F15-16 ($p<0.05$), F11-12, F20-23, F24-26, F27-30, and F31-37 ($p<0.001$), with F20-23 displaying more than half of the activity of the positive control, gallic acid (Figure 3.5). This is interesting considering that gallic acid is a pure industrial product free from the contamination and oxidations that the fractions must have encountered during the entire extraction, fractionation, and drying processes. Most of the fractions displaying FRAP activities eluted at the latter stages of the HPLC run (100% acetonitrile as mobile phase). This suggests that they likely contain non-polar antioxidant compounds such as phenols and polyphenols (aromatic compounds) which have been previously reported to be present in diatoms (Grubišić et al., 2022). Further confirmatory analysis such as LC-MS would be necessary to validate this assumption.

ACE Inhibition

Inhibiting ACE activity would prevent or reduce the production of the vasoconstrictor and pro-inflammatory compound, Ang II. Therefore, compounds exhibiting ACE inhibitory activities would possibly serve as lead compounds for the formulation of alternative therapies for hypertension management. A fluorometric assay was used to assess the samples' ability to inhibit ACE's activity. Ethanol fractions F13 and F19 displayed significantly higher ($p<0.05$) ACE inhibitory activities than the crude extract, and interestingly, very close activities to the drug captopril used as positive control (Figure 3.6). Further analyses would be necessary to decipher the metabolites responsible for this activity. F17-18, which is suspected to contain chlorophyll, also displayed high ACE inhibitory activities although not significantly higher than

the extract. We did not find any studies attempting to elucidate chlorophyll's potential to inhibit ACE activity, hence we recommend this for further studies.

We suspected fraction F14 to contain carotenoids such as lycopene, β-carotene, etc., because of its bright orange color. However, by the time the bioassays were performed, much of this coloration was lost, likely due to long storage before running the assays as carotenoids are very labile and can easily oxidize. This is possibly why no bioactivities (such as FRAP and ACE inhibition) were observed in this fraction as would be expected of carotenoids.

Cell Viability Results (Reporter Gene Assay)

As a requirement for anti-inflammatory tests, samples must be tested for toxicity to the cells, since toxic samples could lead to false positive or negative results. The reporter gene assay for anti-inflammatory test used two cell lines (THP-1 and RAW 264.7) as gene carriers. Therefore, toxicity of the samples to these cells was examined (at 8h and 72h for extracts, and 8h for fractions). In line with ISO standard 10993-5 (Tests for *in vitro* cytotoxicity), toxicity limit was set at 30%, hence samples causing viability values less than 70 are considered toxic to the cells.

Figure 3.6 shows the viability test results for cells treated with ethanol samples. The extract did not exhibit any toxicity to the cells even after 72h. Also, after 8h, none of the fractions displayed toxicity to the human monocytic cells which suggests that the components of these fractions may be safe for human consumption if used to formulate antihypertension or anti-inflammation therapy. However, the viability level of murine macrophage cells treated with fraction F13 fell below 70 after 8 hours of treatment, suggesting toxicity to these cells. Ruocco et al. (2018) reported cytotoxic compounds in *N. shiloi*, some of which were identified as toxigenic oxylipins including hydroxyeicosapentaenoic acids (HEPEs). LC-MS analysis of F13 would reveal the compounds eliciting this response, after which it would be necessary to confirm the toxicity of the pure compounds. These points are discussed later in this report.

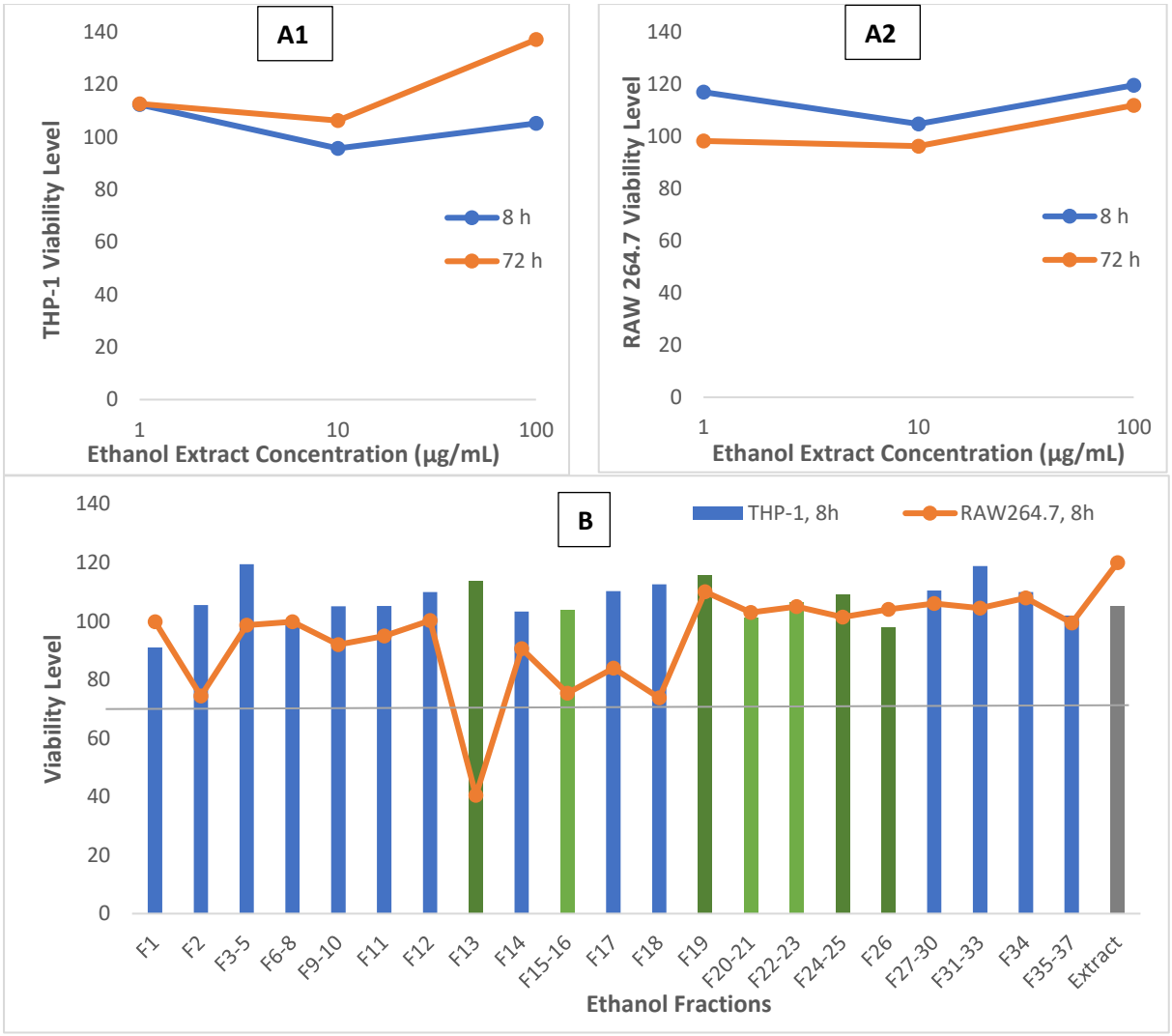

Figure 3.6: Cell viability (%) of ethanol fractions and crude extract. (A) Extract on (1) THP-1 and (2) RAW 264.7 cell lines at 8 and 72h. (B) Fractions and extract at 8h. Bars represent the median ± SD of replicate samples; n=4. Green bars indicate fractions that were analyzed with LC-MS, while grey bars denote the extract. The horizontal line indicates the acceptance level of biocompatibility.

Anti-inflammatory activity

Pro-inflammatory cytokines such as TNFα, IL-6, and NF-kβ play important roles in activating inflammatory pathways such as RAS and JAK, or upregulating the expression of COX-2, all of which cause or increase inflammatory reactions (Zhang and An, 2007). Reporter genes containing promoter sequences for the expression of genes coding for human TNFα, human IL-6, murine TNFα, and NF-kβ were transfected into different cell lines (THP-1 and RAW 264.7) and treated with LPS (or TNFα for NF-kβ) to stimulate gene expression and production of pro-inflammatory cytokines. The potential of the samples to inhibit these genes expression was tested (at 100, 10, and 1 µg/ml for extracts, and 100 µg/ml for fractions).

Figure 3.7 shows the inhibitory activity of ethanol extract on genes expression coding for pro-inflammatory cytokines. At 100 µg/ml, the crude ethanol extract significantly inhibited the expression of the human genes coding for TNFα (p<0.05) and IL-6 (p<0.0001) carried by human monocytic cells and murine macrophage cells, respectively. To better utilize the available fractions, ethanol fractions were only tested at 100 µg/mL and were not tested on mTNFα [RAW 264.7] as no activities were recorded for them with the extract.

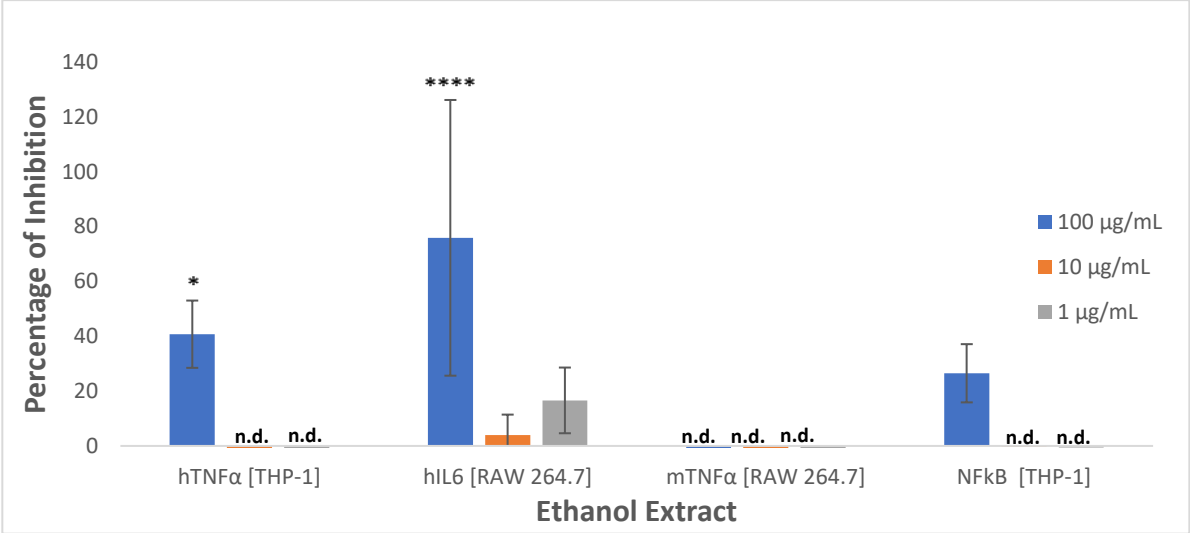

Figure 3.7: Inhibition of inflammatory cytokines production (TNFα, IL6 and NFkB) by the ethanol extract. Bars represent the median ± SD of replicate samples; n=4. N.d. = not detected. * and **** denote significantly higher than dexamethasone (reference sample) at p<0.05 and p<0.0001, respectively.

Ethanol fraction F13 showed significant (p<0.0001) inhibitory activity on the expression of human genes coding for TNFα carried by human monocytic cells (Figure 3.8). This activity is much higher than that of the extract possibly indication a concentration of the active compounds in this fraction.

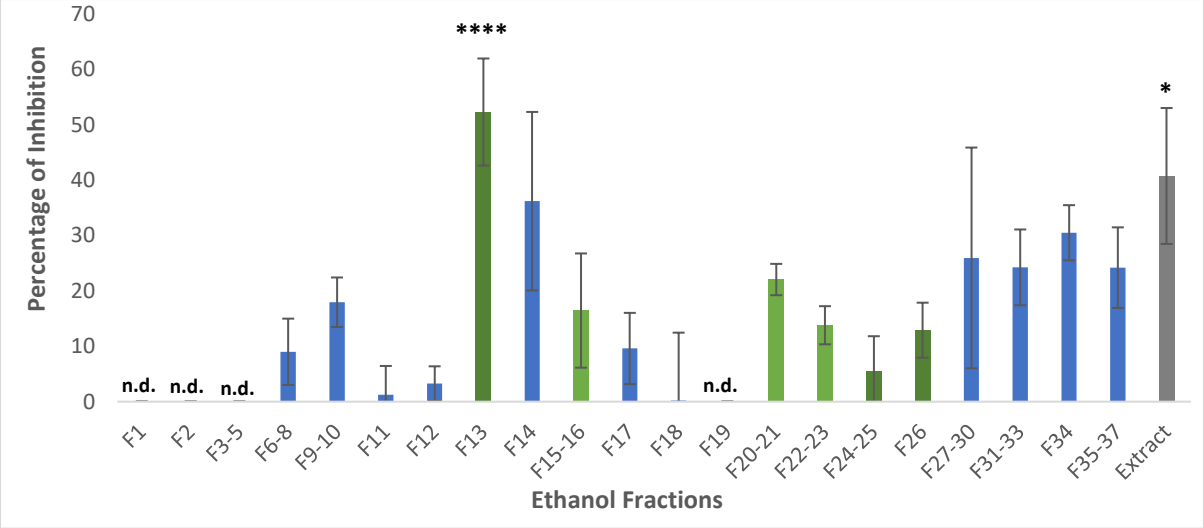

Figure 3.8: Inflammation inhibition of 100 µg/mL of ethanol fractions on hTNFα [THP-1]. Bars represent the median ± SD of replicate samples; n=4. Green bars indicate fractions that were analyzed with LC-MS, while grey bars denote the extract. N.d. = not detected. * and **** denote significantly higher than dexamethasone (reference sample) at $p<0.05$ and $p<0.0001$, respectively. The negative and positive controls are normalized to 0 and 100%, respectively.

The very high inhibitory activity displayed by the ethanol extract on the genes coding for human IL-6 in murine macrophage cell line is likely an additive effect of three fractions which also showed significant activities ($p<0.0001$): F13, F17 and F18 (Figure 3.9). It should be noted that F13 showed some toxicity to these cells and therefore the inhibition recorded by F13 might be a false positive result. Subramoniam et al. (2012) reported chlorophyll a and b with the ability to inhibit the expression of NF-kβ and TNFα but did not study their effect on IL6 expression. F17 and F18 (suspected to contain chlorophyll) inhibited expression of all three cytokines.

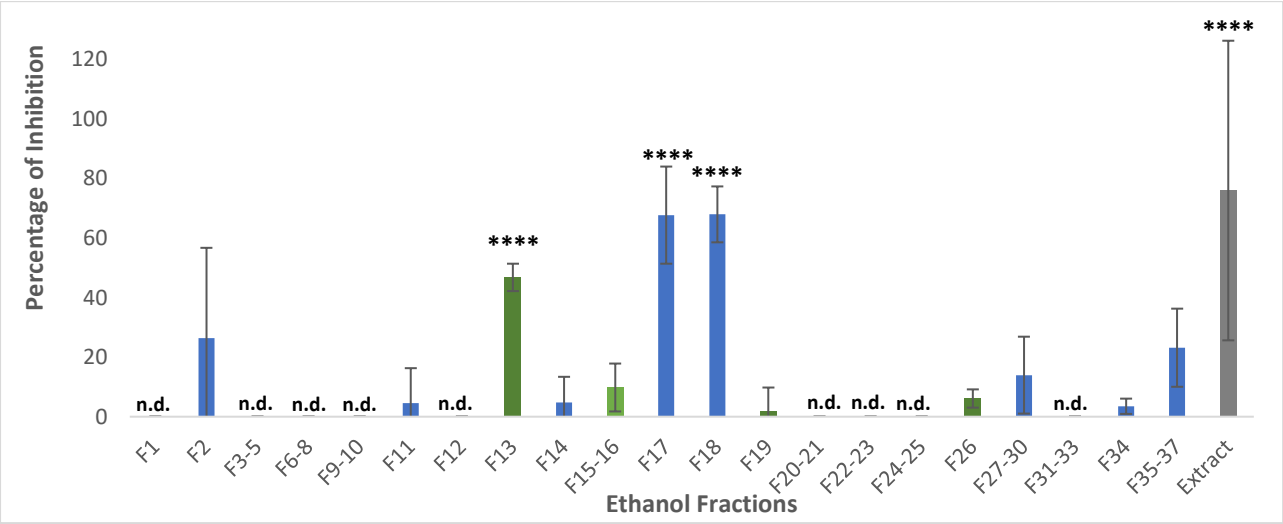

Figure 3.9: Inflammation inhibition of 100 µg/mL of ethanol fractions on hIL6 [RAW 264.7]. Bars represent the median ± SD of replicate samples; n=4. Green bars indicate fractions that were analyzed

with LC-MS, while grey bars denote the extract. N.d. = not detected. **** denote significantly higher than dexamethasone (reference sample) at $p<0.0001$. The negative and positive controls are normalized to 0 and 100%, respectively.

For NF-kβ in human monocytic cell lines, fractions F13 and F15-16 significantly ($p<0.05$) inhibited the gene expression, as did F26 ($p<0.01$), and F17 to F24-25 ($p<0.001$; Figure 3.10). Although fractions from F27-30 to F35-37 displayed significant inhibitory activities, it is suspected that these activities could be a result of chlorophyll degradation products which can stick to HPLC column.

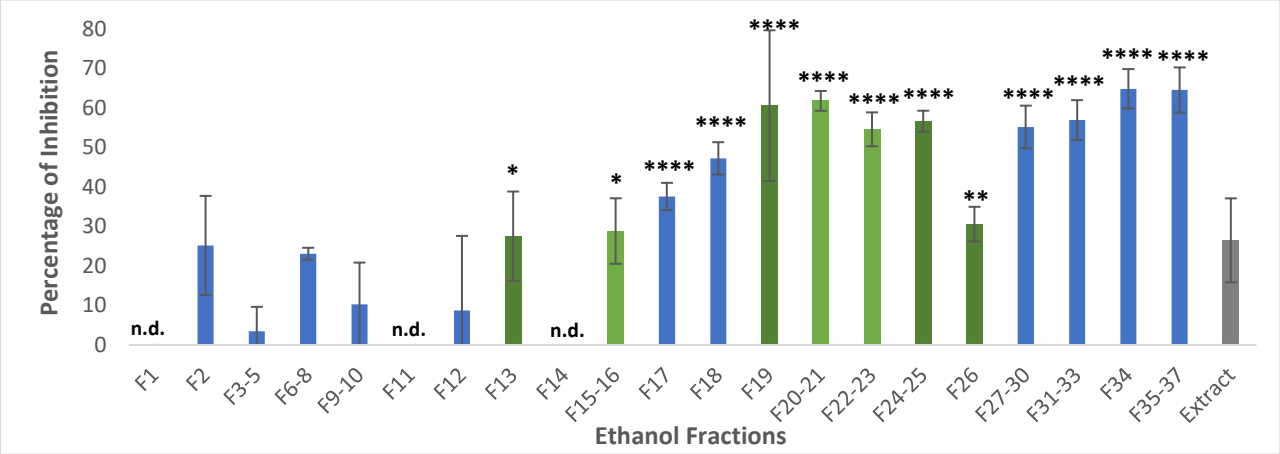

Figure 3.10: Inflammation inhibition of 100 µg/mL of ethanol fractions on NF-kβ [THP-1]. Bars represent the median ± SD of replicate samples; n=4. Green bars indicate fractions that were analyzed with LC-MS, while grey bars denote the extract. N.d. = not detected. *, **, and **** denote significantly higher than dexamethasone (reference sample) at $p<0.05$, $p<0.01$, and $p<0.0001$, respectively. The negative and positive controls are normalized to 0 and 100%, respectively.

In summary, Fraction F13 inhibited the gene expression of all three pro-inflammatory cytokines assayed while F19 inhibited NF-kβ expression. Both fractions also inhibited ACE activity. Fractions F15-16, and all fractions from F20-21 to F26 inhibited NF-kβ expression and displayed FRAP activities. Hence, these fractions were selected for further analysis with LC-MS. Table 3.2 gives a summary of all activities displayed by ethanol fractions.

On the other hand, although fractions F17 and F18 displayed FRAP activities and inhibited ACE activity (to some extent) and the expression of human IL-6 and NF-kβ, we decided not to analyze the color intensive fractions since some works have been done to identify *N. shiloi* pigments. For instance, Grubišić et al. (2022) found significant quantities of fucoxanthin, β-carotene, and Chlorophyll a in *N. shiloi*. The presence of such pigments in *N. shiloi* is of importance to the pharmaceutical, nutraceutical, food, feed, fabric, and cosmetic industries

where they have been used in drug and food formulation, as colorants, etc. (Spolaore et al., 2006). We cannot rule out the possibility of the presence of other color intensive phytochemicals such as flavonoids which have been reported with bioactivities (Ginwala et al., 2019).

Table 3.2: Ethanol fractions displaying bioactivities (significantly higher than extract for DPPH, FRAP and ACE; fractions with names in green font were analyzed with LC-MS).`

Ethanol Fraction	F1	F2	F3-5	F6-10	F11-12	F13	F14	F15-16	F17-18	F19	F20-23	F24-26	F27-30	F31-37
DPPH				✓			✓							
FRAP					✓			✓			✓	✓	✓	✓
ACE						✓				✓				
hTNFα [THP-1]						✓								
hIL6 [RAW 264.7]						✓			✓					
NF-kβ [THP-1]						✓		✓	✓	✓	✓	✓	✓	✓
Viability THP-1						✓								
Viability RAW 264.7						✖								

3.3.2 Ethyl Acetate Extract and Fractions

DPPH Free Radical Scavenging

The activities of ethyl acetate fractions were very similar to those of ethanol (Figure 3.11). Only F19-21 showed significantly higher (p<0.001) DPPH free radical scavenging activity than the crude extract. Based on its color and absorption spectrum similar to ethanol fraction F17-18 (Figures 3.3 and 3.4), we predict that this fraction contains chlorophyll-like compounds responsible for the scavenging activity observed.

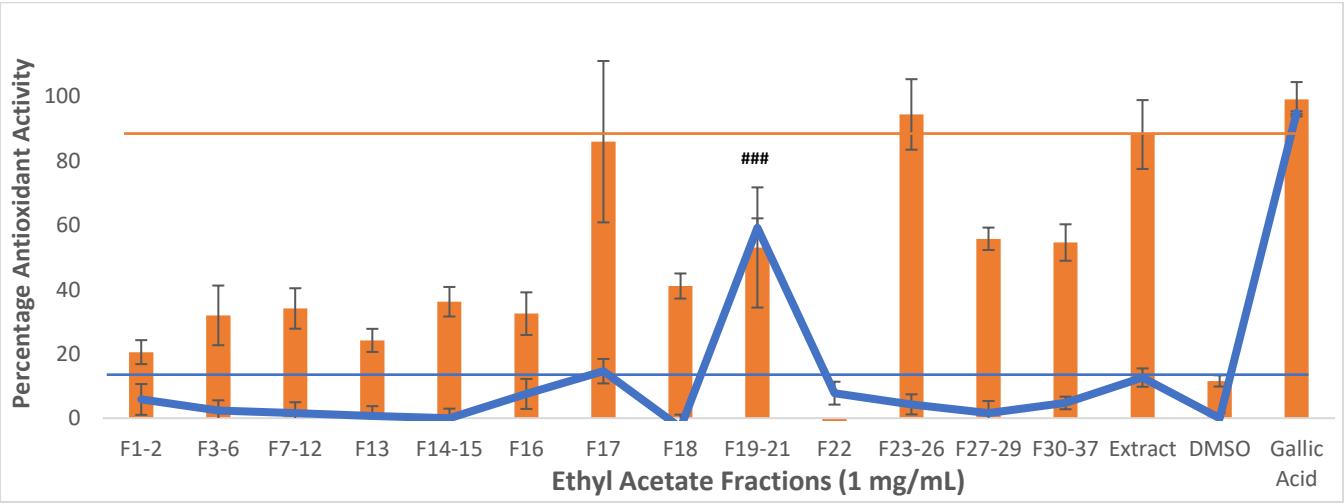

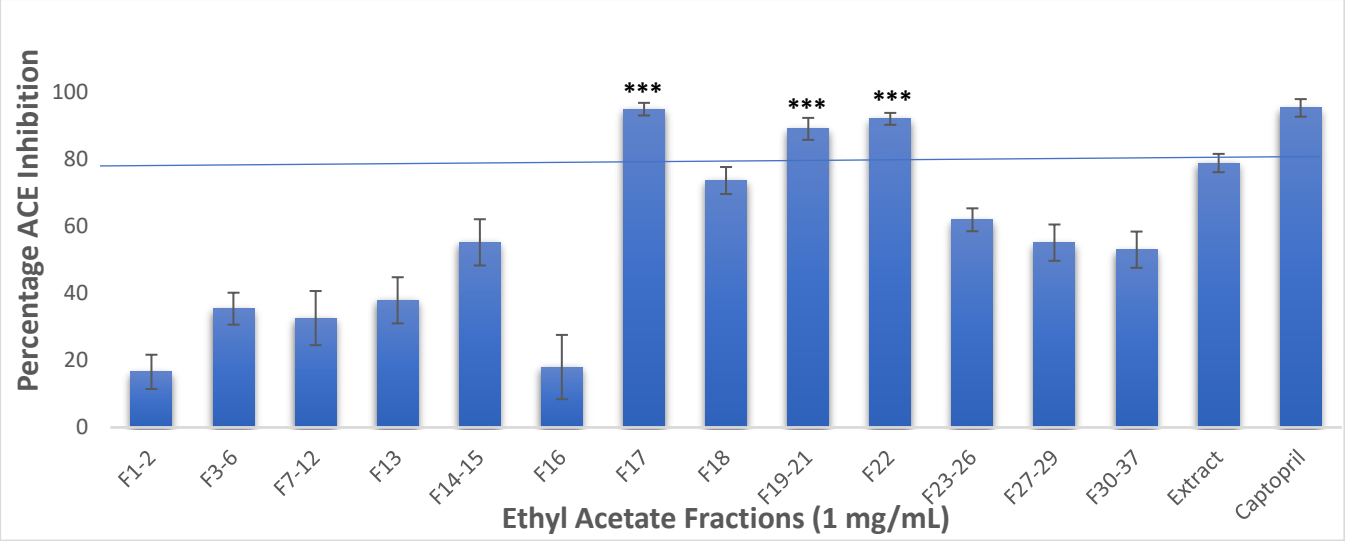

Figure 3.11: Bioactivity of ethyl acetate extract and fractions (A) antioxidant and (B) ACE inhibitory. Bars represent the mean ± SD of replicate samples; n=3. Horizontal lines mark the level of the crude extract. *** and ### denote significantly higher than extract at $p<0.001$ for ACE inhibitory and DPPH free radical scavenging assays, respectively. For ACE inhibition, the negative control is normalized to 0%.

Ferric reducing antioxidant power

Although no ethyl acetate fractions showed significantly higher iron reducing activities than the crude extract, F17 and F23-26 displayed very high activities, with the activity of F23-26 being almost identical to that of the positive control, gallic acid. We suspect synergistic interactions between these fractions which gave the extract its high activity. Perhaps, a good approach is to pool all fractions displaying high activities and compare them to the crude extract to confirm the presence of interactions, but this was not done due to limited quantity of the fractions.

Similar to ethanol F14, ethyl acetate F17 is suspected to contain carotenoids due to its bright orange colors (Figure 3.4). Müller et al. (2011) reported that carotenoids (particularly lycopene which is also red colored) display FRAP activities but not DPPH scavenging activities, which agrees with the observations of ethyl acetate F17. As stated earlier, the absence of similar activity in ethanol F14 could be due to photo-degradation of carotenoids from prolonged storage.

ACE Inhibition

F17, F19-21, and F22 displayed significantly greater ACE inhibitory activities ($p<0.001$) than the extract, with some being identical with the activity of captopril (Figure 3.7). As stated, F17 likely contains carotenoids such as lycopene which have been reported with ACE inhibitory

activities (Han and Liu, 2017). To the best of our knowledge, no work has studied the presence of lycopene in *N. shiloi* and we recommend this for further studies. F19-21 is suspected to contain chlorophyll and related pigments.

In summary, two ethyl acetate fractions (F17 and F19-21) are suspected to contain carotenoids and chlorophylls and displayed activities expected for such compounds. Two others (F22 and F23-26) displayed ACE inhibitory or FRAP activities and should be analyzed with LC-MS, which was not done due to the constraints of time. We suspect the presence of non-polar compounds extracted by ethyl acetate but not ethanol, especially as these fractions eluted with 100% acetonitrile as mobile phase and because ethyl acetate samples generally showed better bioactivities than ethanol in both assays. As highlighted earlier, part of the low activities of ethanol extracts might be due to prolonged storage.

Cell Viability Results

As with ethanol, ethyl acetate extract was not toxic to any of the cells even after 72 hours of treatment (Figure 3.12). The results of the fractions did not arrive on time and so is not included in this report.

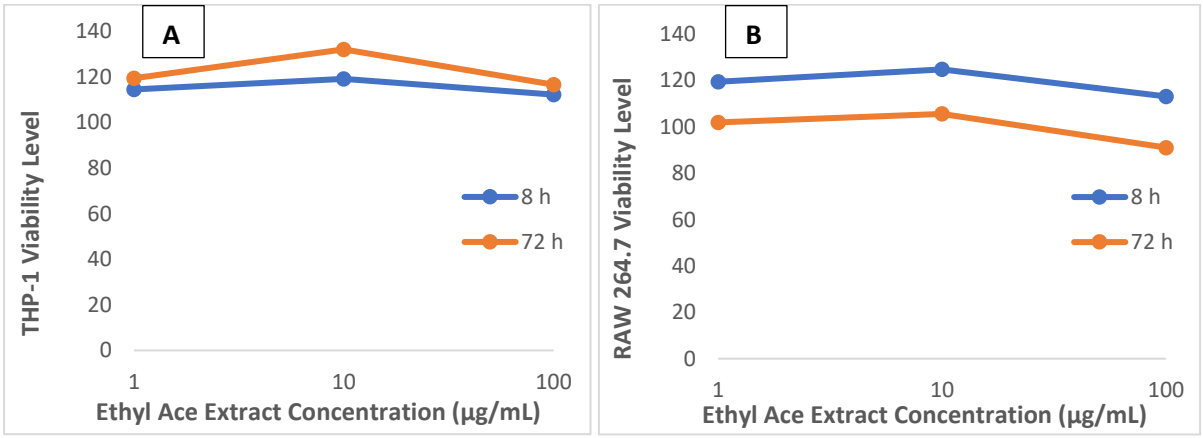

Figure 3.12: Cell viability (%) of ethanol extract on (A) THP-1 and (B) RAW 264.7 cell lines at 8 and 72h.

Anti-inflammatory activity

At 100 µg/mL, the ethyl acetate extract significantly (p<0.0001) inhibited the expression of all the genes in all the carrier cells (Figure 3.13), but as with ethanol extract, the lowest activity was recorded for murine TNFα carried by murine macrophage cells (p<0.05). This result makes it more convincing that the samples displayed more activity on human gene expression than on murine.

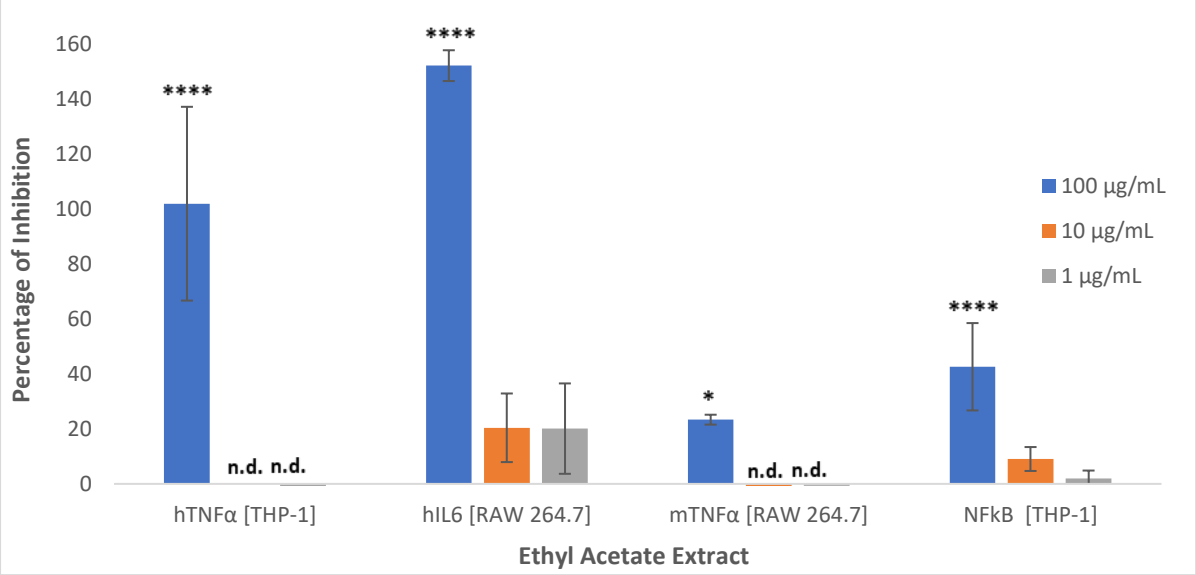

Figure 3.13: Inflammation inhibition of ethyl acetate extract. Bars represent the median ± SD of replicate samples; n=4. * and **** denote significant at $p<0.05$ and $p<0.0001$, respectively.

3.4 LC-MS

Based on the bioactivity assays results (and also the anti-inflammatory assay report from a partner of Algae4IBD project, in the CZ-Openscreen platform in Check Republic; https://www.openscreen.cz/), five ethanol fractions (F13, F15-16, F19, F20-23, and F24-26) were subjected to LC-MS analysis. The aim is to identify metabolites with known exact mass and molecular formula in the fractions by comparing the mass spectrum patterns against two libraries (Wiley and NIST) using XCalibur 4.1.50. Only results with a matching of 70% or greater were accepted. For all accepted compounds, the exact mass (and the isotopic abundance) was confirmed by searching the molecular formula on Sisweb's exact mass calculator. In addition, the names and molecular formular were searched in Chemspider, PubChem, and SpectraBase databases to find the structure and other information about the compounds. Table 3.3 lists all accepted compounds from library search. Figures 3.14-3.18 show the LC-MS chromatograms and spectrum patterns of the compounds, and molecular structure found in Chemspider (when available). Unless otherwise indicated, no reference to the use or activity of the detected compounds was found in the literature. The compounds in some of the peaks could not be identified by library search since the peaks were not well separated.

Table 3.3: Compounds detected in the ethanol fractions by LC-MS analysis.

Fraction	Name	Formula	Exact Mass (g/mol; Lib search)	RT (min)	Prob. (%)	Library ID N=NIST W=wiley	Exact Mass (u; Sisweb)	Isotopic Abundance (%; Sisweb)	Monoisotopic/Exact Mass (Da/g/mol)	Search ID C= Chemspider S= SpectraBase
F13	Bis[(2,4,6-Tri-tert-butylphenyl)amino)] phenylchlorosilane	$C_{42}H_{65}ClN_2Si$	660.460556	12.75	82.6	W-386065	660.460554	43.3	660.460571	C-73941459
F13	2-ter-Butyl-4-(fluorobis[methyl (trimethylsilyl) amino]silyl)-3,3,5-trimethyl-1, 2-diaza-3-sila-5-cyclopentene	$C_{17}H_{43}FN_4Si_4$	434.25488	12.93	70.6	W-348786	434.254886	58.8	434.254889	S-CgJL0dF7KM7
F15-16	-	$C_{25}H_{54}N_4Si_3Th$	726.403683	13.06	74.3	W-388577	726.403684	58.3	-	-
F15-16	34,36,37-Trioxo-35,38-dimethoxy-4,27-dimethyl-1,7,11,20,24,30-hexaazaheptacyclo(28.3.1.1.1.1.1.1.0)ocataconta-35-(2),3,5,13,(14),15,17,38(25),26,28-nonaene	$C_{36}H_{42}N_6O_5$	638.321667	13.14	98.5	W-384805	638.321668	64.6	638.321655	C-4677868
F19	β',N-(2,6-diacetyl-1,5-diazanonane-1,9-diyl)-α',β'-dihydro-4-hydroxy-N,N'-(propane-1,3-diyl)-3,4'-oxy-di[benzenepropanamide]	$C_{32}H_{40}N_4O_6$	576.294785	13.70	80.1	W-379722	576.294785	67.9		
F19	2,2-isopropylidenebis((5-(dimethylfurfuryl-dimethylfurfuryl)furan)	$C_{39}H_{44}O_6$	608.31379	13.78	70.8	W-382777	608.313790	63.8	608.313782	29316307
F20-23	L-Proline, N-(pentafluorobenzoyl)-, octadecyl ester	$C_{30}H_{44}F_5NO_3$	561.324135	14.70	81.1	N-188889	561.324134	70.7	-	-
F24-26	Dodecyl(dimethyl)phosphine oxide	$C_{14}H_{31}OP$	246.211252	14.22	76.3	N-621193	246.211253	85.2	246.211252	12808

Fraction F13: Two compounds corresponding to two peaks were detected and identified as Bis[(2,4,6-Tri-tert-butylphenyl)amino)]phenylchlorosilane with the IUPAC name 1-Chloro-1-phenyl-N,N'-bis[2,4,6-tris(2-methyl-2-propanyl)phenyl]silanediamine and 2-ter-Butyl-4-(fluorobis[methyl (trimethylsilyl) amino]silyl)-3,3,5-trimethyl-1, 2-diaza-3-sila-5-cyclopentene with IUPAC name 1-[2-(1,1-dimethylethyl)-3,3,5-trimethyl-1,2-diaza-3-silacyclopent-5-en-4-yl]-1-fluoro-N,N'-dimethyl-N,N'-bis(trimethylsilyl)-silanediamine. These compounds are not peptides, and their structures (Figure 3.14) are not similar to known ACE inhibitors (Figure 1.7). We cannot predict which of the compounds is responsible for the bioactivities observed since no activity report was found for them. It is possible that different compounds are responsible for different bioactivities and cytotoxicity observed in this fraction.

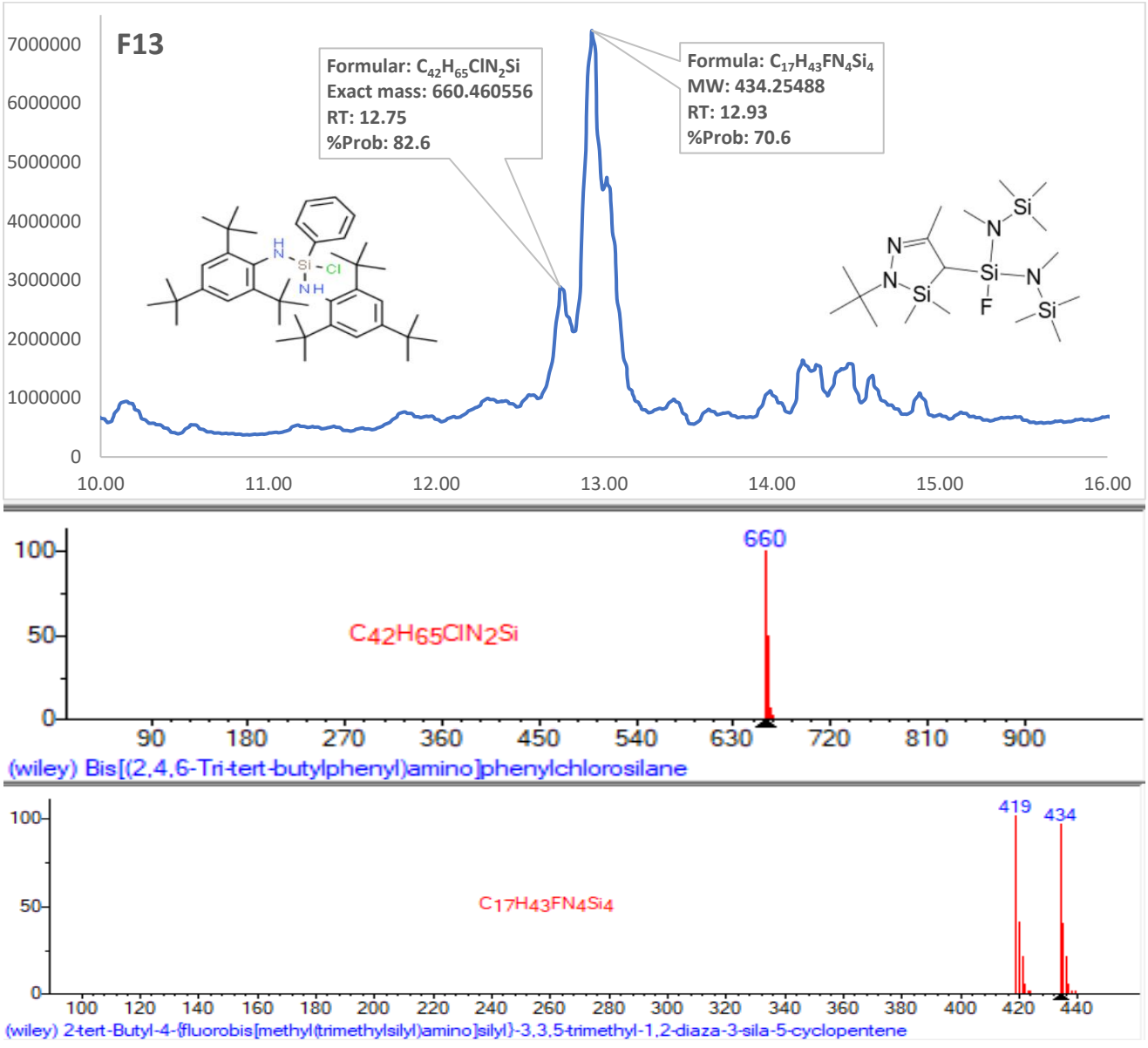

Figure 3.14: LC-MS chromatograms, molecular structure and spectrum patterns of compounds detected in F13.

Fraction F15-16: Figure 3.15 shows the details of compounds detected in F15-16. The first compound with the formular C25H54N4Si3Th is unnamed and the second is 34,36,37-Trioxo-35,38-dimethoxy-4,27-dimethyl-1,7,11,20,24,30-hexaazaheptacyclo(28.3.1.1.1.1.1.1.0) ocata conta-35-(2),3,5,13,(14),15,17,38(25),26,28-nonaene with the IUPAC name (17S,18S)-18-{3-[(2-Aminoethyl)amino]-3-oxopropyl}-20-(carboxymethyl)-7-ethyl-3,8,13,17-tetramethyl-12-vinyl-17,18-dihydro-2-porphyrincarboxylic acid. No activity record was found for these compounds.

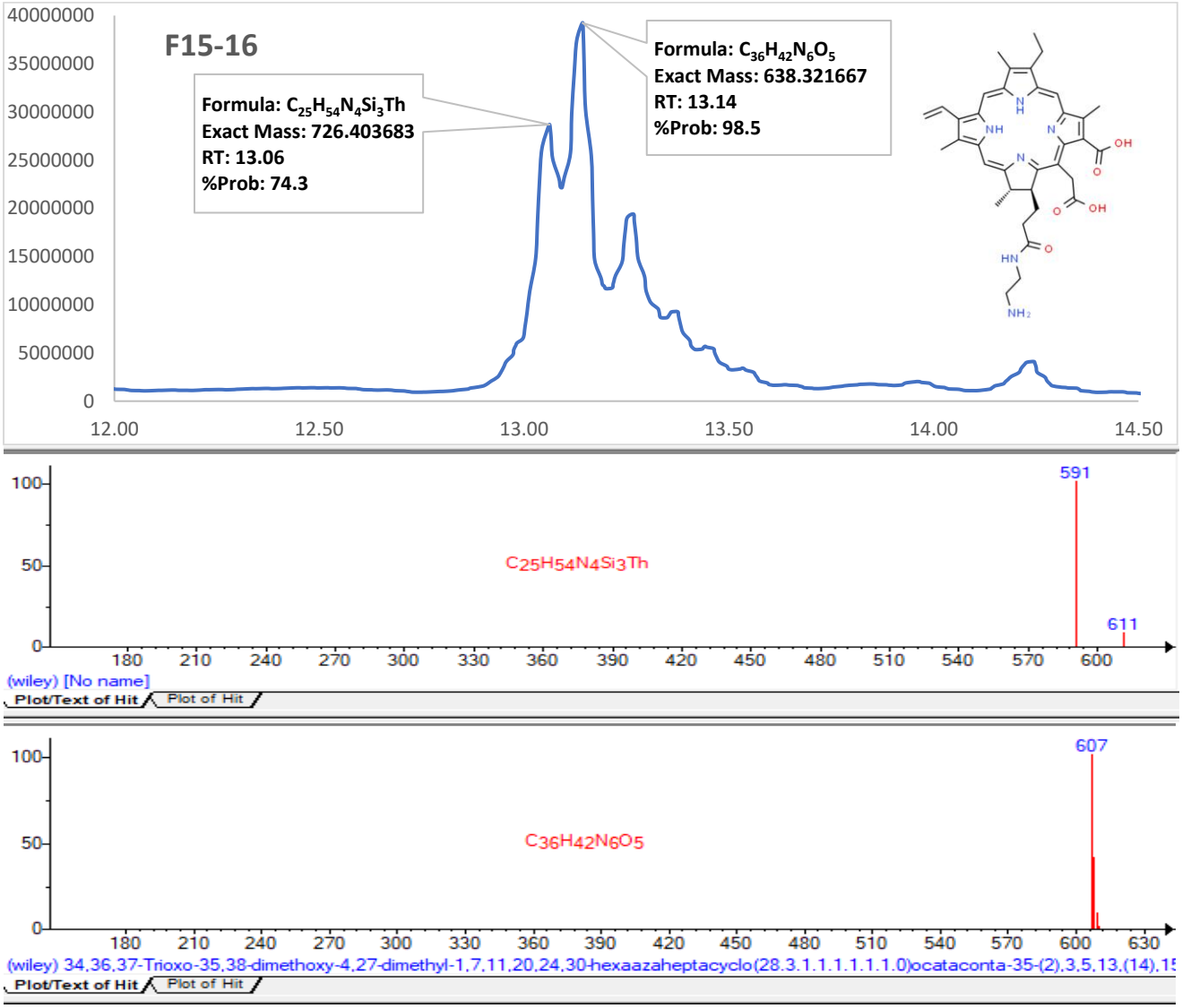

Figure 3.15: LC-MS chromatograms, molecular structure, and spectrum patterns of compounds detected in F15-16.

Fraction F19: For the first of the two compounds detected in this fraction, 328 structures fit the molecular formula $C_{32}H_{40}N_4O_6$ and we are unable to determine the exact one that fits the name β',N-(2,6-diacetyl-1,5-diazanonane-1,9-diyl)-α',β'-dihydro-4-hydroxy-N,N'-(propane-1,3-diyl)-3,4'-oxy-di [benzenepropanamide]. The second is 2,2-isopropylidenebis((5-(dimethylfurfuryl-dimethylfurfuryl)furan) with the IUPAC name 2,2'-(2,2-Propanediyl)bis[5-(2-{5-[2-(2-furyl)-2-propanyl]-2-furyl}-2-propanyl)furan]. The structure is displayed in Figure 3.16. No biological activity was previously reported for these compounds.

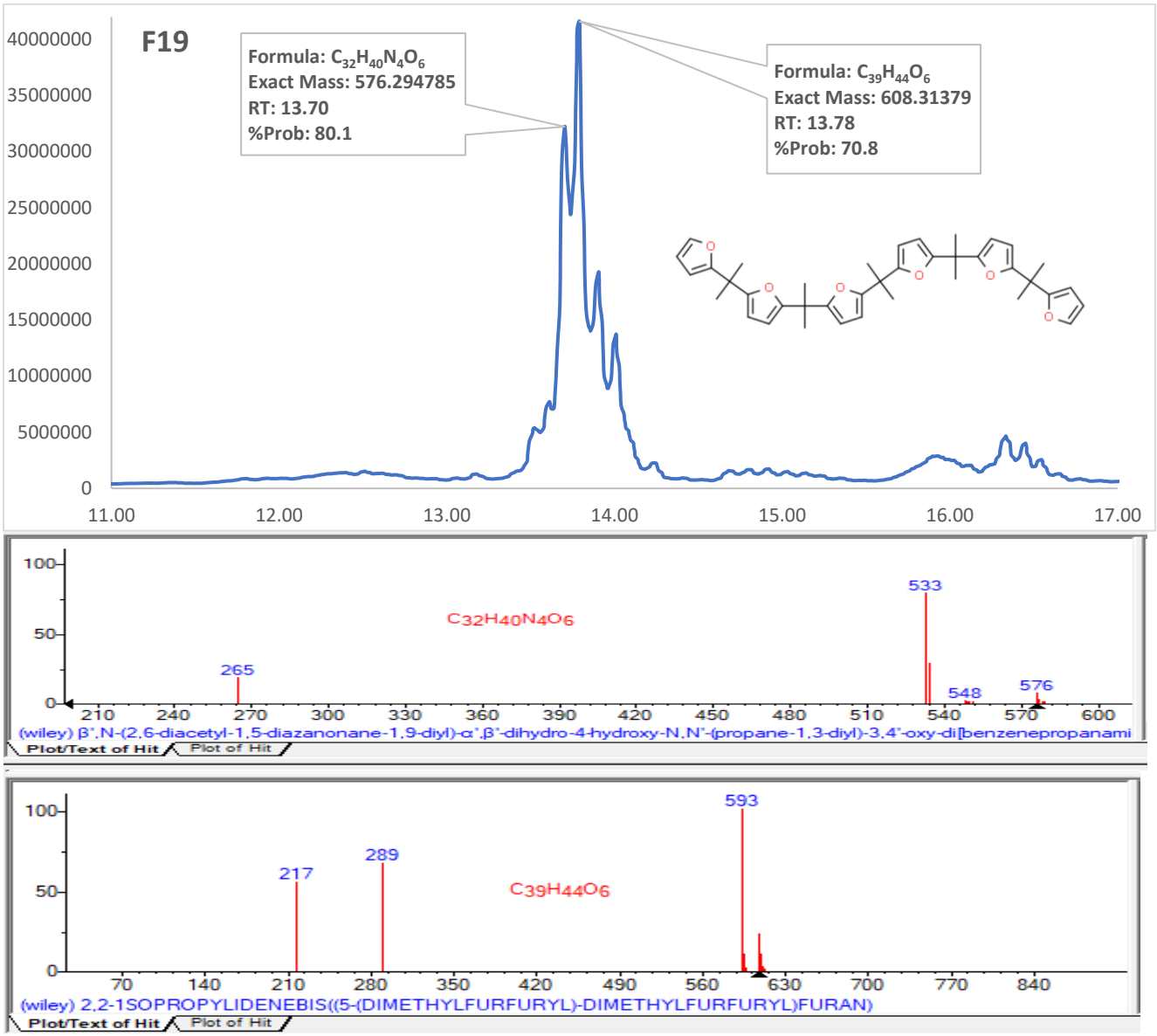

Figure 3.16: LC-MS chromatograms, molecular structure and spectrum patterns of compounds detected in F19.

Fraction 20-23: The main peaks in this fraction were not well separated which prevented the identification of the compounds present in the fraction. L-Proline, N-(pentafluorobenzoyl)-, octadecyl ester (with structure in Figure 3.17) was detected but no information about this compound was found in the literature.

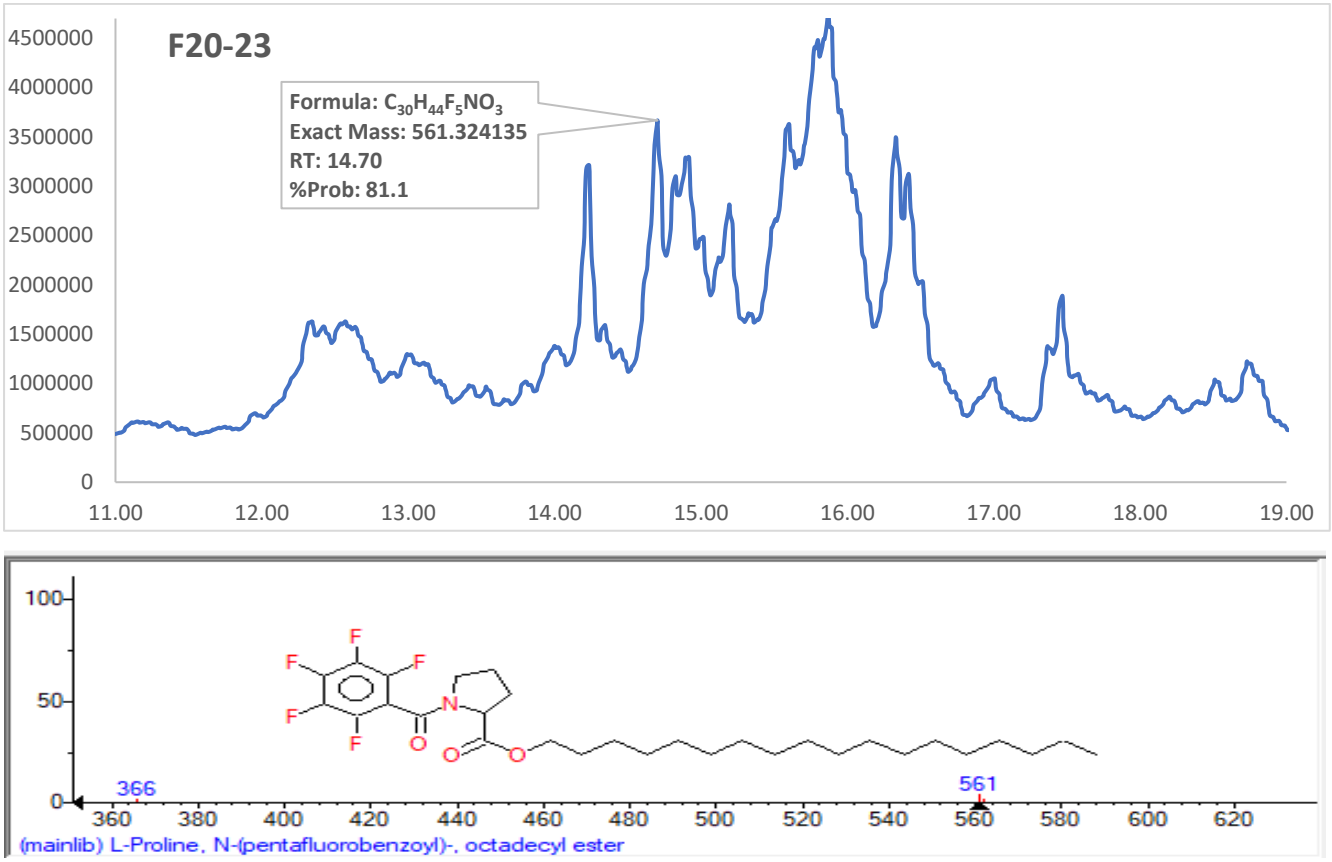

Figure 3.17: LC-MS chromatograms, molecular structure and spectrum patterns of compounds detected in F20-23.

Fraction F24-26: Like F20-23, peaks in F24-26 were poorly separated making it difficult to identify the compounds present in the fraction, except for dodecyl(dimethyl)phosphine oxide (IUPAC name), displayed in Figure 3.18. This compound has been employed as a surfactant to increase amphiphile penetration of monolayers (Zhao et al., 2000).

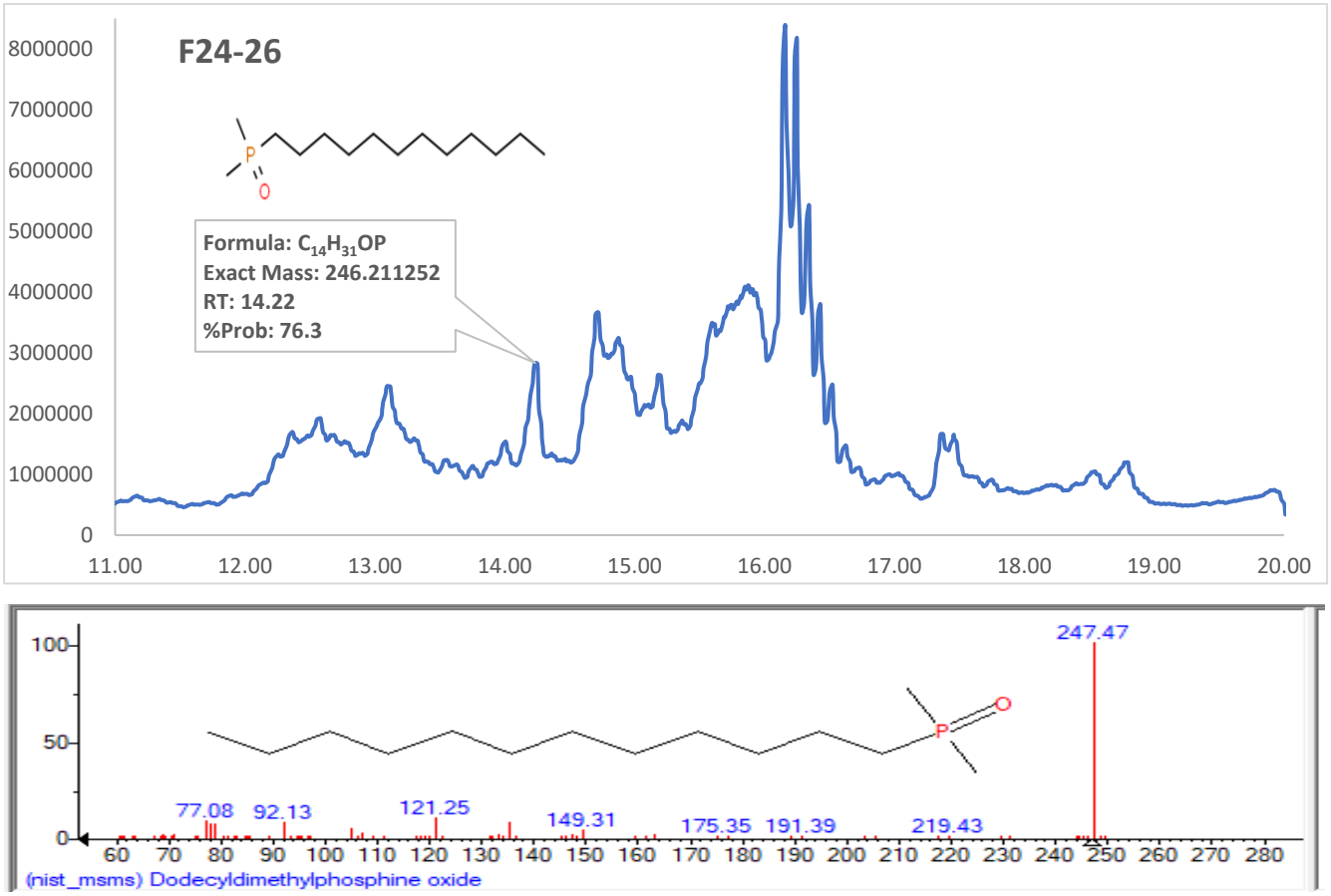

Figure 3.18: LC-MS chromatograms, molecular structure and spectrum patterns of compounds detected in F24-26.

In summary, LC-MS analysis detected several compounds in the samples which would be very interesting to investigate further since the activities and possible industrial value of many of them have not been reported.

3.5 Suggestions for Improvement

We have made several considerations leading to suggestions to improve and validate the results obtained from this study.

Foremost, according to the Chemical Analysis Working Group (CAWG) of the Metabolomics Standards Initiative (MSI), to adequately validate the identification of non-novel metabolites, it is necessary to have at least two independent and orthogonal data in relation to an

authentic (or reference) compound analyzed under identical experimental conditions (Sumner et al., 2007). Examples of such orthogonal data are retention time/index and mass spectrum, retention time and NMR spectrum, accurate mass and tandem MS, accurate mass and isotope pattern, full ^{1}H and/or ^{13}C NMR, 2-D NMR spectra, etc. Such rigorous identification protocol was not possible to carry out in this work. We predicted the metabolites structure using mass spectrum data but could not compare the retention times/index of the peaks to that of a reference or standard of the predicted compound as they are not found commercially. We recommend further studies employing the described in-depth validation protocol to adequately confirm the identity of the metabolites detected in this study.

Furthermore, as pointed out, some compounds in the fractions subjected to LC-MS analysis were not identified by the library search. This could either be because of the poor separation of the peaks which prevented matching of their mass spectra with those available in spectral libraries, or because they contain novel compounds that have not yet been fully identified and deposited in such libraries. To improve identification, the LC protocol should be optimized to achieve a good separation of the peaks. This could provide better matching of the mass spectra with those in spectral libraries and possible tentative identification of the metabolites. For novel compounds, this separation will be valuable in obtaining the accurate mass of the compounds which can help in predicting the elemental compositions. Such fractions should therefore be further subjected to chromatographic techniques to achieve better peak resolution and other techniques able to elucidate compound structures, such as NMR spectrometry or x-ray crystallography (Sumner et al., 2007).

After validating the presence of the identified and novel compounds, it would be necessary to confirm their bioactivity especially as there is not enough information available about their properties and uses. For commercially available compounds, similar *in vitro* bioactivity tests performed in this work could be done with pure compounds. If bioactivity is confirmed *in vitro*, *in vivo* efficacy experiments will be required as compounds sometimes display different activities *in vitro* and *in vivo* (Georgiadis et al, 2003). There would also be a need for toxicological validation and pharmacokinetic investigations to validate efficacy and safety of the pure compounds.

3.6 Insights into Industrial Application

Bioactive and biocompatible compounds confirmed in *N. shiloi* can be mass-produced in different ways to attain industrial application. First, like other microalgae, *N. shiloi* can be cultured under controlled abiotic/biotic conditions to overproduce desired metabolites (Demirel et al., 2020). This would involve optimizing the levels of culture parameters such as stirring, pH, light intensity, temperature, salt concentration and nutrients concentration in the culture media. Bioactive compounds can also be mass-produced through chemical synthesis and industrial production.

Whichever method is employed, mass-producing these metabolites will be a step forward towards their applications in different industries. In healthcare, the findings of this study would be of immense importance in ethnomedicine which employs natural substances in disease management and has been used in managing some metabolic and immunological disorders (Bouyahya et al., 2020). Also, this research would be important to the pharmaceutical and nutraceutical industries in the fight against hypertension, inflammation, and CVDs. It would be interesting, for example, to confirm which compound(s) are responsible for the bioactivities observed in ethanol fraction F13 such as inhibition of the gene expression of proinflammatory cytokines and the activity of ACE (and even COX-2 inhibition reported by Kautzmann (2021)). Structure-activity relationship and lead optimization studies can lead to improvement of compound structures (such as addition or deletion of functional groups) to achieve better efficacy and physiological responses, reduce toxicity, or increase absorption and bioavailability/bio-accessibility (Guha, 2013). In fact, there is a possibility of formulating medications that bypass the side effects of current ACE inhibitors. For example, compounds confirmed to display ACE inhibition can be tested for selective inhibition of its C- and N-domains. Molecular docking experiments can be employed to study their binding conformation and affinity to different domains *in silico* ACE models (Pekkoh et al., 2022; Trott and Olson, 2010). Those selectively inhibiting ACE C-domain might bypass the side effects of current ACE inhibitor drugs (captopril, enalapril, etc.) such as dry cough and angioedema, which would be an advancement in pharmaceutical management of hypertension (Shrimpton et al., 2020). Altogether, the findings of this study can be of use to different industries if followed up with further experiments.

3.7 Other Industrial Applications of *N. shiloi* Compounds

Apart from the bioactive compounds identified in this study, *N. shiloi* has other chemicals, pigments and macromolecules that are of interest to different industries. For example, *N. shiloi* has some potential applications in the production of vegetable oil, due to its relatively high content of essential fatty acids such as alpha linolenic acid (C18:2; 1.88%), arachidonic acid (C20:4; 9.29%), docosahexaenoic acid (C22:6; 1.24%), and EPA (C20:5; 6.79%; Grubišić et al., 2022; Kautzmann, 2021 (unpublished)). The proportion of these PUFAs can be increased by culturing under controlled conditions. Currently, fish is the primary source of essential fatty acids (Pieber et al., 2012), which is unacceptable to vegetarians and other consumers who are repulsed by its fishy smell, and a concern to public health due to heavy metal accumulation in fish which is passed on to the oil (Afshan et al., 2014; Pieber et al., 2012). Microalgae is in fact, the primary source of the EPA in fishes that graze on them, hence, microalgal- (including *N. shiloi*) derived oil could be a product of choice.

Furthermore, there is an increasing demand for natural pigments such as carotenoids (carotenes and xanthophylls) in the industry, where they have already found application as colorants and anti-aging agents (food and cosmetic), and therapeutics (nutraceutical; Fu et al., 2015). β-carotene, the precursor of vitamin A, is essential for the proper functioning of the retina and protects the skin against photoaging (Pieber et al., 2012). *N. shiloi* contains about 0.36 mg/100 g DW β-carotene which is considerably high (Grubišić et al., 2022). Also, fucoxanthin has been reported with anti-cancer, anti-obesity, anti-diabetic, and anti-malarial activities. Presently, the primary source of fucoxanthin is brown algae containing about 1 mg/g DW (Xiao et al., 2012) compared to *N. shiloi* (cultured under normal growth conditions) which contains about 0.39 mg/g DW (Grubišić et al., 2022). Fu et al. (2015) commented that growing diatoms under controlled conditions might aid them to outcompete brown algae in fucoxanthin production. Thus, pigment-rich *N. shiloi* has a high potential for application in food and cosmetic industries.

Again, after fatty acids and pigment extraction, microalgal industrial waste stream has a large content of protein and carbohydrate, which, of course, applies to *N. shiloi* reported with 56.2% DW protein and 17.1% DW carbohydrate contents when cultured under normal conditions (Grubišić et al., 2022). If proven non-toxic and bio-accessible, this waste fiber can be fortified with essential nutrients and used in food and feed formulation as an alternative protein source

in animal production. It will also provide bulk biomass to diet, which would be useful in fighting obesity, diabetes, colorectal cancer, and other diseases related to excess caloric intake.

With the increasing emphasis on sustainability and clean energy alternatives to fossil fuel, carbohydrate- and lipid-rich microalgae, such as *N. shiloi,* have the potential for utilization in the production of ethanol and generation of biofuels as a renewable energy source. Presently, some companies use valuable foodstuff such as tubers and corn for this purpose, which raises a concern of food and energy competition (Mielenz, 2021). Utilizing microalgal waste stream for this purpose will be a significant advancement in this industry. Presently, energy production from microalgae is not economically feasible (Fu et al., 2015), but advances in technology might turn things around in the future.

In summary, *N. shiloi* contains a wide range of chemicals which gives it a potential for application in several industries. Further experiments are to pinpoint these chemicals, mass-produce them, validate their activities, and apply them in industry.

3.8 Conclusion and recommendations

This study aims at discovering the potential of *N. shiloi* in ameliorating the effects of hypertension and its associated complications such as oxidative stress and cardiovascular inflammation, and to identify compounds responsible for such potential. The findings could be of great importance to different industries such as food, pharmaceutical, nutraceutical, etc., as it will pave the way for further research that might result in formulation of improved hypertension therapy that will hopefully overcome the drawbacks of currently used hypertension therapies.

Different HPLC-separated fractions of *N. shiloi* separately extracted with ethanol and ethyl acetate displayed significant antioxidant (mostly FRAP), ACE inhibitory, and anti-inflammatory activities. LC-MS analysis of the active non-color-intensive ethanol fractions showed the presence of some identified and unidentified compounds with no record of use or biological activity.

For further studies, we recommend a better peak resolution to better identify all the compounds with greater accuracy and validation of these results using more stringent protocols and techniques such as NMR spectrometry or x-ray crystallography. We also

recommend confirmation of the bioactivity, and evaluation of toxicity, and pharmacokinetics of such compounds (if commercially available or after purification) through *in vitro* or *in vivo* experiments. A detailed characterization of the components of the color intense fractions will also be of importance to the food, nutraceutical, and cosmetic industries. Finally, we recommend continuing the analysis of the active ethyl acetate fractions as they might contain even more interesting compounds.

References

Afshan, S., Ali, S., Ameen, U.S., Farid, M., Bharwana, S.A., Hannan, F., & Ahmad, R. (2014). Effect of Different Heavy Metal Pollution on Fish. *Res. J. Chem. Env. Sci*., 2(1), 74-79.

Alonso, A. Marsal, S. & Julià, A. (2015). Analytical methods in untargeted metabolomics: state of the art in 2015. *Front. Bioeng. Biotechnol.*, 3, 23

Bárcenas-Pérez, D., Lukeš, M., Hrouzek, P., Zápal, J., Kuzma, M., Kopecký, J., Kubáč, D., Arredondo-Vega, B.O., & Cheel, J. (2022). Bio-production of eicosapentaenoic acid from the diatom *Nanofrustulum shiloi* via two-step high performance countercurrent chromatography. *J. Appl. Phycol.*, 34(6), 2995.

Baudin, B. (2005). Angiotensin I converting-enzyme (ACE) in the diagnosis of sarcoidosis. *Pathol. Biol*., 53, 183–188.

Beal, M. F. (2003). Mitochondria, oxidative damage, and inflammation in Parkinson's disease. *Ann. N.Y. Acad. Sci.,* 991, 120– 131.

Begum, H., Yusoff, F. M., Banerjee, S., Khatoon, H., & Shariff, M. (2016). Availability and utilization of pigments from microalgae. *Crit. Rev. Food Sci. Nutr*., 56, 2209–2222.

Bernstein, K. E., Ong, F. S., Blackwell, W. B., Shah, K. H., Giani, J. F., Gonzalez-Villalobos, R. A., Shen, X. Z., Fuchs, S., & Touyz, R. M. (2013). A Modern Understanding of the Traditional and Nontraditional Biological Functions of Angiotensin-Converting Enzyme. *Pharmacol*. *Rev.*, 65(1), 1–46.

Bernstein, K. E., Khan, Z., Giani, J. F., Cao, D., Bernstein, E. A., & Shen, X. Z. (2018). Angiotensin-converting enzyme in innate and adaptive immunity, *Nat. Rev. Nephrol*. 14(5) 325–336.

Bernstein, K. E., Koronyo, Y., Salumbides, B. C., Sheyn, J., Pelissier, L., Lopes, D. H., Shah, K. H., Bernstein, E. A., Fuchs, D. T., Yu, J. J., Pham, M., Black, K. L., Shen, X. Z., Fuchs, S., & Koronyo-Hamaoui, M. (2014). Angiotensin-converting enzyme overexpression in myelomonocytes prevents Alzheimer's-like cognitive decline. *J. Clin. Investig*., 124(3), 1000–1012.

Bouyahya, A., Omari, N. E., Elmenyiy, N., Guaouguaou, F. E., Balahbib, A., El-Shazly, M., & Chamkhi, I. (2020). Ethnomedicinal use, phytochemistry, pharmacology, and toxicology of Ajuga iva (L.,) schreb. *J. Ethnopharmacol*., 258, 112875.

Brand-Williams, W., Cuvelier, M. E., & Berset, C. (1995). Use of a free radical method to evaluate antioxidant activity. *Lebensm. Wiss. Technol.*, 28, 25–30.

Brandt, C., & Pedersen, B.K. (2010). "The role of exercise-induced myokines in muscle homeostasis and the defense against chronic diseases". *J. biotechnol. biomed*., 520258.

Brasier, A.R. (2006). "The NF-kappaB regulatory network". Cardiovasc. *Toxicol*. 6(2): 111–130.

Calliste, C.A., Trouillas, P., Allais, D.P., Simon, A., & Duroux, J.L. (2001). Free radical scavenging activities measured by electron spin resonance spectroscopy and B16 cell antiproliferative behaviors of seven plants. *J. Agric. Food Chem*., 49, 3321–3327.

Cao, D. Y., Saito, S., Veiras, L. C., Okwan-Duodu, D., Bernstein, E. A., Giani, J. F., Bernstein, K. E., & Khan, Z. (2020). Role of angiotensin-converting enzyme in myeloid cell immune responses, *CellMol. Biol. Lett*. 25, 31.

CEM Corporation (2017). Automated Extraction System EDGE. http://cem.com/edge/. Accessed on February 13, 2023.

Chandra, S., Saklani, S., Kumar, P., Kim, B., & Coutinho, H. D. M. (2022). Nutraceuticals: Pharmacologically active potent dietary supplements. *Biomed Res. Int*., 2022, 2051017.

Chapman, R. L. (2013). Algae: The world's most important 'plants'-an introduction. Mitigation and Adaptation Strategies for Global Change, 18(1), 5–12.

Clementina, S., Alessandra, B., Elena, E., Giovanna, R., Anna, P., Raffaella, C., Maria, F., & Adrianna, I. (2014). Diatom-derived polyunsaturated aldehydes activate cell death in human cancer cell lines but not normal cells. *PLoS One*, 9 (7), e101220.

Colak, E. (2008). New markers of oxidative damage to macromolecules. *J. Med. Biochem*., 27, 1–16.

Corradi, H. R., Schwager, S. L., Nchinda, A. T., Sturrock, E. D., & Acharya, K. R. (2006). Crystal structure of the N domain of human somatic angiotensin I-converting enzyme provides a structural basis for domain-specific inhibitor design. *J. Mol. Biol*., 357(3), 964-74.

Cushman, D. W. & Cheung, H. S. (1971). Spectrophotometric assay and properties of the angiotensin converting enzyme of rabbit lung. *Biochem. Pharmacol*., 20, 1637–1648.

Dagenais, N. J., & Jamali, F. (2005). Protective effects of angiotensin II interruption: evidence for antiinflammatory actions. *Pharmacotherapy*, 25(9), 1213-1229.

Del Rio, L. A. (2015). ROS and RNS in plant physiology: an overview. *J. Exp. Bot.,* 66, 2827–37

Demirel, Z., Imamoglu, E., & Dalay, M. C. (2020). Growth Kinetics of *Nanofrustulum shiloi* Under Different Mixing Conditions in Flat-plate, *Braz Arch Biol Technol*. 63, 20190201.

Di Meo, S., Reed, T. T., Venditti, P., & Victor, V. M. (2016). Role of ROS and RNS sources in physiological and pathological conditions. *Oxid Med Cell Longev*., 2016, 1245049.

Douglas, G. C., O'Bryan, M. K., Hedger, M. P., Lee, D. K., Yarski, M. A., Smith, A. I., & Lew, R. A. (2004). The novel angiotensin-converting enzyme (ACE) homolog, ACE2, is selectively expressed by adult Leydig cells of the testis. *Endocrinology*, 145(10), 4703-4711.

DrugBank. https://go.drugbank.com/drugs/DB08887. Accessed on June 03, 2023.

Fleith, M., & Clandinin, M.T. (2005). Dietary PUFA for Preterm and Term Infants: Review of Clinical Studies. *Crit. Rev. Food Sci. Nutr*., 45, 205–229.

Fleming, I. (2006). Signaling by the Angiotensin-Converting Enzyme. *Circ. Res*. 98(7), 887–896.

Fu, W., Wichuk, K., & Brynjo´lfsson, S. (2015). Developing diatoms for value-added products: challenges and opportunities. *N. Biotechnol.*, 32(6), 547-551.

Fuhrer, T., & Zamboni, N. (2015). High-throughput discovery metabolomics. *Curr. Opin. Biotechnol*. 31, 73–78.

Gaddam, R. R., Chambers, S., & Bhatia, M. (2014). ACE and ACE2 in Inflammation: A Tale of Two Enzymes. *Inflamm. Allergy Drug Targets*, 13(4), 224–234.

Gao, Q., Xu, L., & Cai, J. (2021). New drug targets for hypertension: A literature review. *Biochem. Biophys. Acta. Mol. Basis Dis*., 1867(3), 166037.

Giles, G.I., Tasker, K.M., & Jacob, C. (2001). Hypothesis: the role of reactive sulfur species in oxidative stress. Free Radic. *Biol. Med*. 31, 1279–83

Ginwala, R., Bhavsar, R., Chigbu, D. G. I., Jain, P., & Khan, Z. K. (2019). Potential Role of Flavonoids in Treating Chronic Inflammatory Diseases with a Special Focus on the Anti-Inflammatory Activity of Apigenin. *Antioxidants*, 8 (2), 35.

Gonzalez-Villalobos, R. A., Shen, X. Z., Bernstein, E. A., Janjulia, T., Taylor, B., Giani, J. F., Blackwell, W. L. B., Shah, K. H., Shi, P. D., & Fuchs, S. (2013). Rediscovering ACE: novel insights into the many roles of the angiotensin-converting enzyme. *J. Mol. Med*., 91(10), 1143-1154.

Grondelle, R. & Boeker, E. (2017). Limits on Natural Photosynthesis. *J. Phys. Chem. B*., 121(30), 7229-7234.

Grossman, E. (2008). Does Increased Oxidative Stress Cause Hypertension? *Diabetes Care*, 31(2), S185–S189.

Grubiši´c, M., Šantek, B., Zori´c, Z., Coši´c, Z., Vrana, I., ˇGašparovi´c, B., Což-Rakovac, R., ˇIvanˇci´c & Šantek, M. (2022). Bioprospecting of Microalgae Isolated from the Adriatic Sea: Characterization of Biomass, Pigment, Lipid and Fatty Acid Composition, and Antioxidant and Antimicrobial Activity. *Molecules*, 27(4), 1248.

Guha, R. (2013). On Exploring Structure–Activity Relationships. In: Kortagere, S. (eds) *In Silico Models for Drug Discovery.* Methods in Molecular Biology, vol 993.

Han, G.M., & Liu, P. (2017). Higher serum lycopene is associated with reduced prevalence of hypertension in overweight or obese adults. *Eur. J. Integr. Med*., 13, 34–40.

Harrison, C., & Acharya, K.R. (2015). A new high-resolution crystal structure of the Drosophila melanogaster angiotensin converting enzyme homologue, AnCE. *FEBS open bio*, 5, 661–667.

Heinecke, J. W. (1997). Mechanisms of oxidative damage of low-density lipoprotein in human atherosclerosis. *Curr. Opin. Lipidol*., 8, 268–274.

Huang, C., McAllister, M.J., Slusher, A.L., Webb, H.E., Mock, J.T., and Acevedo, E.O. (2015). Obesity Related Oxidative Stress: the Impact of Physical Activity and Diet Manipulation. Sports Med. Open, 1:32.

Huentelman, M.J., Grobe, J.L., Vazquez, J., Stewart, J.M., Mecca, A.P., Katovich, M.J., Ferrario, C.M., & Raizada, M.K. (2005). Protection from angiotensin II-induced cardiac hypertrophy and fibrosis by systemic lentiviral delivery of ACE2 in rats. *Exp. Physiol*., 90(5), 783-790.

Huuskonen, M.S., Jarvisalo, J., Koskinen, H., & Kivisto, H. (1986). Serum Angiotensin-Converting Enzyme and Lysosomal Enzymes in Tobacco Workers. *Chest,* 89(2) 224–228.

Iyer, S.N., Chappell, M.C., Averill, D.B., Diz, D.I., & Ferrario, C.M. (1998). Vasodepressor actions of angiotensin-(1-7) unmasked during combined treatment with lisinopril and losartan. *Hypertension*, 31(2), 699-705.

Kautzmann, B. (2022). Bioprospecting anti-inflammatory compounds in three diatoms, *Cylindrotheca closterium, Cylindrotheca fusiformis* and *Nanofrustulum shiloi*. Unpublished.

Khan, Z., Shen, X.Z., Bernstein, E.A., Giani, J.F., Eriguchi, M., Zhao, T.V., Gonzalez-Villalobos, R. A., Fuchs, S., Liu, G.Y., & Bernstein, K.E. (2017). Angiotensin-converting enzyme enhances the oxidative response and bactericidal activity of neutrophils. *Blood,* 130, 328–339.

Khurana, V. & Goswami, B. (2022). Angiotensin converting enzyme (ACE). *Clinica Chimica Acta,* 524, 113–122

Kinross, A.D., Hageman, K.J., Doucette, W.J., & Foster, A.L. (2020). Comparison of Accelerated Solvent Extraction (ASE) and Energized Dispersive Guided Extraction (EDGE) for the analysis of pesticides in leaves. *J. Chromatogr. A*., 1627, 461414.

Kjeldsen, S.E. (2018). Hypertension and cardiovascular risk: General aspects. *Pharmacol Res,* 129, 95-99.

Kociolek, J.P., Blanco, S., Coste, M., Ector, L., Liu, Y., Karthick, B., Kulikovskiy, M., Lundholm, N., Ludwig, T., Potapova, M., Rimet, F., Sabbe, K., Sala, S., Sar, E., Taylor, J., Van de Vijver, B., Wetzel, C.E., Williams, D.M., Witkowski, A., & Witkowski, J. (2023). DiatomBase. *Nanofrustulum shiloi* (J.J.Lee, Reimer & McEnery) Round, Hallsteinsen & Paasche, 1999. World Register of Marine Species. https://www.marinespecies.org/aphia.php?p=taxdetails&id=613135. Accessed on February 16, 2022.

Kohlstedt, K., Brandes, R.P., Muller-Esterl, W., Busse, R., & Fleming, I. (2004). Angiotensin-Converting Enzyme Is Involved in Outside-In Signaling in Endothelial Cells, *Circ. Res*. 94 (1), 60–67.

Kuda, T., Hishi, T., & Maekawa, S. (2006). Antioxidant properties of dried product of 'haba-nori', an edible brown alga, *Petalonia binghamiae* (J. Agraradh) Vinogradova. *Food Chem*., 98, 545– 550.

Labunskyy, V.M., Hatfield, D.L., & Gladyshev, V.N. (2014). Selenoproteins: molecular pathways and physiological roles. *Physiol. Rev.* 94:739–77

Lauritano, C., Giovanna, R., Vittoria, R., Angela, A., Carolina, F., Mauro, B., Federica, B., Ylenia, C., & Adrianna, I. (2016). New oxylipins produced at the end of a diatom bloom and their

effects on copepod reproductive success and gene expression levels. *Harmful Algae*. 55, 221–229.

Li, C., Gastineau, R., Turmel, M., Witkowski, A., Otis, C., Car, A., & Lemieux, C. (2019). Complete chloroplast genome of the tiny marine diatom *Nanofrustulum shiloi* (Bacillariophyta) from the Adriatic Sea. *Mitochondrial DNA B: Resour*., 4(2), 3374–3376.

Li, Y., Zhang, Q., Li, N., Ding, L., Yi, J., Xiao, Y., Chen, S., & Huang, X. (2021). Ataxin-10 Inhibits TNF-α-Induced Endothelial Inflammation via Suppressing Interferon Regulatory Factor-1. *Mediators Inflamm.*, 7042148.

Liu, J., & Mori, A. (2006). Oxidative damage hypothesis of stress-associated aging acceleration: neuroprotective effects of natural and nutritional antioxidants. *Res. Commun. Biol. Psychol. Psychiat. Neurosci*., 30, 103–119.

Lopez-Sublet, M., Lanzacco, C. L., Danser, A. H. J., Lambert, M., Elourimi, G., & Persu, A. (2018). Focus on increased serum angiotensin-converting enzyme level: From granulomatous diseases to genetic mutations, *Clin. Biochem*. 59, 1–8.

Lyle, A.N., & Griendling, K.K. (2006). Modulation of vascular smooth muscle signaling by reactive oxygen species. *Physiology*, 21:269–80.

Magalhães, L. P., Dos Reis, L. M., Graciolli, F. G., Pereira, B. J., de Oliveira, R. B., de Souza, A. A., Moyses, R. M., Elias, R. M., & Jorgetti, V. (2017). Predictive Factors of One-Year Mortality in a Cohort of Patients Undergoing Urgent-Start Hemodialysis. *PloS one*, 12(1), e0167895.

Majumder, K., & Wu, J. (2014). Molecular targets of antihypertensive peptides: understanding the mechanisms of action based on the pathophysiology of hypertension. Int. J. Mol. Sci., 16(1), 256–283.

Masuyer, G., Yates, C. J., Sturrock, E. D., & Acharya, K. R. (2014). Angiotensin-I converting enzyme (ACE): structure, biological roles, and molecular basis for chloride ion dependence, *Biol. Chem.* 395, 1135–1149.

Megías, C., Pastor-Cavada, E., Torres-Fuentes, C., Girón-Calle, J., Alaiz, M., Juan, R., Pastor, J., & Vioque, J. (2009). Chelating, antioxidant and antiproliferative activity of Vicia sativa polyphenol extracts. *Eur. Food Res. Technol.,* 230(2), 353–359.

Meijvis, S. C. A., Cornips, M. C. A., Endeman, H., RuvenJan, H. J. T., Danser, A. H., Biesma, D. H., Leufkens, H. G. M., Bos, W. J. W., van de Garde, E. M. W. (2011). Prognostic value of serum angiotensin-converting enzyme activity for outcome of community-acquired pneumonia, *Clin. Chem. Lab. Med.* 49(9), 1525–1532.

Mielenz, J. R. (2001). Ethanol production from biomass: technology and commercialization status*. Curr. Opin. Microbiol*., 4, 324–329.

Minhas, A.K., Hodgson, P., Barrow, C.J., & Adholeya, A. (2016). A review on the assessment of stress conditions for simultaneous production of microalgal lipids and carotenoids. *Front. Microbiol*. 7, 546.

Moon, J. & Shibamoto, T. (2009). Antioxidant Assays for Plant and Food Components. *J. Agric. Food Chem*., 57(5), 1655–1666.

Moreira, P., Smith, M. A., Zhu, X., Honda, K., Lee, H.G., Aliev, G., & Perry, G. (2005). Since oxidative damage is a key phenomenon in Alzheimer's disease, treatment with antioxidants seems to be a promising approach for slowing disease progression. Oxidative damage and Alzheimer's disease: are antioxidant therapies useful? *Drug News Perspect*., 18, 13–19.

Mukherjee, A. B.; Zhang, Z., & Chilton, B. S. (2007). Uteroglobin: a steroid-inducible immunomodulator protein that founded the Secretoglobin superfamily. *Endocrine ReV,* 28, 707–725.

Müller, L., Fröhlich, K., & Böhm, V. (2011). Comparative antioxidant activities of carotenoids measured by ferric reducing antioxidant power (FRAP), ABTS bleaching assay (αTEAC), DPPH assay and peroxyl radical scavenging assay. *Food Chem*., 129(1), 139-148.

Naito, Y., Uchiyama, K., & Yoshikawa, T. (2006). Oxidative stress involvement in diabetic nephropathy and its prevention by astaxanthin. *Oxid. Stress Disease*, 21, 235–242.

Nakamura, S., Nakamura, I., Ma, L., Vaughan, D.E., & Fogo, A.B. (2000). Plasminogen activator inhibitor-1 expression is regulated by the angiotensin type 1 receptor *in vivo*. *Kidney Int.,* 58(1), 251- 259.

Natesh, R., Schwager, S.L., Sturrock, E.D., & Acharya, K. R. (2003). Crystal structure of the human angiotensin-converting enzyme–lisinopril complex. *Nature*, 421(6922), 551–554

National center for Biotechnology Information. https://pubchem.ncbi.nlm.nih.gov/compound/1054. Accessed on June 03, 2023.

National center for Biotechnology Information. https://pubchem.ncbi.nlm.nih.gov/substance/472970851. Accessed on June 03, 2023.

National center for Biotechnology Information. https://www.ncbi.nlm.nih.gov/mesh/68015118. Accessed on June 03, 2023.

National Library of medicine – IL1B interleukin 1 beta [Homo sapiens (human)]. https://www.ncbi.nlm.nih.gov/gene?Db=gene&Cmd=ShowDetailView&TermToSearch=3553. Accessed on April 03, 2023.

Naylor, L.H. (1999). Reporter Gene Technology: The Future Looks Bright. *Biochem. Pharmacol.*, 58, 749–757.

Nieri, P., Carpi, S., Esposito, R., Costantini, M., & Zupo, V. (2023). Bioactive Molecules from Marine Diatoms and Their Value for the Nutraceutical Industry. *Nutrients*, 15, 464.

Oyaizu, M. (1986). Studies on products of browning reaction. Antioxidative activities of products of browning reaction prepared from glucosamine. *Jpn. J. Nutr. Diet.* 44(6), 307–315.

Panfoli, I., Candiano, G., Malova, M., De Angelis, L., Cardiello, V., Buonocore G, & Ramenghi, L. A. (2018). Oxidative stress as a primary risk factor for brain damage in preterm newborns. *Front Pediatr*., 6, 369.

Parajuli, N., Ramprasath, T., Patel, V.B., Wang, W., Putko, B., Mori, J., & Oudit, G.Y. (2014). Targeting angiotensin-converting enzyme 2 as a new therapeutic target for cardiovascular diseases. *Can. J. Physiol. Pharmacol*., 92(7), 558-565.

Passos-Silva, D.G., Verano-Braga, T., & Santos, R.A. (2013). Angiotensin-(1- 7): beyond the cardio-renal actions*. Clin. Sci*., 124(7), 443- 456.

Paulose, C.S., Dakshinamurti, K., Packer, S., & Stephens, N.L. (1988). Sympathetic Stimulation and Hypertension in the Pyridoxine-Deficient Adult Rat. *Hypertension,* 11(4), 387–391.

Paz-Elizur, T., Sevilya, Z., Leitner-Dagan, Y., Elinger, D., Roisman, L. C., & Livneh, Z. (2008). DNA repair of oxidative DNA damage in human carcinogenesis: Potential application for cancer risk assessment and prevention. *Cancer Lett.*, 266, 60–72.

Pekkoh, J., Phinyo, K., Thurakit, T., Lomakool, S., Duangjan, K., Ruangrit, K., Pumas, C., Jiranusornkul, S., Yooin, W., Cheirsilp, B., Pathom-Aree, W., & Srinuanpan, S. (2022). Lipid Profile, Antioxidant and Antihypertensive Activity, and Computational Molecular Docking of Diatom Fatty Acids as ACE Inhibitors. *Antioxidants*, 11(2), 186.

Pieber, S., Schober, S., & Mittelbach, M. (2012). Pressurized fluid extraction of polyunsaturated fatty acids from the microalga *Nannochloropsis oculate*. *Biomass Bioenergy*, 47, 474-482.

Preedy, V. R., Reilly, M. E., Mantle, D., & Peters, T. J. (1998). Oxidative damage in liver disease. *J. Int. Fed. Clin. Chem*., 10, 16–20.

Quinlan, C. L., Perevoshchikova, I. V., Hey-Mogensen, M., Orr, A. L., & Brand, M. D. (2013). Sites of reactive oxygen species generation by mitochondria oxidizing different substrates. *Redox. Biol.,* 1, 304–312.

Radi, R. (2018). Oxygen radicals, nitric oxide, and peroxynitrite: redox pathways in molecular medicine. *Proc. Natl. Acad. Sci.*, 115(23), 5839–5848.

Rawat, M., Lakshminrusimha, S., & Vento, M. (2022). Pulmonary hypertension and oxidative stress: Where is the link? *Semin. Fetal Neonatal Med.,* 27(4), 101347

Reis, F. S., Martins, A., Lillian Barros, L., & Ferreira, I. (2012). Antioxidant properties and phenolic profile of the most widely appreciated cultivated mushrooms: A comparative study between in vivo and in vitro samples. *Food Chem., Toxicol*., 50, 1201–1207.

Riordan, J.F. (2003). Angiotensin-I-converting enzyme and its relatives. *Genome Biol.,* 4, 225.

Round, F. E., Hallsteinsen, H., & Paasche, E. (1999). On a previously controversial “fragilarioid” diatom now placed in a new genus *Nanofrustulum*. *Diatom Res*., 14(2), 343-356.

Ruocco, N., Costantini, S., Zupo, V., Lauritano, C., Caramiello, D., Ianora, A., Budillon, A., Romano, G., Nuzzo, G., D’Ippolito, G., Fontana, A., & Costantini, M. (2018). Toxigenic effects of

two benthic diatoms upon grazing activity of the sea urchin: morphological, metabolomic and de novo transcriptomic analysis. *Sci. Rep.,* 8, 5622.

Ruocco, N., Nuzzo, G., D'Ippolito, G., Manzo, E., Sardo, A., Ianora, A., Romano, G., Iuliano, A., Zupo, V., Costantini, M., & Fontana, A. (2020). Lipoxygenase Pathways in Diatoms: Occurrence and Correlation with Grazer Toxicity in Four Benthic Species. *Mar. Drugs*, 18, 66.

Sahin, M.S., Khazi, M.I., Demirel, Z., & Dalay, M.C. (2019). Variation in growth, fucoxanthin, fatty acids profile and lipid content of marine diatoms *Nitzschia sp*. and *Nanofrustulum shiloi* in response to nitrogen and iron. *Biocatal. Agric. Biotechnol*., 17, 390-398.

Salma shaik, & Harikrishnan, N. (2023). Evolution of cytotoxicity of the phytopigments Isolated from *Spirulina platensis* using MTT assay. *J. Popul. Ther. Clin. Pharmacol*., 30(4), 335–343.

Sentandreu, Ángel M., & Toldrá, F. (2006). A fluorescence-based protocol for quantifying angiotensin-converting enzyme activity. *Nat. Protoc*., 1(5), 2423–2427.

Sepulveda, R. T., & Watson, R. R. (2002). Treatment of antioxidant deficiencies in AIDS patients. *Nutr. Res*., 22, 27–37.

Sorriento, D. & Iaccarino, G. (2019). Inflammation and Cardiovascular Diseases: The Most Recent Findings. *Int J Mol Sci*., 20(16), 3879.

Shrimpton, A. J., Walker, S. L. M., & Ackland, G. L. (2020). Angiotensin converting enzyme inhibitors and angiotensin receptor blockers. *BJA Education*, 20(11), 362–367.

Sies, H. (1986). Biochemistry of oxidative stress. *Angew. Chem. Int. Ed. Engl*., 25(12), 1058-1071.

Sies, H. & Jones, D. P. (2007). Oxidative stress. *G. Fink, Encyclopedia of stress (2nd ed.), Elsevier, Amsterdam*, 45-48

Sies, H., Belousov, V. V., Chandel, N. S., Davies, M. J., Jones, D. P., Mann, G. E., Murphy, M. P., Yamamoto, M., & Winterbourn, C. (2022). Defining roles of specific reactive oxygen species (ROS) in cell biology and physiology. *Nat. Rev. Mol. Cell Biol.,* 23(7), 499–515.

Sies, H., Berndt, C., & Jones, D.P. (2017). Oxidative stress. *Annu Rev Biochem*, 86, 715–748.

Spolaore, P., Joannis-Cassan, C., Duran, E., & Isambert, A. (2006). Commercial applications of microalgae—Review. *J. Biosci. Bioeng*., 101(2), 87–96.

Studdy, P.R., Lapworth, R., & Bird, R. (1983). Angiotensin-converting enzyme and its clinical significance–a review, *J. Clin. Pathol*. 36(8), 938–947.

Subramoniam, A., Asha, V. V., Nair, S. A., Sasidharan, S. P., Sureshkumar, P. K., Rajendran, K. N., Karunagaran, D., & Ramalingam, K. (2012). Chlorophyll revisited: anti-inflammatory activities of chlorophyll a and inhibition of expression of TNF-α gene by the same. *Inflammation*, 35(3), 959–966.

Sumner, L. W., Amberg, A., Barrett, D., Beale, M. H., Beger, R., Daykin, C. A., Fan, T. W. M., Fiehn, O., Goodacre, R., Griffin, J. L., Hankemeier, T., Hardy, N., Harnly, J., Higashi, R., Kopka, J.,

Lane, A. N., Lindon, J. C., Marriott, P., Nicholls, A. W., Reily, M. D., Thaden, J. J., & Viant, M. R. (2007). Proposed minimum reporting standards for chemical analysis. *Metabolomics*, 3, 211-221.

Tham, D. M., Martin-McNulty, B., Wang, Y., Wilson, D. W., Vergona, R., Sullivan, M. E., Dole, W., & Rutledge, J. C. (2002). Angiotensin II is associated with activation of NF-kB-mediated genes and downregulation of PPARs. *Physiol Genomics*, 11(1), 21-30.

Trott, O. & Olson, A.J. (2010) AutoDock Vina: Improving the Speed and Accuracy of Docking with a New Scoring Function, Efficient Optimization, and Multithreading. *J. Comput Chem*, 31, 455-461.

Viant, M. R., Kurland, I. J., Jones, M. R., & Dunn, W. B. (2017). How close are we to complete annotation of metabolomes? *Curr Opin Chem Biol*, 36, 64–69.

Waters Corporation (2006). 2424 Evaporative light scattering detector operator's guide. 71500121802/Revision B.

Widodo, N., Wisnasari, S., Rohman, M.S., Yunita, L., Lukitasari, M., Nuril, M., Holil, K., Purwaningroom, D.L. (2017). Alu insertion/deletion of ACE gene polymorphism might not affect significantly the serum bradykinin level in hypertensive patients taking ACE inhibitors. *Egypt. J. Med. Hum. Genet*., 18(2), 187-191.

World Health Organization (2022). https://www.who.int/health-topics/cardiovascular-diseases#tab=tab_1. Accessed on December 03, 2022.

World Health Organization (2022). https://www.who.int/news-room/fact-sheets/detail/hypertension. Accessed on December 03, 2022.

World Health Organization. https://www.who.int/health-topics/hypertension. Accessed on June 06, 2023.

Xiao, B., Li, Y., Lin, Y., Lin, J., Zhang, L., Wu, D., Zeng, J., Li, J., Liu, J., & Li, G. (2022). Eicosapentaenoic acid (EPA) exhibits antioxidant activity via mitochondrial modulation. *Food Chem*., 373, 131389.

Xiao, X., Si, X., Yuan, Z., Xu, X., & Li, G. (2012). Isolation of fucoxanthin from edible brown algae by microwave-assisted extraction coupled with high-speed countercurrent chromatography. *J. Sep. Sci*., 35, 2313–7.

Yates, C. J., Sturrock, E. D., & Acharya, K. R. (2014). Angiotensin-I converting enzyme (ACE): structure, biological roles, and molecular basis for chloride ion dependence, *Biol. Chem*. 395, 1135–1149.

Zeisel, S. H. (1999). Regulation of "nutraceuticals". *Science*, 285, 1853–1855.

Zhang, J., & An, J. (2007). Cytokines, Inflammation and Pain. *Int Anesthesiol Clin*., 45(2), 27–37.

Zhang, X., Zhang, P., Liu, Y., Liu, Z., Xu, Q., Zhang, Y., Liu, L., Yang, X., Li, L., & Xue, C. (2023). Effects of Caprylic Acid and Eicosapentaenoic Acid on Lipids, Inflammatory Levels, and the JAK2/STAT3 Pathway in ABCA1-Deficient Mice and ABCA1 Knock-Down RAW264.7 Cells. *Nutrients*, *15*(5), 1296.

Zhao, J., Vollhardt, D., Wu, J., Miller, R., Siegel, S., & Li, J. B. (2000). Effect of dodecyl dimethyl phosphine oxide penetration into phospholipid monolayers: morphology and dynamics. *Colloids Surf. A Physicochem. Eng. Asp*., 166(1–3), 235-242.

Zhao, Y., & Xu, C. (2008). Structure and Function of Angiotensin Converting Enzyme and Its Inhibitors. *Chin. J. Biotech.*, 24(2), 171-176.

Zheng, H., & Cao, J. J. (2020). Angiotensin-Converting Enzyme Gene Polymorphism and Severe Lung Injury in Patients with Coronavirus Disease 2019. *Am. J. Pathol*., 190(10), 2013–2017.